Ectopic expression of an Arabidopsis glutaredoxin increases thermotolerance in maize during reproductive developmental stages

by

Stuart A. Sprague

B.S., Kansas State University, 2012

AN ABSTRACT OF A DISSERTATION

submitted in partial fulfillment of the requirements for the degree

DOCTOR OF PHILOSOPHY

Department of Horticulture and Natural Resources
College of Agriculture

KANSAS STATE UNIVERSITY
Manhattan, Kansas

2018

Abstract

Drought and heat stress are two of the biggest constraints to global food production. Abiotic stress response pathways are complex and consist of osmotic adjustors, macromolecule stabilizers, and antioxidants to counteract the damaging nature of abiotic stress induced reactive oxygen species (ROS) accumulation. In this work, we studied the effect of overexpression of an *Arabidopsis* glutaredoxin, *AtGRXS17,* on heat tolerance in maize (*Zea mays* L.) and drought tolerance in rice (*Orzya sativa* L.). Glutaredoxins (GRXs) are proteins cable of reducing disulfide bonds, therefore regulating the cellular redox status, and require glutathione for regeneration. Ectopic expression of *AtGRXS17* in maize resulted in increased heat stress tolerance during flowering. AtGRXS17 enhanced heat tolerance by increasing kernel set and total grain yield during heat treatments, compared to wild type controls. Our results indicated that *AtGRXS17*-expressing maize plants produce heat tolerant pollen with higher germination rates than wild type when challenged during heat treatments. Furthermore, *AtGRXS17*-expressing plants were less susceptible to post pollination heat induced kernel abortion. Rice plants expressing *AtGRXS17* were also tolerant to abiotic stress. *AtGRXS17*-expressing rice was more tolerant to drought stress challenges and consistently survived drought treatments. A non-targeted metabolomics study revealed distinct changes in profiles of key metabolite groups in response to drought stress. Soluble sugars and amino acids accumulate as osmotic adjustors while antioxidants, such as glutathione, accumulate to mediate ROS accumulation and regulate redox activity. All genotypes accumulated amino acids, soluble sugars, and raffinose family oligosaccharides in response to drought stress. Our results indicated *AtGRXS17*-expression affected several pathways known to increase drought tolerance. Altered sugar metabolites suggested a redox modulation of sucrose synthase activity and significant increases in the

secondary sulfur assimilation pathway metabolites suggested altered sulfur metabolism. This research provides new insights into ability of GRXs to improve heat tolerance and crop yield in maize and functions of GRXs in affecting metabolite profiles contributing to increased drought tolerance in rice.

Ectopic expression of an Arabidopsis glutaredoxin increases thermotolerance in maize during reproductive developmental stages

by

Stuart A. Sprague

B.S., Kansas State University, 2012

A DISSERTATION

submitted in partial fulfillment of the requirements for the degree

DOCTOR OF PHILOSOPHY

Department of Horticulture and Natural Resources
College of Agriculture

KANSAS STATE UNIVERSITY
Manhattan, Kansas

2018

Approved by:

Major Professor
Dr. Sunghun Park

Copyright

Abstract

Drought and heat stress are two of the biggest constraints to global food production. Abiotic stress response pathways are complex and consist of osmotic adjustors, macromolecule stabilizers, and antioxidants to counteract the damaging nature of abiotic stress induced reactive oxygen species (ROS) accumulation. In this work, we studied the effect of overexpression of an *Arabidopsis* glutaredoxin, *AtGRXS17*, on heat tolerance in maize (*Zea mays* L.) and drought tolerance in rice (*Orzya sativa* L.). Glutaredoxins (GRXs) are proteins cable of reducing disulfide bonds, therefore regulating the cellular redox status, and require glutathione for regeneration. Ectopic expression of *AtGRXS17* in maize resulted in increased heat stress tolerance during flowering. AtGRXS17 enhanced heat tolerance by increasing kernel set and total grain yield during heat treatments, compared to wild type controls. Our results indicated that *AtGRXS17*-expressing maize plants produce heat tolerant pollen with higher germination rates than wild type when challenged during heat treatments. Furthermore, *AtGRXS17*-expressing plants were less susceptible to post pollination heat induced kernel abortion. Rice plants expressing *AtGRXS17* were also tolerant to abiotic stress. *AtGRXS17*-expressing rice was more tolerant to drought stress challenges and consistently survived drought treatments. A non-targeted metabolomics study revealed distinct changes in profiles of key metabolite groups in response to drought stress. Soluble sugars and amino acids accumulate as osmotic adjustors while antioxidants, such as glutathione, accumulate to mediate ROS accumulation and regulate redox activity. All genotypes accumulated amino acids, soluble sugars, and raffinose family oligosaccharides in response to drought stress. Our results indicated *AtGRXS17*-expression affected several pathways known to increase drought tolerance. Altered sugar metabolites suggested a redox modulation of sucrose synthase activity and significant increases in the

secondary sulfur assimilation pathway metabolites suggested altered sulfur metabolism. This research provides new insights into ability of GRXs to improve heat tolerance and crop yield in maize and functions of GRXs in affecting metabolite profiles contributing to increased drought tolerance in rice.

Table of Contents

List of Figures

List of Tables

Acknowledgements

I would like to thank everyone who supported my studies and professional development here at K-State and our family like environment in Horticulture and Natural Resources.

Dr. Sunghun Park deserves my most sincere gratitude and appreciation for all he has done for me. He was always there for me offering advice on experiments, teaching, and professional development. He constantly helped inspire confidence within myself and without his support I would not be where I am today. He is a rare example of leading by example. His critical thinking about experimental designs, research outcomes, and their useful application has shown me how to confront issues and critically assess them as a scientist. His kind and warm attitude and sincere concern with the well-being of his students is unquantifiable. Thank you Dr. Park.

Each of my committee members had a unique role that helped my development during graduate studies. I would like to thank Dr. Kimberly Williams. She is a fantastic example of someone who cares about student learning and is passionate about helping students understand the application of course material. She was my undergraduate advisor and helped me find my career passion. Without her expertise on greenhouse production and nutrient management I would not have been able to conduct the greenhouse experiments correctly. I would like to thank Dr. Frank White for his critical review of my work and his ability to be critical yet caring. This balance is an excellent model for my scientific career. I would like to thank Dr. Jason Griffin who helped me start thinking about professional development and time management skills early in my graduate studies. Without some of the resources he provided me I would have had a much more difficult journey through graduate school. I would like to thank Dr. Deann Presley for her advice and suggestions for my dissertation and defense and the days leading up to it.

Our lab has a family like atmosphere and everyone deserves my sincere appreciation for the role they played in helping me get here. Kim Park constantly provides seeds for our experiments and technical advice for everything tissue culture related. Trevor Steiner helped with many tasks and without his help during the 2017 field trial I would have not been able to conduct this research. Tej Man Tamang and Tayebeh Kakeshpour are excellent graduate students who perfectly fit into our team atmosphere and always ask how they can help or contribute to a project. Former graduate students Dr. Ying Hu and Dr. Qingyu Wu constantly provided good advice and collaboration for my work and writing.

I would like to thank all collaborators for our work. Dr. Barbara Valent, and researchers working for her Dr. Ely Oliveira-Garcia and Melinda Dalby, were invaluable for much of my work. Dr. Kendal Hirschi and Dr. Ninghui Cheng provided advice on the direction of our projects. Dr. Krishna Jagadish SV and his researchers, Anuj Chiluwal, Blake Bergkamp, Nithin Shetty, Dr. Impa Somayanda, Dr. Raju Bheemanahalli, and Dr. David Sebela, for their assistance in both rice and maize work. Dr. Sanzhen Liu was a great help providing technical advice on best procedures for maize tissue gene expression analysis.

My family has been a tremendously supportive pillar for me. My parents support reminded me that I could make it by concentrating on the task at hand. My wife Brianna has made many sacrifices for my career that I cannot begin to thank her for all that she has done to support this endeavor.

Dedication

I dedicate this work to my family. My wife Brianna has made this possible with her constant support. My first born daughter Clara who has helped me see the world in a new light. My parents Randy and Mary for always being there. My brother Wayne who has always been a good brother and hard worker. I am proud of all of them.

Chapter 1 - Ectopic expression of *AtGRXS17* in maize confers heat tolerance during reproductive developmental stages

ABSTRACT

Increases in global world population and increased predicted temperatures will negatively impact crop production. Genetic improvement and improved cropping practices have greatly increased yields of cereal crops over the last century but there is still much room for improvement. Maize is the highest yielding crop in the world and, despite its subtropical ancestral origins, maize flowers can be quite sensitive to high temperatures. Our previous work indicates *AtGRXS17* is critical for temperature-dependent postembryonic growth, and ectopic expression of this gene has been demonstrated as useful in combating multiple abiotic stress in tomato during vegetative growth and development. Here, we define a precise time for the ability of AtGRXS17 to confer thermotolerance during reproductive growth stages in maize. In field tests, three independent *AtGRXS17*-expressing maize events displayed significantly higher kernel set, resulting in increased yields in comparison to the non-transgenic counterparts. Pollen produced by *AtGRXS17*-expressing plants has improved germination under elevated temperatures in comparison to controls. Fertilized ovules also are more heat tolerant than wild type and are less likely to abort under heat treatments. No differences in expression pattern of stress responsive or embryo specific genes were measured between genotypes. Our data provide novel insights into the impact of glutaredoxins on temperature dependent postembryonic growth and development and heat stress tolerance during embryonic growth.

INTRODUCTION

The population of humans on earth is currently estimated to rise by a staggering 83 million people per year and reach a global total of almost 10 billion by 2050, representing an increase of almost 29% from our current population of 7.6 billion (United Nations, 2017). Climate models now predict that the mean global temperature will increase anywhere from 2.5°F (1.4°C) to 10°F (5.55°C) in the next 100 years (Melillo et al., 2014) These increases are theorized to also be associated with an increase in unpredictable weather patterns, reducing our ability to cope though modified planting dates and best practices, and, thus, increasing our reliance on genetic improvements (Easterling et al., 2000). Bouts of extreme high temperatures can devastate crops, including maize (*Zea mays* L.), the largest world crop by grain weight (Tripathi et al., 2016). Models have predicted from a 46%-82% reduction in average cereal yields due to increasing temperatures by the end of the next century, depending on which model is used for interpretation, and agronomists have suggested that maize will be the most impacted species of the four major crops (Schlenker and Roberts, 2009, Zhao et al., 2017). The combination of predicted increased populations and decreased crop yields due to temperature necessitates an urgency in conventional and molecular breeding programs to develop heat tolerant cultivars.

Due to the spatial separation of Rubisco from oxygen, C4 species tend to have higher optimal temperature for growth and development than C3 species. C4 species are still susceptible to heat stress as photosynthesis is severely impacted at leaf temperatures above 30°C (Crafts-Brandner et al., 2002). When exposed to temperatures only 4°C warmer than optimal, maize hybrid vegetative growth and biomass yield increase but kernel set and yield drastically decrease (Hatfield, 2016). Models predict that maize grain yield will decrease 8.3% for each 1°C increase in average temperature (Lobell and Field, 2007). Although yield loss can occur due to decreased

florets on reproductive plant organs such as the tassel and ear, heat stress can significantly decrease yield primarily due to an effect on pollen and ovules resulting in reduced fertilization and kernel abortion (Lizaso et al., 2018). Despite millions of pollen grains produced per plant, decreased pollen production and viability can contribute to decreased yields as viability is strongly correlated with ambient vapor pressure deficit (VPD). VPD, in turn, is a function of temperature (Fonseca and Westgate, 2005). High temperature induced yield reductions were found to be highly correlated to number of kernels and can be affected up to 15 days post silking (Ordóñez et al., 2015). Some studies have found heat induced kernel abortion can explain up to 95% of yield loss (Rattalino Edreira et al., 2011). Maize plants subjected to heat stress in the field, but pollinated with fresh greenhouse grown pollen, were still found to display reduced kernel set (Cicchino et al., 2010).

The molecular response of plants to heat stress includes reduction in photosynthesis, and reactive oxygen species (ROS) accumulation, compromising cell membranes, proteins, and, nucleic acids due to oxidative stress. In tomato pollen, heat stress induces heat shock factors (HSFs), heat shock proteins (HSPs), ROS scavengers, and sugars (Frank et al., 2009). HSFs, post transcriptionally regulated transcription factors, are strongly and quickly induced by elevated temperatures (Ohama et al., 2017). In maize, 25 HSFs were identified to be induced or repressed by heat stress in various tissues (Lin et al., 2011). HSFs regulate transcription of several different heat shock proteins (HSPs), named according to molecular weights. HSP100, HSP90, HSP70, HSP60 and small heat shock proteins (sHSPs), are considered the first line of defense against heat stress as their transcripts can be detected within seconds of stress initiation, and they are crucial molecular chaperones for protein stabilization (Kotak et al., 2007). HSPs transcript levels, including HSP90, HSP70, and sHSP26, are upregulated in maize leaf tissue

when temperatures increase (Frey et al., 2015). HSP70 and HSP90 are involved in reducing oxidative stress, as inhibition of these proteins increased H_2O_2 and resulted in oxidative stress and increased cell death (Sable et al., 2018). ROS production from mitochondria, chloroplasts, and peroxisomes increase due to heat stress (Apel and Hirt, 2004). Despite this potential for oxidative stress, ROS production through NADPH oxidase is dependent upon phosphorylation and calcium signals (Kobayashi et al., 2007). ROS accumulation can act as a signaling molecule and is able to modulate HSP70 production (Piterková et al., 2013). To combat ROS excesses, a strict balancing act must be maintained within the complex antioxidant system, and enzymes such as ascorbate peroxidase (APX), catalase (CAT), superoxide dismutase (SOD), and glutaredoxins (GRXs) assist in keeping ROS levels in check under normal growth conditions and after ROS inducing events, including heat stress, to prevent unnecessary cellular damage.

Glutaredoxins (GRXs) are small ubiquitous oxidoreductases, present in nearly all living organisms, that contribute to detoxification of ROS (Wu et al., 2017). Monothiol GRXs reduce glutathionylated proteins utilizing their reduced thiol group, and the reduced form is regenerated by reduced glutathione (GSH) (Rouhier et al., 2004). This oxidoreductase activity affects the redox state, and activity, of target proteins and the plant cell. GRXs are important in heavy metal detoxification, iron-sulfur cluster (ISC) binding and transport, floral development signaling, and abiotic stress tolerance (Stroher et al, 2016, Inigo et al., 2016, Knuesting et al., 2015, Hu et al., 2015). AtGRXS17 has been implicated in most of these roles. First, AtGRXS17 was identified to be critical for post-embryonic growth and development of Arabidopsis when challenged with elevated temperatures (Cheng et al., 2011). Abnormal meristem maintenance and root architecture were observed in homozygous *atgrxs17* knockout lines. Furthermore, ectopic expression of *AtGRXS17* in tomato resulted in plants with significantly higher thermotolerance

than wild type plants during vegetative growth and development (Wu et al., 2012). In this study we expressed *AtGRXS17* in the maize inbred line B104 to investigate the effect of AtGRXS17 on yield when challenged with heat stress during reproductive developmental stages. Total grain yield and total kernel number were measured when plants were challenged with elevated temperatures, both in the greenhouse and the field. Pollen germination rates and kernel abortion were also measured.

MATERIALS AND METHODS

Cloning the maize glutaredoxin ZmGRXS17

The NCBI database was utilized to identify the maize homolog of *AtGRXS17,* accession number NM_001156291.2, in the B73 reference genome. Primer sequences, forward 5'-CACCATGGCGAGCGGCGGG-3' and reverse 5'-CTACATTGACAGGGTCGACTTCAGCTC-3', were devised from the sequence. PCR was performed on cDNA synthesized according to manufacturer's instructions using RevertAid cDNA synthesis kit (Thermo Scientific™) from total RNA, which was isolated with the RNeasy Mini Kit (QIAGEN®). *ZmGRXS17* was then cloned into pENTR™/D-TOPO® vector for entry into the gateway system. Plasmids were transformed into competent *E. coli* cells via the freeze/thaw method and screened by PCR to confirm the presence of *ZmGRXS17*. The sequenced gene was transferred to pIPKb004 via gateway cloning and confirmed by PCR after transferring to *E. coli*. Plasmids were transformed into *Agrobacterium tumefaciens* GV3101 and confirmed by PCR. Nucleotide and amino acid sequence comparison was carried out using the NCBI BLAST tool.

Stress treatments for expression analysis of the maize glutaredoxin ZmGRXS17

Wild-type B104 seedlings were grown in Metro-Mix® 900 (Sun Gro®) at 28°C/24°C, 16hr/8hr photoperiod, and 600μmol/m^2/s photons of photosynthetically active radiation (PAR) intensity and irrigated as needed with constant liquid feed fertilizer. At V4 growth stage, visible leaf collar on the 4th true leaf, uniform experimental units were randomly assigned to various levels of either drought or heat treatments. Plants randomly assigned to different levels of heat treatment were exposed to 42°C for 0, 2, 4, 8, or 24 hr. Plants exposed to drought had all media carefully removed from roots without damaging primary or lateral roots and plants were placed in dry,

empty pots in upright position mimicking natural conditions, and returned to optimal growing conditions, as stated above, for 0, 2, 4, 8, or 24 hr of drought treatment. All leaf blade tissue above the 4th collar was harvested at the specified time after initiation of stress treatment, immediately frozen in liquid nitrogen and stored in the -80°C freezer for further analysis.

qPCR gene expression analysis of endogenous ZmGRXS17

Total RNA was isolated from leaf tissue using RNeasy Mini Kit (QIAGEN®) according to manufacturer's instructions. 1.0 µg RNA was used for cDNA synthesis using RevertAid cDNA synthesis kit (Thermo Scientific™). Each 20uL qRT-PCR reaction consisted of 9.4 µL diluted cDNA solution (2ng/µL), 0.3 µL of each primer (20µM), and 10 µL iQ SYBR Green Supermix (Bio-Rad). Primers, 5'-CCTGAGTCTGCAACTGAGAAG-3' and 5'-CATCACTGGGCTGGAGTTAAT-3', were designed against the maize B73 reference for *ZmGRXS17,* and primers, 5'-CCGTCATCGCCTCACGAAGAG-3' and 5'-AGAGCCTGCCTTACGGAATTGG-3', which are based on the cyclin-dependent kinase gene CDK, were used as an expression control.

Cloning AtGRXS17 for ectopic expression in Zea mays

AtGRXS17 driven by the maize ubiquitin-1 promotor was amplified by PCR from an existing construct. CACC was added to the 5' end of the cassette using forward primer, 5'-CACCTGCAGTGCAGCGTG-3', for compatibility with the gateway cloning system. Reverse primer, 5'- AATTCCCGATCTAGTAACATAGATGACACCG-3', complementary to the nopaline synthase (nos-T) terminator was used. The blunt end PCR product was directionally cloned into pENTR™/D-TOPO® vector for entry into the gateway system. Plasmids were transformed into competent *E. coli* cells via the freeze/thaw method, screened by PCR to confirm successful integration of the expression cassette, and a representative clone was sequenced. The

plasmid ptfGRX.gw1 was created by transferring the sequenced cassette to ptf101.gw1 via gateway cloning. Integration was confirmed by PCR after transferring to *E. coli*. Plasmids were transformed into *Agrobacterium tumefaciens* EHA101 and confirmed by PCR and restriction digestion analysis with *Eco*R1 and *Eco*R1+*Bam*H1.

DNA isolation and Southern blot analysis

Maize gDNA was isolated from leaf tissue of transgenic and wild type plants using 2% cetyl trimethylammonium bromide (CTAB) and phenol:cholroform:isoamyl alcohol (25:24:1). 50 µg gDNA was digested to completion overnight with *Hind*III and separated on a 0.7% agarose gel by overnight electrophoresis. The gDNA was blotted onto a positively charged Zeta-Probe GT nylon membrane using the alkali transfer method. All remaining Southern blot steps were carried out according to manufacturer's instructions for the AlkPhos Direct Labeling and Detection System (CDP-Star GE Healthcare Life Sciences). The probe for the BAR gene was generated by PCR from the ptf101.gw1 vector used for transformation using 5'-ATGAGCCCAGAACGACGCCC-3' and 5'-TCAGATCTCGGTGACGGGCAGG-3'. The membrane was prehybridized, hybridized overnight at 60°C, and washed at 65°C. Detection was carried out using CDP-Star with different exposure times to X-ray autoradiography film. All events tested were confirmed to have at least one stable integration of the transgene. Wild-type B104 was used as negative control, and the linearized ptfGRX.gw1 was used as a positive control.

RNA isolation, RT-PCR, and qPCR Analysis of AtGRXS17 in Zea mays

Total RNA was isolated from leaf tissue of transgenic and wild type maize plants using the RNeasy Mini Kit (QIAGEN®). 1µg total RNA was used to synthesize first strand cDNA using Revert Aid First Strand cDNA Synthesis kit. 2µL of cDNA was used as template for PCR.

Primers were complementary to the transgene, *AtGRXS17*. qRT-PCR was carried out according to previous reports using 5'-CACGAGAGCGGTGAACTAAA-3' and 5'-CCAGCTTCATCCTGACTTTCT-3' to produce an 80bp amplicon using *CDK* as internal control.

Greenhouse experiment 1

Transgenic and wild type plants were grown in 3 gallon pots filled with equal volumes of Metro-Mix 900 soilless growth media and were watered as needed with constant liquid feed on a pot by pot basis. During vegetative growth, V1-VT, plants were grown at optimal temperatures (28ºC /22ºC) and under supplemental lighting systems. Before pollinations were carried out, the thermostat was set to a target temperature of 37°C to initiate heat stress. Plants were manually self-pollinated for three days starting on the first day of silking. Twenty-four hours after the last pollination, the thermostat was reset to optimal conditions.

Summer 2017 field trial

Transgenic and wild type plants were grown in a split plot design with four replications at the Agronomy Research Station in Manhattan, KS. One row per genotype was grown for each replication. Seeds were planted May 15, 2017 at a spacing of 10 in. and a row width of 24 in. Approximately two months after sowing (at VT), heat tents with a thermostat controlled passive vent were placed over plots designated for heat treatment. The thermostat was set to 37°C, opening the vent at this temperature and staying closed below, to increase the temperature compared to ambient conditions. The heat tents remained in place through physiological maturity until harvest.

Greenhouse experiment 2

Greenhouse Experiment 2 consisted of two single copy insertion transgenic lines and wild type plants grown in one gallon pots filled with equal volumes of Metro-Mix 900 soilless growth media and were watered as needed with liquid feed on a pot by pot basis. During vegetative growth and tasseling, V1-VT, plants were grown at optimal temperatures of 28ºC /22ºC. Plants were randomly assigned to several treatments. Six plants per genotype (n=6) were designated as control and were pollinated. Six plants per genotype (n=6) were designated as heat and were moved to an adjacent greenhouse exactly 24 hours after pollination under the same environmental conditions, except, the thermostat was set to 37 ℃. In addition to these treatments, twenty-seven plants per genotype had cob tissues collected at different time points for gene expression analysis.

Pollen viability and vigor analysis

Pollen stressed for 0, 2, and 3 days at 37°C was collected from plants of each genotype and incubated on a 12% sucrose, .03% calcium chloride, .01% boric acid media solidified with .7% W/V bacto agar at 25°C, 30°C, 35°C, or 40°C for two hours and then moved to 4°C to arrest development. In the *in vitro* study, germination was scored as a pollen grain with a pollen tube as long as the grain radius. Vigor was analyzed by measuring the length of the pollen tube divided by the diameter of the pollen grain to account for differences in distance from the objective.

qPCR of ovules

Ovules collected from greenhouse experiment 2 were used for qRT-PCR analysis. RNA isolation, cDNA synthesis, and qRT-PCR was carried out as described above. HSFs, ABA-responsive elements, HSPs, sugar metabolism, receptor kinases, and cell cycle phase gene expression was analyzed.

Grain quality parameters

Nutritional composition for Ca^{2+}, Mg^{2+}, K^{+}, Cu^{+}, Fe^{3+}, Mn^{2+}, Zn^{+}, and SO_4^{2-} was determined by nitric-perchloric acid digestion and analyzed by inductively coupled plasma spectrometry. Total carbon was measured by LECO CN 2000 combustion and reported on a weight percentage.

RESULTS

ZmGRXS17 is upregulated by abiotic stress treatments

The expression profile of the endogenous maize glutaredoxin, *ZmGRXS17*, was measured in response to heat and drought stress. *ZmGRXS17* transcripts quickly accumulate in response to high temperature stress and reach 4.7 times the initial levels at 2 hours (Figure 1). This transcript level was the maximum value detected in the experiment, and *ZmGRXS17* expression decreased to 3.0 times initial levels by 4 hours. The expression level did not change at 8 or 24 hours. *ZmGRXS17* expression increased during drought stress, and transcript levels doubled from initial values by 2 hours. This expression level remained constant until reaching a maximum of two and a half times the expression of the nonstressed plants at 24 hours. The effect of drought stress on *ZmGRXS17* expression was less than heat stress during the 24-hour time period analyzed. Heat stress initiated a faster accumulation of *ZmGRXS17* than drought stress, peak at 2 hours compared to 24 hours for drought, and higher maximum accumulation, 4.7-times compared to 2.5-times for drought.

ZmGRXS17 is highly conserved

ZmGRXS17 was cloned from B104 using primers based on the B73 reference. Nucleotide sequence alignment revealed high similarity between B104 and B73. Four nucleotides differed between these cultivars resulting in a 64.2% and 64.3% sequence identity between B73 and *Arabidopsis*, and B104 and *Arabidopsis*, respectively. The nucleotide substitutions were silent mutations and encoded the same amino acid sequence. Amino acid sequence alignment revealed a highly conserved relationship between maize and *Arabidopsis* (Figure 2). Exact matches between amino acids comprised 65.9% of the identities, amino acid substitutions with similar hydrophobicity accounted for 15.2%, and substitutions not of opposite polarity accounted for

7.2% totaling, 88.3%. All three CGFS active sites, unique to class II glutaredoxins, are present in the maize homolog.

Generation of AtGRXS17-expressing maize

The inbred line, *Zea mays* L. cv. B104, was transformed via *Agrobacterium*-mediated plant transformation. *AtGRXS17* driven by the maize ubiquitin-1 promoter (Ubi-1) and terminated by the *Agrobacterium* nopaline synthase terminator was transferred to the Gateway destination vector ptf101.gw1. Integration was confirmed by restriction digestion analysis, PCR, and sequencing. Integration and expression of *AtGRXS17* was measured by semi-quantitative RT-PCR, quantitative RT-PCR (qRT-PCR), and Southern blot hybridization. RT-PCR was carried out by amplifying the *AtGRXS17* cDNA using primers, extending the entire 1500bp coding region of *AtGRXS17* from the start to the stop codon. The correct band size was observed in all transgenic samples and plasmid positive control but not in the wild type negative control (Figure 3A). Southern blot hybridization determined two, one, multiple, and one stable integration of T-DNA into the genome for *AtGRXS17*-expressing lines *-4*, *-5*, *-6*, *-10*, respectively (Figure 3C). qRT-PCR analysis revealed *AtGRXS17-5* displayed the highest expression, followed by *AtGRXS17-6*, and *AtGRXS17-10* (Figure 3B). Morphological traits of *AtGRXS17*-expressing maize were observed in greenhouse grown plants. The phenotype of transgenic plants was morphologically indistinguishable from wild type plants, displaying no differences at any vegetative growth stages, V1 to VT (Figure 4A, C), or tasseling, flowering, and kernel set and fill, VT-R6 (Figure 4B, D).

AtGRXS17-expression increases thermotolerance in maize

Under optimal temperatures (28ºC/22ºC), *AtGRXS17*-expressing lines *-4*, *-5*, *-6*, and *-10*, and wild-type B104 plants display no difference in kernel set and development (Figure 4D). A heat

stress (37ºC/32ºC) period of ten days was initiated one day before pollinations began, and silks were manually self-pollinated daily until pollen shedding was complete. Despite greenhouse cooling efforts at 37ºC, maximum daily temperatures exceeded 40ºC during the first five days of treatment and average daily temperatures exceeded 35ºC. Nevertheless, heat stress had much less impact on the kernel set of *AtGRXS17*-expressing maize plants than wild-type corn plants (Supplemental Figure 2). Kernel set in the heat stress treatment for *AtGRXS17-4*, *-5*, *-6*, *-10*, and wild type was 123.8, 111.8, 126.2, 111.3, and 30.5 kernels/plant, respectively. Consistent with all plants grown at control conditions, kernel set between *AtGRXS17*-expressing plants and wild type did not differ.

AtGRXS17-expressing Corn Plants Have Increased Kernel Set in the Field

AtGRXS17-expressing events *-5*, *-6*, and *-10* were grown in the field and compared to wild type plants. Each event performed better than wild type plants under heat tent treatments, and *AtGRXS17-5* and *AtGRXS17-10* performed better than wild type under ambient conditions (Figure 5A). On average, heat tents had a maximum daily temperature 3.58°C higher and average daily temperature 1.95°C higher than ambient conditions (Supplemental Figure 1). *AtGRXS17*-expressing plants yielded 6-fold more grain than wild type, as measured by total grain weight per plant (Figure 5B). Ambient conditions, which routinely exceeded 35°C during pollination, also produced differences in total grain yield between both line *-5* and *-10*, and wild-type. There were no differences between thousand kernel weight (TKW) or ears per plant between genotypes or treatments (data not shown). However, kernel set per plant, in heat tents, was higher than wild type in all transgenic events (Figure 6). Kernel number per plant was highly correlated (R2=.979) with total grain yield across all treatments and genotypes.

AtGRXS17-expressing Corn Produces pollen that is less sensitive to heat challenge

Pollen germinated under control (Day 0, 25°C) conditions (88%) and produced pollen tubes more than four times as long (4.06) as the grain diameter. Pollen was severely affected by the 37°C temperature stress in the greenhouse as measured by both germination rate and pollen tube length. Both pollen parameters were also negatively impacted when directly exposed to high temperature incubation treatments. Pollen collected from *AtGRXS17*-expressing plants displayed no differences in morphology, tube length, or grain diameter compared to wild type pollen under normal growth conditions compared (Figure 7A). No difference in germination rate between any genotypes were observed when 0 Day pollen (non-stressed) was incubated at 25°C, 30°C, 35°C, or 40°C for germination (Figure 7A). However, differences between genotypes appeared when pollen is collected from plants stressed for 2 Days. While there are no differences between genotypes at 25°C, wild type pollen is more sensitive to all other incubation temperatures and germinated less than pollen collected from *AtGRXS17*-expressing plants (Figure 7B). Differences become more pronounced after 3 days, where wild type pollen is nearly unable to germinate (Figure 7C). Despite the clear difference in germination rate, pollen tube length did not differ between genotypes.

AtGRXS17-expressing plants have less kernel abortion than wild-type

AtGRXS17-expressing and wild type plants were subjected to 37°C 24 hours after pollination. *AtGRXS17*-expressing corn plants displayed significantly higher kernel set than wild type plants due to this treatment and displayed no differences in kernel set control conditions (Figure 10). Wild type plants experienced an 81% reduction in kernel set, compared to a 38% and 42% reduction in lines 5 and 10, respectively. Wild type produced an average of nearly 61 kernels per plant compared to 233 and 188 for lines -*5*, and -*10*.

Heat stress affects stress responsive genes in maize ovules

The effect of heat stress and *ZmGRXS17*-expression on the expression of several heat responsive and ovule developmental genes was measured. Heat treatments induced changes in expression of most genes measured in ovules at one hour at 37°C, but no differences in expression due to *AtGRXS17*-expression were measured. Heat shock factors *ZmHSF3* and *ZmHSF4* were strongly upregulated 19.2-fold and 13.2-fold increases at 1 hr and returned near baseline to 3.2-fold and 1.9-fold at 24 hr, respectively (Figure 11A, B). Heat shock proteins experienced greater increases. *ZmHSP26, ZmHSP70,* and *ZmHSP90* increased 7.9-fold, 57.8-fold, and 195.8-fold at 1 hr and maintained 3.2-fold, 4.9-fold, and 15-fold higher expression at 24 hr, respectively (Figure 11C, D, E). Expression of the regulatory starch biosynthesis gene, *ADP-glucose pyrophosphorylase* (*AGPase*), was significantly reduced under heat stress, decreasing 29.7% at 1 hr and 27.0% at 24 hours. The expression of plasma membrane localized receptor proteins *DEFECTIVE KERNEL 1* (*DEK1*) was unaffected by stress, while *CRINKLY 4* (*CR4*) decreased 34.4% due to heat stress.

DISCUSSION

In tomato, *AtGRXS17* confers thermotolerance during vegetative developmental stages and was recently shown to mitigate heat induced pollen damage (Wu et al., 2015; Müller et al., 2016). The loss of function mutants (*atgrxs17*) of *Arabidopsis* are sensitive to heat stress and display an abnormal shoot apical meristem (SAM), floral development, ROS accumulation, and defective cell cycle control through altered polar auxin perception (Cheng et al., 2011). Flowers and roots were most affected by heat stress as *AtGRXS17* expression in wild type *Arabidopsis* was reported to be highest in those organs. The *Arabidopsis* mutant phenotype was demonstrated to be temperature dependent by demonstrating that *atgrxs17* plants were unable to transition to reproductive development when grown under long days and elevated temperatures but quickly produced flowers and seeds when moved to optimal temperatures. Agreeing with Cheng et al., the SAM and transition to reproductive development was found to be severely altered in *atgrxs17* mutants under elevated temperatures (Knuesting et al., 2015). Additionally, several potential AtGRXS17-interacting proteins were identified, including Sucrose synthase1 (SUS1) and Brassinosteroid-signaling kinase2 (BSK2).

In *Arabidopsis*, *GRXS15* mutants (*grxs15*) produced fewer seeds due to embryo abortion shortly after fertilization (Moseler et al., 2015). In contrast to the two *atgrxs17* studies above, this phenotype was due to ISC binding. Despite AtGRXS15 lacking oxidoreductase activity, ISC binding is mediated by redox status because the ability of GRXS15 to bind ISCs is GSH dependent. The yeast orthologs of GRXS17, GRX3 and GRX4, are able and necessary, to bind and deliver ISC to target proteins in the cytosol and nucleus in a GSH dependent manner (Mühlenhoff et al., 2010). Further, they are vital for iron-sensing processes and regulate transcription factors necessary for iron status sensing (Pujol-Carrion et al., 2006). The role of

AtGRXS17 in iron status has also been studied in *Arabidopsis*. AtGRXS17 interacts with cytosolic iron assembly (CIA) processes and, as a result of a complete loss of function of AtGRXS17 in *atgrxs17* mutants, DNA damage responsive genes are highly upregulated (Iñigo et al., 2016). The *atgrxs17* plants are more sensitive to iron deficient medium as measured due to increased ROS production, suggesting iron homeostasis-mediated redox status is affected (Yu et al., 2017).

Despite the well-studied effect of GRXs on redox status, iron homeostasis, and the resulting abiotic stress tolerance in dicots, monocot crops have not been as extensively studied. In maize, mutants for aa CC-type glutaredoxin gene *MALE STERILE CONVERTED ANTHER 1 (msca1)*, germ cells are more sensitive to ROS accumulation, and germ cell development is negatively impacted (Chaubal et al., 2003). Miss-expression of this gene through a mutation termed *Aberrant phyllotaxy2* (Abph2), caused enlarged shoot meristems and a distorted phyllotaxy, leading to further suggestions that GRXs play a role in auxin metabolism (Yang et al., 2015).

Our results indicated that CGFS-type GRXs are responsive to abiotic stress in maize. Within two hours, *ZmGRXS17* expression increased nearly five-fold in response to elevated temperatures. Maize pollen germination is sensitive to elevated temperatures (Schoper et al., 1985). The inbred line B104 provided an ideal background to study the effect of *AtGRXS17* expression on thermotolerance of reproductive processes because it was found to be sensitive to pollen moisture content induced viability reduction (Fonseca and Westgate, 2005). The pollen moisture content necessary to decrease viability to 50% germination was 53.6%, which was the highest moisture content to result in a 50% reduction in viability of all 11 genotypes measured. B104 pollen viability was severely affected by 37ºC greenhouse temperatures. Pollen tube length did not differ between genotypes, but germination rates of *AtGRXS17*-expressing plant pollen was 2

to 3 times higher than wild type, 48 and 72 hours after initiation of the 37ºC greenhouse treatment, depending on incubation temperature and transgenic event. The differences continued over time, and pollen collected from wild type plants stressed for three days was nearly unable to germinate. Less than 5% of wild type pollen germinated after 3 days of heat stress, while transgenic pollen maintained near 20% germination rates.

Pollen viability is an important component in understanding maize yield, but because heat stress does not affect the anthesis silk interval, the effect of heat stress on reduced kernel set must be due to reduced pollen viability or kernel abortion (Lizaso et al., 2018). Heat treatments applied for 15 days leading up to silking resulted in a 52% reduction in kernel set, compared to a 75% reduction in kernel set when heat treatments were initiated at silking for 15 days, suggesting kernel abortion may be more sensitive to heat stress than pollen (Rattalino Edreira and Otegui, 2013). Our results indicated that heat stress initiated after pollination can reduce kernel set by up to 81%. Chosen for their consistent heat tolerant phenotype and single copy T-DNA insertions, *AtGRXS17* expressing lines *-5* and *-10* were less affected by this stress than wild type, experiencing 38% and 42% reductions, respectively.

Heat tolerant *AtGRXS17* expressing tomato plants were found to have increased expression of several *HSFs* and *HSPs* (Wu et al., 2012). In maize, 25 distinct *HSFs* have been identified, and tissue localization of the expression of each gene were reported (Yong-Xiang et al., 2011). *Hsf04* was reported to be expressed in husks and seeds, and *Hsf*03 was reported as expressed only in seeds. However, both of these *HSFs* were found to increase several thousand fold in leaf tissue. This drastic increase may be due to the low expression in leaf tissue under normal growth conditions, which may also explain why they were not listed as detected in leaf tissue. Regardless, our results indicated that *Hsf03* and *Hsf04* are expressed in ovules and are

upregulated 16.8-fold and 14.7-fold at one hour of stress. HSFs are post translationally activated so their expression level might not be an accurate indicator of their activity on *HSP* expression. Nevertheless, in our study their increased transcription clearly was an indication of *HSP* expression. Our results indicated that *Hsp90* increased the most followed by *Hsp70* and *Hsp26*. *Hsp90* expression increased 195.8-fold, *Hsp70* increased 57.8-fold, and the *sHSP*, *Hsp26*, expression increased 7.9-fold at 1 hour, but none differed between genotypes. HSPs contribute to cellular membrane stability and are drastically upregulated in response to stress but often do not differ in expression levels between tolerant and susceptible genotypes (Frova and Gorla, 1993). For example, when flint and dent type corn with contrasting heat tolerances were mapped for responsible quantitative trait loci, only six candidate genes were proposed based on the QTL, and none were HSPs (Frey et al., 2016). When maize inbred lines were analyzed, *Hsp90*, *Hsp26*, and *Hsp70* were all expressed in leaf tissue, regardless of heat tolerance (Frey et al., 2015). Although the *sHSP*, *Hsp17*, was detected in a segregating population of maize plants with differing cell membrane stability, the effect of this loci was not significant, again suggesting HSPs, including sHSPs, may not be critical for the difference between a tolerant or susceptible heat response in maize (Ottaviano et al., 1991).

In response to drought stress, starch biosynthesis genes were downregulated, and starch degradation pathways were activated in maize ovaries (Kakumanu et al., 2012). Our results indicated that a large subunit of the regulatory ADP-glucose pyrophosphorylase (AGPase) starch biosynthesis gene, *AGPLLZM* (formerly *AGPL1)* was downregulated due to heat stress. *AGPLLZM* expression decreased 29.7% at 1 hr and 27.0% at 24 hours. No differences between genotypes were detected within any time point. However, after 1 hr, wild type ovules *AGPLLZM* expression declined 42% ($p \leq .01$), *AtGRXS17-5* declined 19% (ns), and *AtGRXS17-10* declined

23% (ns), indicating that *AtGRXS17*-expressing plants ovules starch metabolism is less affected than wild type in response to elevated temperatures. It was previously reported that starch content was significantly decreased in *AGPLLZM* homozygous mutants, *agpllzm*, and in wild type plants *AGPLLZM* was upregulated 6.78-fold due to glucose treatment (Huang et al., 2014, Huang et al., 2011). Therefore, a larger decrease in *AGPLLZM* may indicate less soluble sugars are available within the kernel for starch biosynthesis. This is consistent with early reports where maize cobs cultured in vitro were exposed to temperatures, 30ºC and 35ºC, and 35ºC induced kernel abortion due to less starch biosynthesis (Hanft and Jones, 1986). That study provided additional evidence that this may be due to the inhibition of unloading of sucrose from the pedicel to the endosperm. Surprisingly, overexpression of *sh2*, which codes for another large subunit AGPase, results in higher kernel set (Hannah et al., 2012). The primary findings from that study were that by increasing starch synthesis at early stages of seed development, sink strength was increased, somehow avoiding abortion cell fate. The second finding was that this was a maternally relevant molecular reaction. That is, when transgenic *sh2* expressing plants were used as pollen donors for wild type silks, the increased kernel set was not observed. AGPase plays a pivotal role in photoperiod dependent starch metabolism and can be induced by trehalose, glucose, and sucrose (Fritzius et al., 2001, Mugford et al., 2014, Sokolov et al., 1998). Overexpression of a cytosolic invertase, an enzyme that hydrolysis sucrose to glucose and fructose, in *Arabidopsis* resulted in delayed flowering and reduced branching (Heyer et al., 2004). Curiously, these phenotypes are similar to the previously characterized *atgrxs17* loss of function mutant (Cheng et al., 2011, Knuesting et al., 2015). Consistent with the theoretical interaction of AtGRXS17 and SUS1, as proposed by Knuesting et al., *AtGRXS17*-expressing rice plants display altered sugar accumulation (see Chapter 2). In addition to the hypothesis that

AtGRXS17 affects sugar metabolism through sucrose synthase (SUS) interactions, AGPase activity is activated through reduction of disulfide bonds by thioredoxins (TRXs), the family of oxidoreductases which GRXs belong, and monothiol mechanisms (Ballicora, 1999). Perception of long days and the transition of the SAM to floral development are a result of transcription factors such as FLOWERING LOCUS T (FT) and sucrose accumulation in SAMs, which is dependent upon adequate sucrose biosynthesis (Moghaddam and Van den Ende, 2013). Taken together, one model suggests that *AtGRXS17* expression may influence sugar metabolism, creating stronger sink potential in developing ovules.

Two membrane proteins CRINKLY 4 (CR4), a receptor-like kinase, and DEFECTIVE KERNEL (DEK1), a calpain-like proteinase, co-localize together and have been shown to be critical for normal kernel development in maize (Tian et al., 2007, Doll et al., 2017). Receptor-like kinases (RLK) control SAM size and loss of function *Arabidopsis* mutants for *clv1* have altered SAM cell size, abnormal phyllotaxy, and abnormal gynoecium development (Clark et al., 1993, Clark et al., 1997). Maize *cr4* mutants display larger cells in the SAM and altered endosperm formation (Becraft et al., 1996, Jin et al., 2000). *Dek1* expression levels were unchanged due to heat stress but *Cr4* was significantly affected. Wild type transcript levels decreased 42% ($p \leq .01$) while *AtGRXS17-5* decreased 30% (ns) and *AtGRXS17-10* decreased 29% (ns). RLKs have recently been shown to be activated due to glutathionylation by GRXs (Bender et al., 2015). This suggests that the overexpression of *AtGRXS17* may be able to maintain higher activity of these enzymes through glutathionylation. Brassinosteroid (BR) signaling kinase 2 (BSK2) was also identified as a potential partner of AtGRXS17 (Knuesting et al., 2015). BR accumulation and signaling has important implications for source sink relationships and overexpression of BR biosynthesis genes in rice results in increased transcription of *SUS* and *UDP-glucose*

pyrophosphorylase (*UGPase*), leading to increased grain filling rate (Wu et al., 2008). *UGPase* activity in rice is critical for callose deposition and subsequent temperature dependent viable pollen development (Chen et al., 2007). *AtGRXS17*-expressing rice plants accumulate more uridine diphosphate-glucose (UDP-glucose) than wild type plants (see Chapter 2). It was later determined that overexpression of either a biosynthesis gene or downstream signaling factor could increase starch content in pollen and seeds through the upregulation of the *Carbon Starved Anther* (*CSA*) gene (Zhu et al., 2015). In rice, *csa* mutants are male sterile under long days due to less starch accumulation (Zhang et al., 2013). Reverse UGPase activity results in the catabolism of UDP-glucose, produced by SUS, and is coupled to ADP-glucose production an important metabolite for AGPase dependent starch biosynthesis (Kleczkowski, et al., 2004). Interestingly, the increase in AGPase activity and starch biosynthesis, is mediated by light and sucrose application, reducing the disulfide bond that forms the inactive dimer, resulting in two active AGPase monomers (Hendriks et al., 2003). Taken together, this suggests that AtGRXS17 may influence redox dependent sugar metabolism and starch accumulation in sink tissues.

AtGRXS17-expressing plants are more heat tolerant than wild type plants and display higher kernel set when challenged with elevated temperatures around flowering. In our study we determined that *AtGRXS17*-expressing plants produced thermotolerant pollen and ovules resulting in increased yield compared to wild type plants when grown at above optimal temperatures. *AtGRXS17*-expressing plants accumulate similar levels of *HSFs*, *HSPs*, but transcription of starch synthesis genes and receptor like kinases are less affected by stress than wild type. Here we present evidence for the hypothesis that AtGRXS17 affects sugar signaling pathways in a redox dependent manner in sink tissues increasing thermotolerance.

REFERENCES

Apel, K., and Hirt, H. (2004) Reactive Oxygen Species: Metabolism, Oxidative Stress, and Signal Transduction. *Annual Review of Plant Biology* 55:1 373-399.

Ballicora, M.A., Frueauf, J.B., Fu, Y., Schürmann, P., Preiss, J. (1999) Activation of the Potato Tuber ADP-glucose Pyrophosphorylase by Thioredoxin. *The Journal of Biological Chemistry* 275: 1315-1320.

Baxter, A., Ron, M., Suzuki, N. (2014) ROS as key players in plant stress signaling. *Journal of Experimental Botany* 65: 1229–1240.

Becraft, P.W., Stinard, P.S., McCarty, D.R. (1996) CRINKLY4: A TNFR-Like Receptor Kinase Involved in Maize Epidermal Differentiation. *Science* 273: 1406-1409.

Chaubal R., Anderson, J.R., Trimnell, M.R., Fox, T.W., Albertsen, M.C., Bedinger, P. (2003) The transformation of anthers in the msca1 mutant of maize. *Planta* 216: 778-788.

Bender, K.W., Wang, X., Cheng, G.B., Kim, H.S., Zielinski, R.E., Huber, S.C. (2015) Glutaredoxin AtGRXC2 catalyses inhibitory glutathionylation of Arabidopsis BRI1-associated receptor-like kinase 1 (BAK1) in vitro. *Biochemical Journal* 467 (3): 399-413.

Chen, R., Zhao, X., Shao, Z., Wei, Z., Wang, Y., Zhu, L., et al. (2007) Rice UDP-Glucose Pyrophosphorylase1 Is Essential for Pollen Callose Deposition and Its Cosuppression Results in a New Type of Thermosensitive Genic Male Sterility. *The Plant Cell* 19(3): 847–861.

Cheng N.H., J.Z. Liu, X. Liu, Q. Wu, S.M. Thompson, J. Lin, J. Chang, S.A. Whitham, S. Park, J.D. Cohen, K.D. Hirschi. (2011) Arabidopsis monothiol glutaredoxin, AtGRXS17, is critical for temperature-dependent postembryonic growth and development via modulating auxin response. *Journal of Biological Chemistry*. 286: 20398-20406.

Cicchino, M., Edreira, J.I.R., Uribelarrea, M., and Otegui, M.E. (2010) Heat Stress in Field-Grown Maize: Response of Physiological Determinants of Grain Yield All rights reserved. *Crop Science* 50:1438-1448.

Crafts-Brandner, S. J., and Salvucci, M. E. (2002). Sensitivity of Photosynthesis in a C4 Plant, Maize, to Heat Stress. *Plant Physiology* 129(4): 1773–1780.

Easterling, D.R., Meehl, G.A., Parmesan, C., Changnon, S.A., Karl, T.R., Mearns, L.O. (2000) Climate Extremes: Observations, Modeling, and Impacts. *Science* 289: 2068-2074.

Doll, N.M., Depège-Fargeix, N., Rogowsky, P.M., Widiez, T. (2017) Signaling in Early Maize Kernel Development. *Molecular Plant* 10: 375-388.

Fonseca A.E., Mark E. Westgate. (2005) Relationship between desiccation and viability of maize pollen. *Field Crops Research* 94: 114-125.

Frank, G., Pressman, E., Ophir, R., Althan, L., Shaked, R., Freedman, M., et al. (2009) Transcriptional profiling of maturing tomato (Solanum lycopersicum L.) microspores reveals the involvement of heat shock proteins, ROS scavengers, hormones, and sugars in the heat stress response. *Journal of Experimental Botany* 60(13):3891-908.

Frey F.P., Urbany, C., Hüttel, B., Reinhardt, R., Stich, B. (2015) Genome-wide expression profiling and phenotypic evaluation of European maize inbreds at seedling stage in response to heat stress. *BMC Genomics* 16:123.

Frey, F.P., Presterl, T., Lecoq, P. et al. (2016) First steps to understand heat tolerance of temperate maize at adult stage: identification of QTL across multiple environments with connected segregating populations. *Theoretical and Applied Genetics* 129: 945.

Frova, C., Gorla, M.S. (1993) Quantitative expression of maize HSPs: genetic dissection and association with thermotolerance. *Theoretical and Applied Genetics* 86: 213-220.

Fritzius, T., Aeschbacher, R., Wiemken, A., Wingler, A. (2001) Induction of ApL3 expression by trehalose complements the starch-deficient Arabidopsis mutant adg2-1 lacking ApL1, the large subunit of ADP-glucose pyrophosphorylase. *Plant Physiology* 126(2):883-9.

Hannah, L.C., Futch, B., Bing, J., Shaw, J.R., Boehlein, S., Stewart, J.D., et al. (2012) A shrunken-2 Transgene Increases Maize Yield by Acting in Maternal Tissues to Increase the Frequency of Seed Development. *The Plant Cell* 24(6): 2352-2363.

Hatfield J.L., Prueger, J.H. (2015) Temperature extremes: Effect on plant growth and development. *Weather and Climate Extremes* 10: 4-10.

Hatfield, J.L. (2016) Increased Temperatures Have Dramatic Effects on Growth and Grain Yield of Three Maize Hybrids. *Agricultural & Environmental Letters* 1:150006.

Hendriks, J.H.I., Kolbe, A., Gibon, Y., Stitt M, Geigenberger, P. (2003) ADP-glucose pyrophosphorylase is activated by posttranslational redox-modification in response to light and to sugars in leaves of Arabidopsis and other plant species. *Plant Physiology* 133(2):838-49.

Heyer, A.G., Raap, M., Schroeer, B., Marty, B., Willmitzer, L. (2004) Cell wall invertase expression at the apical meristem alters floral, architectural, and reproductive traits in Arabidopsis thaliana. *The Plant Journal* 39: 161-169.

Hu, Y., Wu, Q., Sprague, S.A., Park, J., Oh, M., Rajashekar, C.B., Koiwa, H., Nakata, P.A., Cheng, N.H., Hirschi, K.D., White, F.F., Park, S. (2015) Tomato expressing Arabidopsis glutaredoxin gene AtGRXS17 confers tolerance to chilling stress via modulating cold responsive components. *Horticulture Research*. 2: 15051.

Clark, S.E., Running, M.P., Meyerowitz, E.M. (1993) CLAVATA1, a regulator of meristem and flower development in Arabidopsis. *Development* 119: 397-418.

Clark, S.E., Williams, R.W., Meyerowitz, E.M. (1997) The CLAVATA1Gene Encodes a Putative Receptor Kinase That Controls Shoot and Floral Meristem Size in Arabidopsis. *Cell* 89: 575-585.

Hanft, J.M., Jones, R.J. (1986) Kernel Abortion in Maize. *Plant Physiology* 81(2): 503-510.

Huang, B., Chen, J., Zhang, J. et al. (2011) Characterization of ADP-Glucose Pyrophosphorylase Encoding Genes in Source and Sink Organs of Maize. *Plant Molecular Biology Reporter* 29: 563.

Huang, B., Hennen-Bierwagen, T.A., Myers, A.M. (2014). Functions of Multiple Genes Encoding ADP-Glucose Pyrophosphorylase Subunits in Maize Endosperm, Embryo, and Leaf. *Plant Physiology* 164(2): 596–611.

Iñigo, S., Durand, A.N., Ritter, A., Le Gall, S., Termathe, M., Klassen, R., et al. (2016) Glutaredoxin GRXS17 associates with the cytosolic iron-Sulfur cluster assembly pathway. *Plant Physiology* 172: 858-873.

Jin, P., Guo, T., Becraft, P.W. (2000) The maize CR4 receptor-like kinase mediates a growth factor-like differentiation response. *Genesis* 27: 104-116.

Kakumanu, A., Ambavaram, M.M.R., Klumas, C., Krishnan, A., Batlang, U., Myers, E., Grene, R., Pereira, A. (2012) Effects of drought on gene expression in maize reproductive and leaf meristem tissue revealed by RNA-Seq. *Plant Physiology* 160: 846-867.

Kleczkowski, L.A., Geisler, M., Ciereszko, I., Johansson, H. (2004) UDP-Glucose Pyrophosphorylase. An Old Protein with New Tricks. *Plant Physiology* 134(3): 912–918.

Knuesting, J., Riondet, C., Maria, C., Kruse, I., Becuwe, N., Konig, N., Berndt, C., Tourrette, S., Guilleminot-Montoya, J., Herrero, E., Gaymard, F., Balk, J., Belli, G., Scheibe, R., Reichheld, J.P., Rouhier, N., Rey, P. (2015) Arabidopsis Glutaredoxin S17 and its partner the nuclear factor

Y subunit C11/Negative Cofactor 2 alpha, contribute to maintenance of the shoot apical meristem under long-day photoperiod. *Plant Physiology*. 167: 1643-U1822.

Kobayashi, M., Ohura, I., Kawakita, K., Yokota, N., Fujiwara, M., Shimamoto, K., et al. (2007). Calcium-dependent protein kinases regulate the production of reactive oxygen species by potato NADPH oxidase. *Plant Cell* 19 1065–1080.

Kotak, S., Larkindale, J., Lee, U., von Koskull-Döring, P., Vierling, E., Scharf, K.D. (2007) Complexity of the heat stress response in plants. *Current Opinion in Plant Biology*. 10: 310-316.

Lin, Y.X., Jiang, H.Y., Chu, Z.X., Tang, X.L., Zhu, S.W., Cheng, B.J. (2011) Genome-wide identification, classification and analysis of heat shock transcription factor family in maize. *BMC Genomics* 12:76.

Lizaso, J.I., Ruiz-Ramosa, M., Rodrígueza, L., Gabaldon-Lea, C., Oliveira, J.A., Lorite, I.J., Sánchez, D., García, E., Rodríguezae, A. (2018) Impact of high temperatures in maize: Phenology and yield components. *Fields Crop Research* 216: 192-140.

Lobell, D.B, Field, C.B. (2007) Global scale climate–crop yield relationships and the impacts of recent warming. *Environmental Research Letters* 2: 014002.

Melillo, J.M., Richmond, T.C., Yohe, G.W., Eds. (2014) Climate Change Impacts in the United States: The Third National Climate Assessment. *U.S. Global Change Research Program*

Mühlenhoff, U., Molik, S., Godoy, J.R., Uzarska, M.A., Richter, N., Seubert, A., et al. (2010) Cytosolic Monothiol Glutaredoxins Function in Intracellular Iron Sensing and Trafficking via Their Bound Iron-Sulfur Cluster. *Cell Metabolism* 12:137-385.

Moghaddam, M.R.B. and Van den Ende, W. (2013) Sugars, the clock and transition to flowering. *Frontiers in Plant Science* 4:22.

Moseler, A., Aller, I., Wagner, S., Nietzel, T., Przybyla-Toscano, J., Mühlenhoff, U., et al. (2015) The mitochondrial monothiol glutaredoxin S15 is essential for iron-sulfur protein maturation in Arabidopsis thaliana. *Proceedings of the National Academy of Sciences of the United States of America* 112: 13735-13740.

Mugford, S.T., Fernandez, O., Brinton, J., Flis, A., Krohn, N., Encke, B., et al. (2014) Regulatory Properties of ADP Glucose Pyrophosphorylase Are Required for Adjustment of Leaf Starch Synthesis in Different Photoperiods. *Plant Physiology* 166(4): 1733-1747.

Muller, F., Xu, J., Kristensen, L., Wolters-Arts, M., de Groot P.F.M., Jansma, S.Y., et al. (2016) High Temperature-Induced Defects in Tomato (Solanum lycopersicum) Anther and Pollen Development Are Associated with Reduced Expression of B-Class Floral Patterning Genes. *PLoS ONE* 11(12): e0167614.

Ohama, N., Hikaru, S., Shinozaki, K., Yamaguchi-Shinozaki, K. (2017) Transcriptional Regulatory Network of Plant Heat Stress Response. *Trends in Plant Science* 22: 53-65.

Ordóñez, R.A., Savin, R., Cossani, C.M., Slafer, G.A. (2015) Yield response to heat stress as affected by nitrogen availability in maize. *Field Crops Research* 183: 184-203.

Ottaviano, E., Sari Gorla, M., Pè E., Frova, C. (1991) Molecular markers (RFLPs and HSPs) for the genetic dissection of thermotolerance in maize. *Theoretical and Applied Genetics* 81: 713-719.

Piterková, J., Luhová, L., Mieslerová, B., Lebeda, A., Petřivalský, M. (2013) Nitric oxide and reactive oxygen species regulate the accumulation of heat shock proteins in tomato leaves in response to heat shock and pathogen infection. *Plant Science* 207:57-65.

Pujol-Carrion, N., Belli, G., Herrero, E., Nogues, A., Maria Angeles de la Torre-Ruiz. (2006) Glutaredoxins Grx3 and Grx4 regulate nuclear localisation of Aft1 and the oxidative stress response in Saccharomyces cerevisiae. *Journal of Cell Science* 119: 4554-4564.

Rattalino Edreira, J.I., Carpici, E.B., Sammarro, D., Otegui, M.E. (2011) Heat stress effects around flowering on kernel set of temperate and tropical maize hybrids. *Field Crops Research* 123: 62-73.

Rattalino Edreira, J.I., Otegui, M.E. (2013) Heat stress in temperate and tropical maize hybrids: A novel approach for assessing sources of kernel loss in field conditions. *Field Crops Research* 142: 58-67.

Rouhier N., Gelhaye, E., Jacquot, J.P. (2004) Plant glutaredoxins: still mysterious reducing systems. *Cellular and Molecular Life Sciences* 61:1266-1277.

Sable A., Rai, K.M, Choudhary, A., Yadav, V.K., Agarwal, S.K., Sawant, S.V. (2018) Inhibition of Heat Shock proteins HSP90 and HSP70 induce oxidative stress, suppressing cotton fiber development. *Scientific Reports* 8: 3620.

Schlenker, W., Roberts, M.J. (2009) Nonlinear temperature effects indicate severe damages to U.S. crop yields under climate change. *Proceedings for the National Academy of Sciences* 106 (37): 15594-15598.

Schoper, J.B., Lambert, R.J., Vasilas, B.L. (1985) Pollen viability, pollen shedding, and combining ability for tassel heat tolerance in maize. *Crop Science* 27: 27-31.

Sokolov L.N., Déjardin, A., Kleczkowski, L.A. (1998) Sugars and light/dark exposure trigger differential regulation of ADP-glucose pyrophosphorylase genes in Arabidopsis thaliana (thale cress). *Biochemical Journal* 336:681–687.

Stroher, E., Grassl, J., Carrie, C., Fenske, R., Whelan, J., Millar, A.H. (2016) Glutaredoxin S15 is involved in Fe-S cluster transfer in mitochondria influencing lipoic acid-dependent enzymes, plant growth, and arsenic tolerance in Arabidopsis. *Plant Physiology* 170: 1284-1299.

Tian, Q., Olsen, L., Sun, B., Lid, S. E., Brown, R. C., Lemmon, B. E., et al. (2007) Subcellular Localization and Functional Domain Studies of DEFECTIVE KERNEL1 in Maize and Arabidopsis Suggest a Model for Aleurone Cell Fate Specification Involving CRINKLY4 and SUPERNUMERARY ALEURONE LAYER1. *The Plant Cell* 19(10) 3127–3145.

Tripathi, A., Tripathi, D.K., Chauhan, D.K., Kumar, N., Singh, G.S. (2016) Paradigms of climate change impacts on some major food sources of the world: A review on current knowledge and future prospects. *Agriculture, Ecosystems & Environment* 216: 356-373.

United Nations, Department of Economic and Social Affairs, Population Division. (2017) World Population Prospects: The 2017 Revision, Key Findings and Advance Tables. ESA/P/WP/248. ESA/P/WP/248.Wu, C., Trieu, A., Radhakrishnan, P., Kwok, S.F., Harris, S., Zhang, K. (2008) Brassinosteroids Regulate Grain Filling in Rice. *The Plant Cell* 20(8): 2130-2145.

Wu, Q., Yang, J., Cheng, N.H., Hirschi, K.D., White, F.F., Park, S.H. (2017) Glutaredoxins in plant development, abiotic stress response, and iron homeostasis: From model organisms to crops. *Environmental and Experimental Botany* 139: 91-98.

Wu, Q., Hu, Y., Sprague, S.A., Kakeshpour, T., Park, J., Nakata, P.A., Cheng, N.H, Hirschi, K.D., White, F.F., Park, S.H. (2017) Expression of a monothiol glutaredoxin, AtGRXS17, in tomato (Solanum lycopersicum) enhances drought tolerance. *Biochemical and Biophysical Research Communications* 491: 1034-1039.

Yang, F., Bui, H.T., Pautler, M., Llaca, V., Johnston, R., Lee, B.-H., Kolbe, A., Sakai, H., Jackson, D. (2015) A Maize Glutaredoxin Gene, Abphyl2, Regulates Shoot Meristem Size and Phyllotaxy. *The Plant Cell* Jan 27: 121-131.

Zhang, H., Xu, C., He, Y., Zong, J., Yang, X., Si, H., Sun, Z., Hu, J., Liang, W., Zhang, D. (2013) Mutation in CSA creates a new photoperiod-sensitive genic male sterile line applicable for hybrid rice seed production. *Proceedings of the National Academy of Sciences* 110(1):76-81.

Zhao, C., Liu, B., Piao, S., Wang, X., Lobell, D.B., Huang, Y., et al. (2017) Temperature increase reduces global yields. *Proceedings of the National Academy of Sciences* 114: 9326-9331.

Zhu, X., Liang, W., Cui, X., Chen, M., Yin, C., Luo, Z., et al. (2015) Brassinosteroids promote development of rice pollen grains and seeds by triggering expression of Carbon Starved Anther, a MYB domain protein. *The Plant Journal* 82: 570-581.

FIGURES

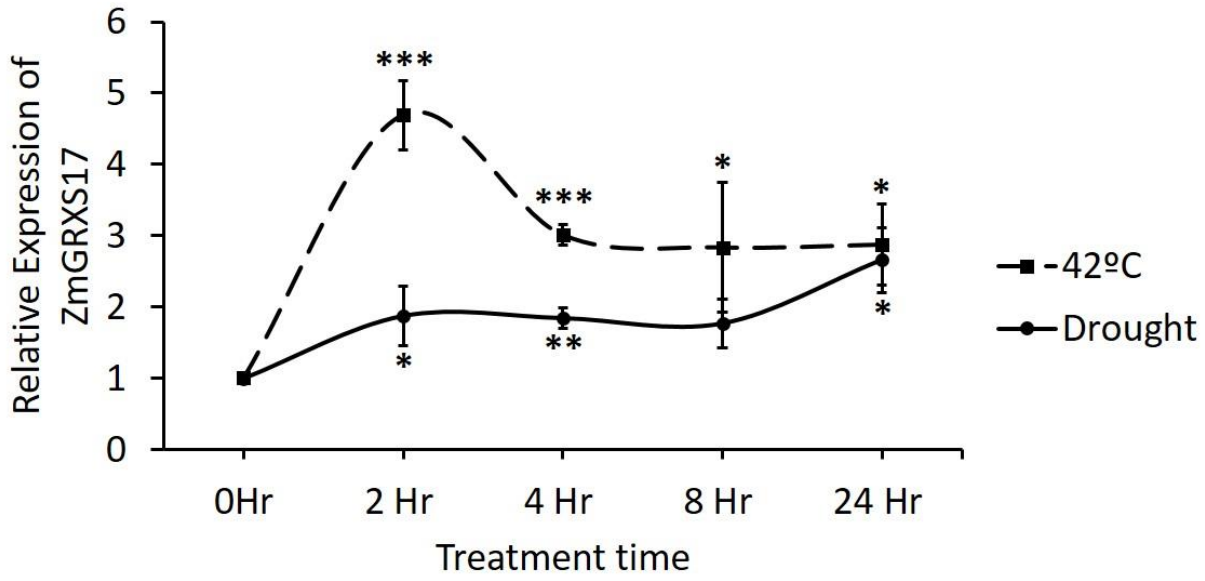

Figure 1. 1 Expression analysis by qRT-PCR of *ZmGRXS17* expression in B104 seedlings in response to heat and drought stress.

Normalized relative expression of *ZmGRXS17* in response to 42°C and drought stress over a 24-hour period in growth chamber grown V4 developmental stage wild type maize plants. Plants were collected at 0, 2, 4, 8, and 24 Hr. Data are means ± se (n=3) and were analyzed using two-way ANOVA and Student's t-test. Asterisks denote difference between corresponding time point and 0 Hr control (*P<0.05, **P<0.01, ***P<.001).

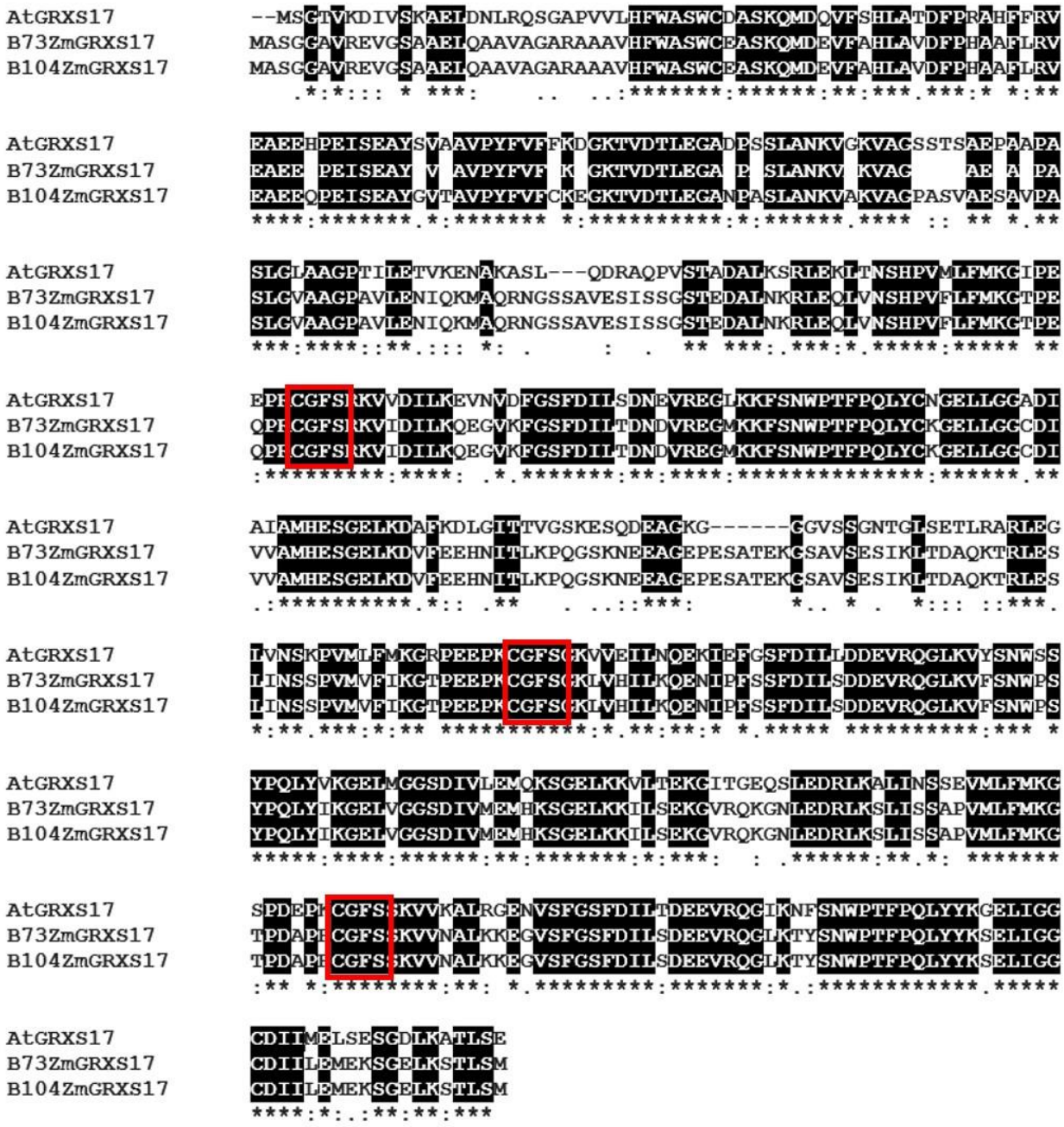
AtGRXS17
B73ZmGRXS17
B104ZmGRXS17

Figure 1. 2 GRXS17 is highly conserved between *Arabidopsis* and maize at the protein level. *ZmGRXS17* from B73 from the reference genome and B104 sequence determined from cloning *ZmGRXS17* were both compared to *Arabidopsis*. (*) indicate positives (65.9%), (:) indicate substitution with similar hydrophobicity (15.2%), and (.) indicate substitutions not of opposite polarity (7.2%) accounting for a total of 88.3%. Red boxes indicate conserved active site CGFS motif.

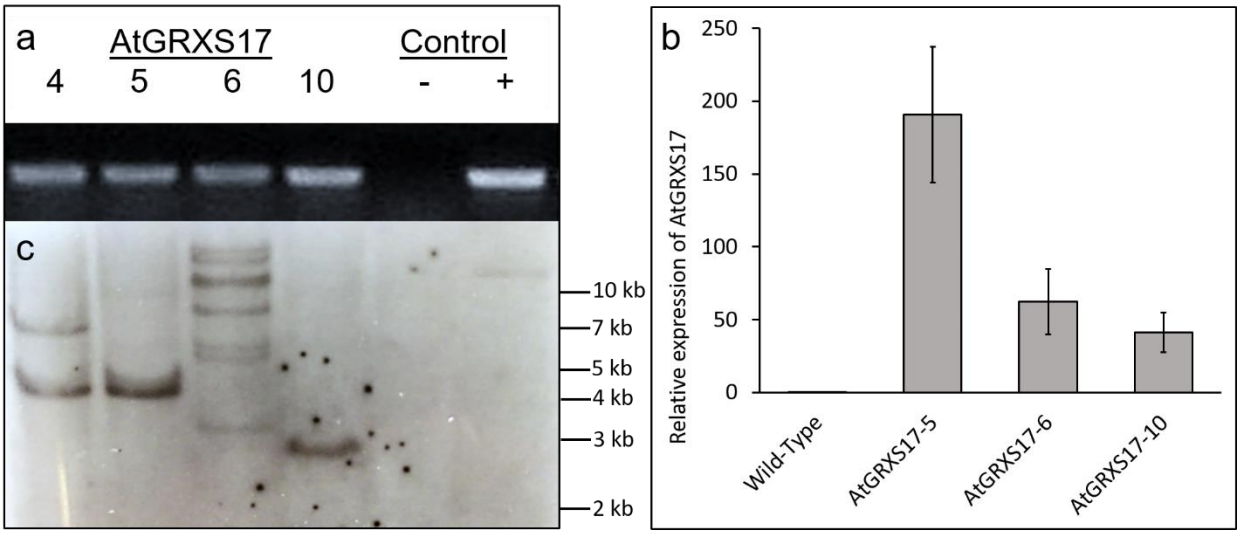

Figure 1. 3 Expression and Southern blot analysis of *AtGRXS17*-expressing plants

(a) Semi-quantitative RT-PCR analysis of the transgenic *AtGRXS17* expression in lines -4, -5, -5, -10, and (b) qRT-PCR analysis on select transgenic lines. (c) Southern blot hybridization to detect the integration of T-DNA into the maize genome. Values are means ± SD (n=3).

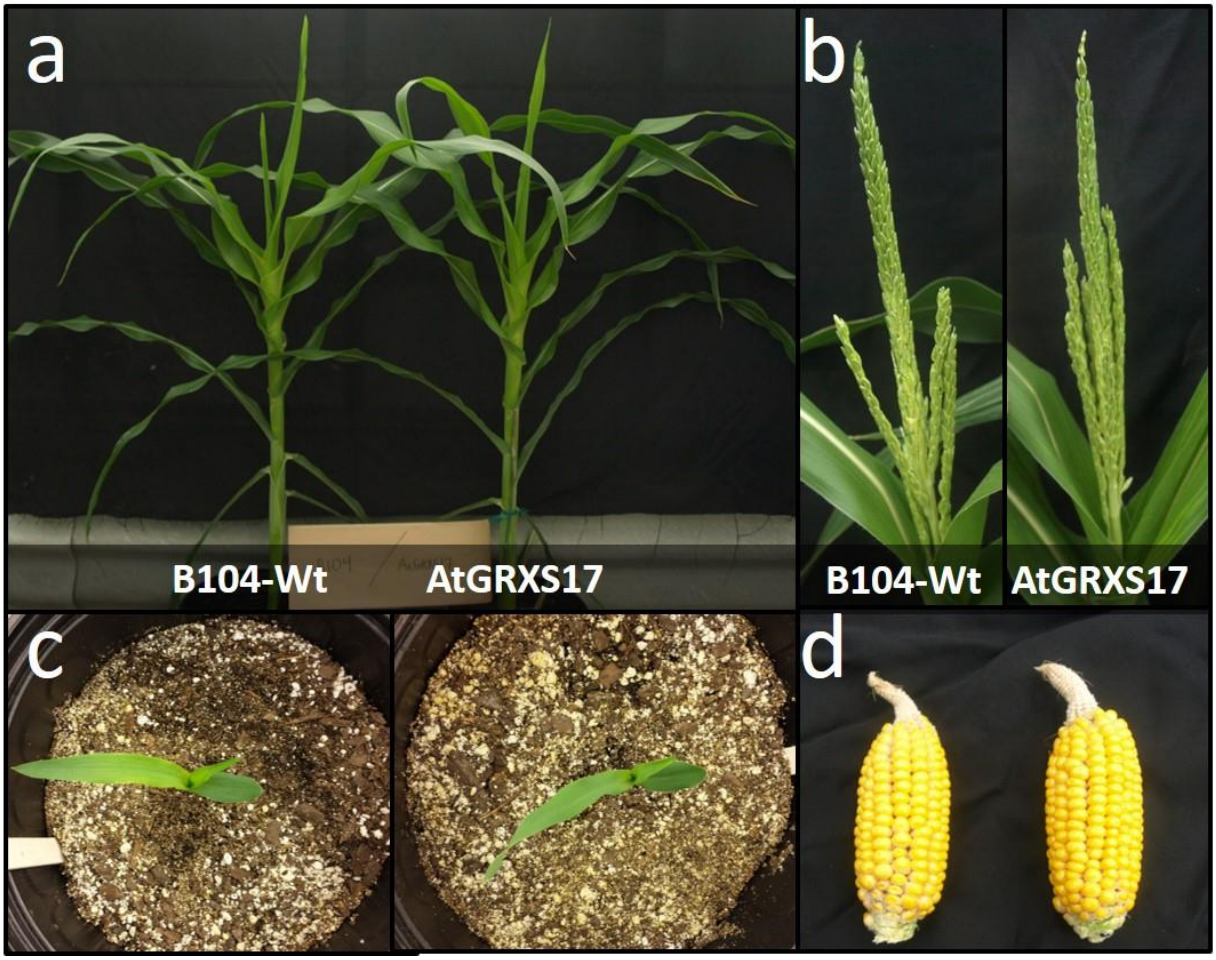

Figure 1. 4 *AtGRXS17*-expressing maize plants are phenotypically indistinguishable from wild-type plants.

Typical morphology at different developmental stages: (a) late vegetative, (b) tasseling, (c) seedling, and (d) kernel set between *AtGRXS17*-expressing and wild type plants.


a
Wild type
AtGRXS17-5
AtGRXS17-6
AtGRXS17-10
Ambient
Tents

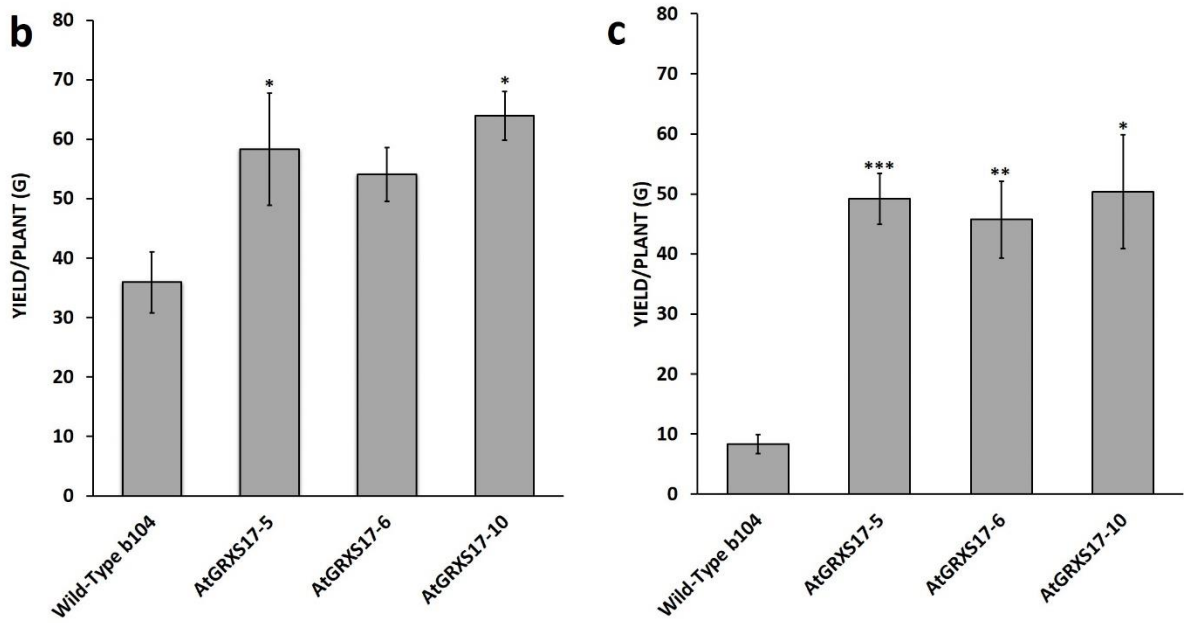

Figure 1. 5 The effect of *AtGRXS17* expression on total grain yield in field grown maize

(a) Representative cobs harvested from field grown plants in 2017 field trial. Top panel and (b) represent cobs harvested from plants grown at ambient temperatures. Bottom panel and (c) are representative cobs harvested from plants grown inside heat tents. Data are means ± se of four rows per genotype (n=4) and were analyzed with GLM code in SAS. Asterisks indicate level of significance (*p≤.05, **p≤.01, *p≤.001)

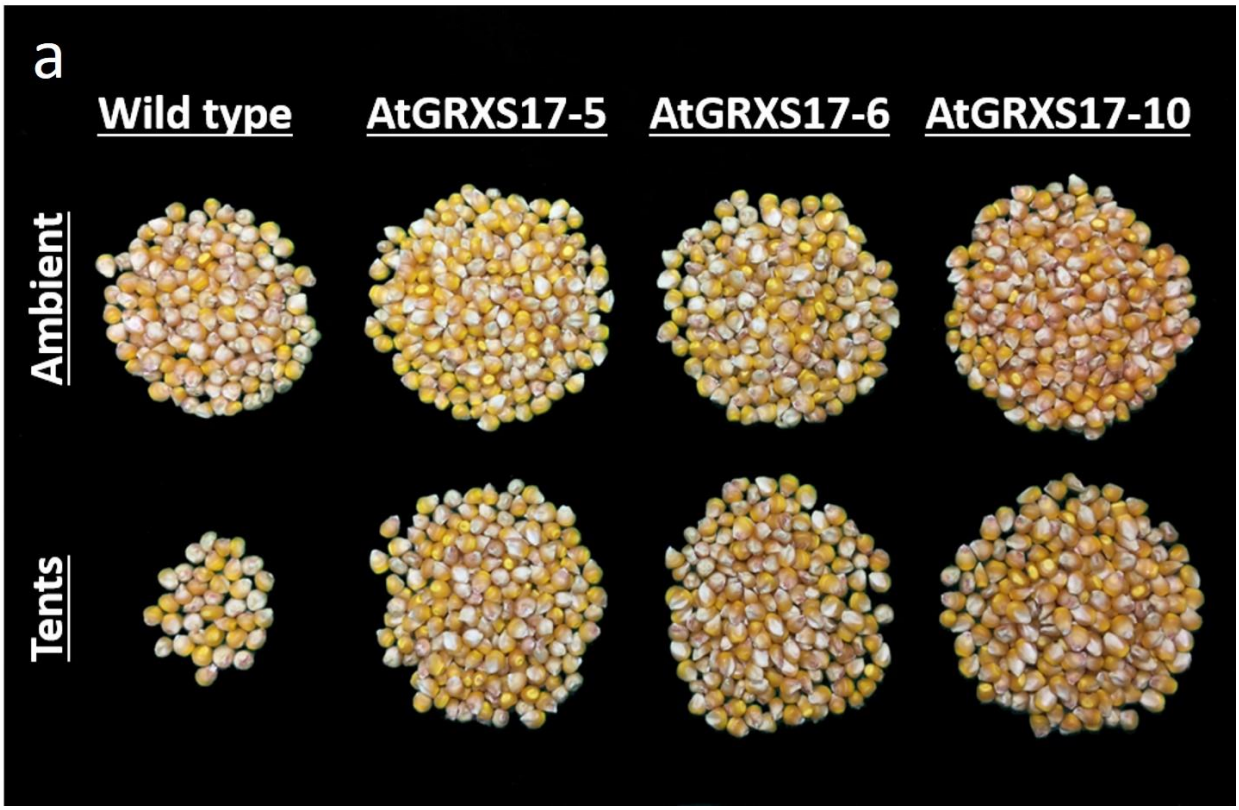
a
Wild type
AtGRXS17-5
AtGRXS17-6
AtGRXS17-10
Ambient
Tents

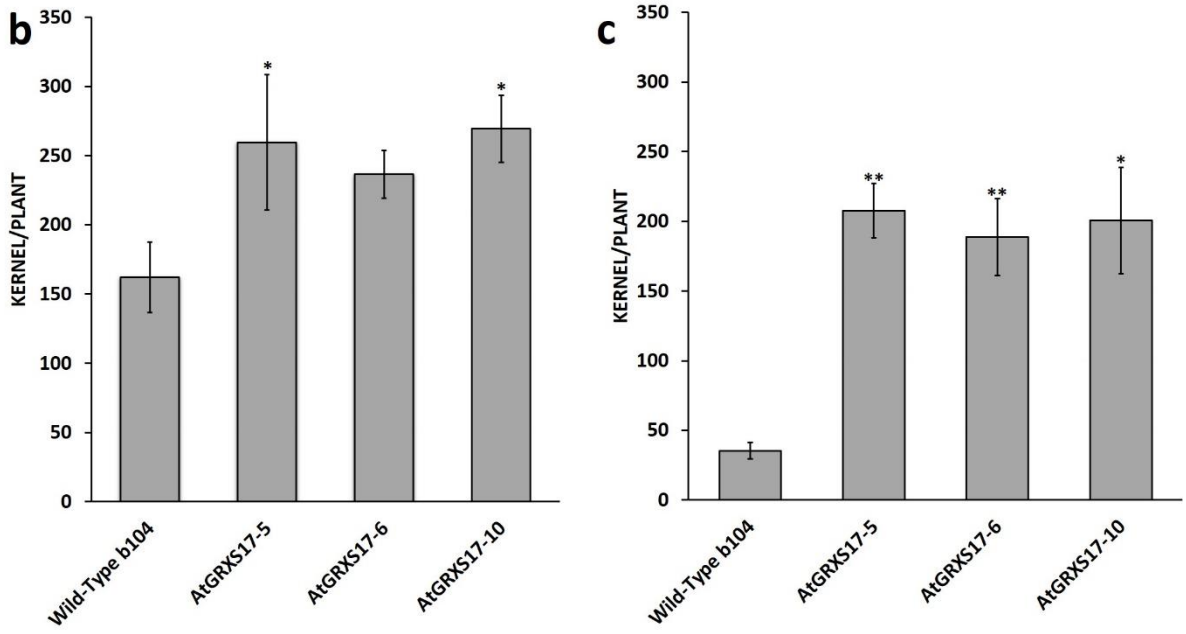
b
KERNEL/PLANT
350
300
250
200
150
100
50
0
*
*
Wild-Type b104
AtGRXS17-5
AtGRXS17-6
AtGRXS17-10
c
KERNEL/PLANT
350
300
250
200
150
100
50
0
**
**
*
Wild-Type b104
AtGRXS17-5
AtGRXS17-6
AtGRXS17-10

Figure 1. 6 The effect of *AtGRXS17* expression on maize kernel set

(a) Representative kernel set per plant harvested from field grown plants in 2017 field trial. Top panel and (b) represent kernels harvested from plants grown at ambient temperatures. Bottom panel and (c) are representative cobs harvested from plants grown inside heat tents. Data are means ± se of four rows per genotype (n=4) and were analyzed with GLM code in SAS. Asterisks indicate level of significance (*p≤.05, **p≤.01, *p≤.001)

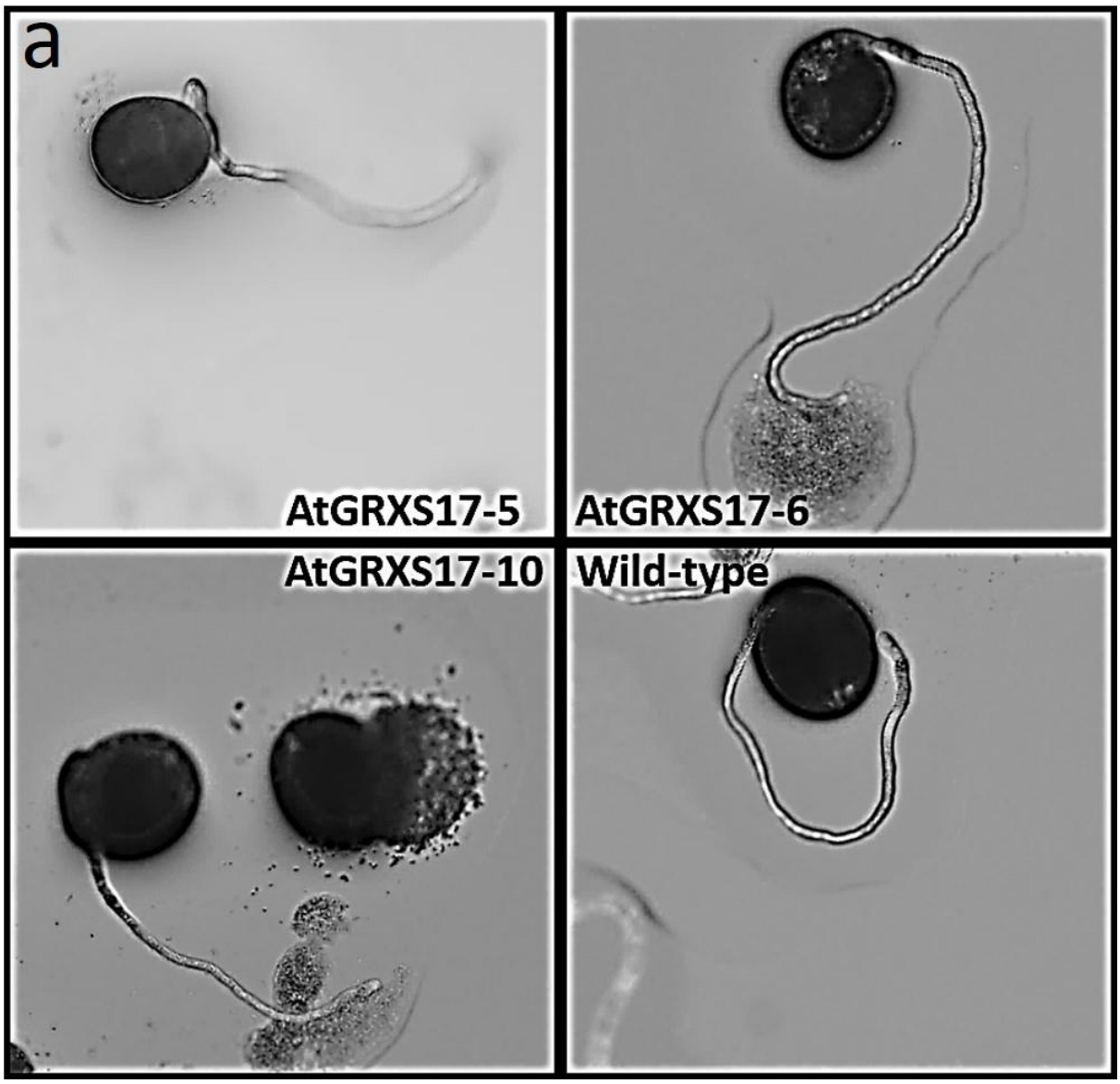
a
AtGRXS17-5
AtGRXS17-6
AtGRXS17-10
Wild-type

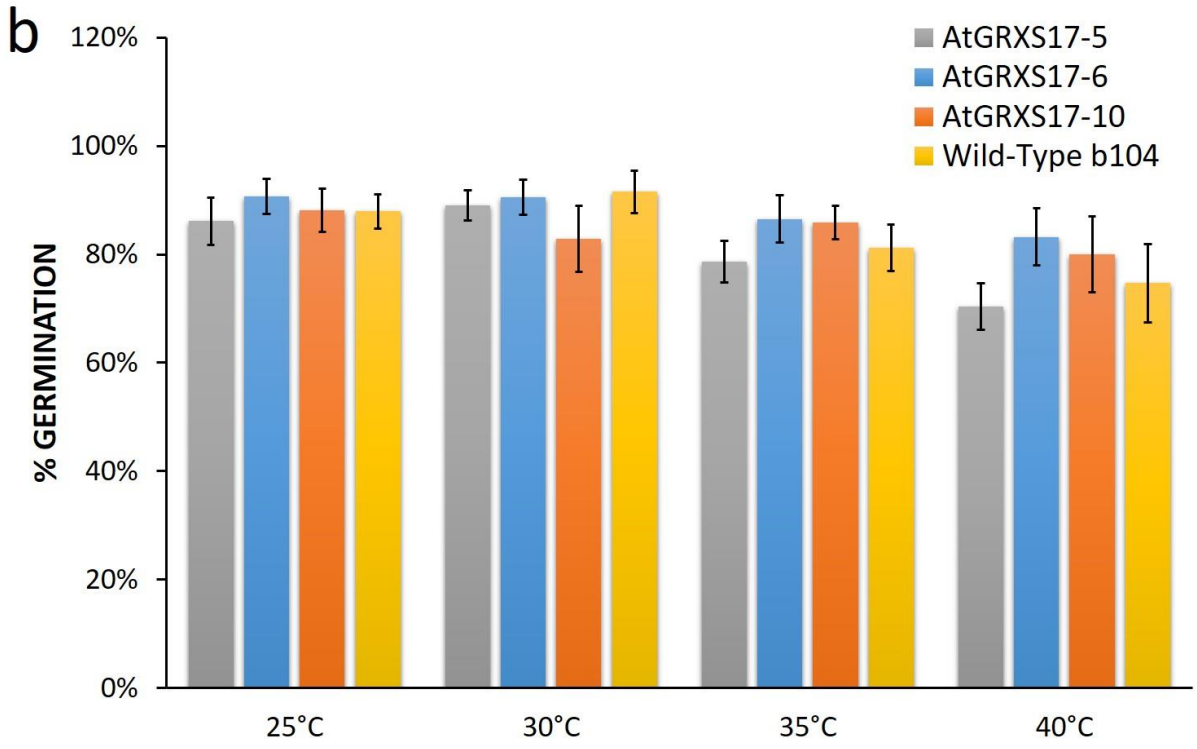

Figure 1. 7 Germination of pollen at different temperatures from non-stressed plants

(a) Pollen grains and germination tubes morphology and (b) germination rates at different incubation temperatures of all genotypes. Pollen was collected from plants before heat treatment was initialized. Data are means ± se of at least 8 images per genotype per treatment (n=8) and were analyzed using two-way ANOVA and Student's t-test. Asterisks indicate level of significance (*p≤.05, **p≤.01, *p≤.001).

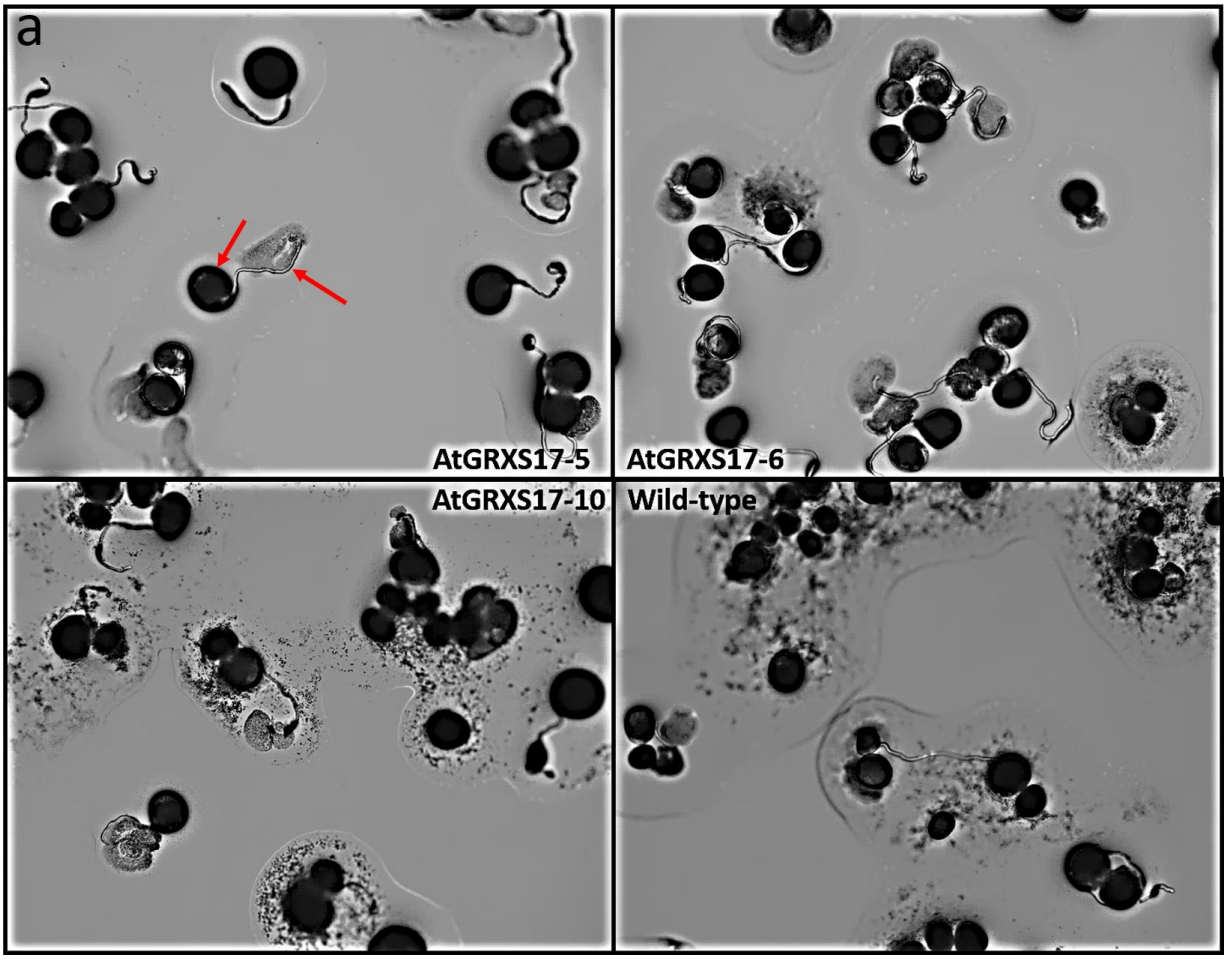
a
AtGRXS17-5
AtGRXS17-6
AtGRXS17-10
Wild-type

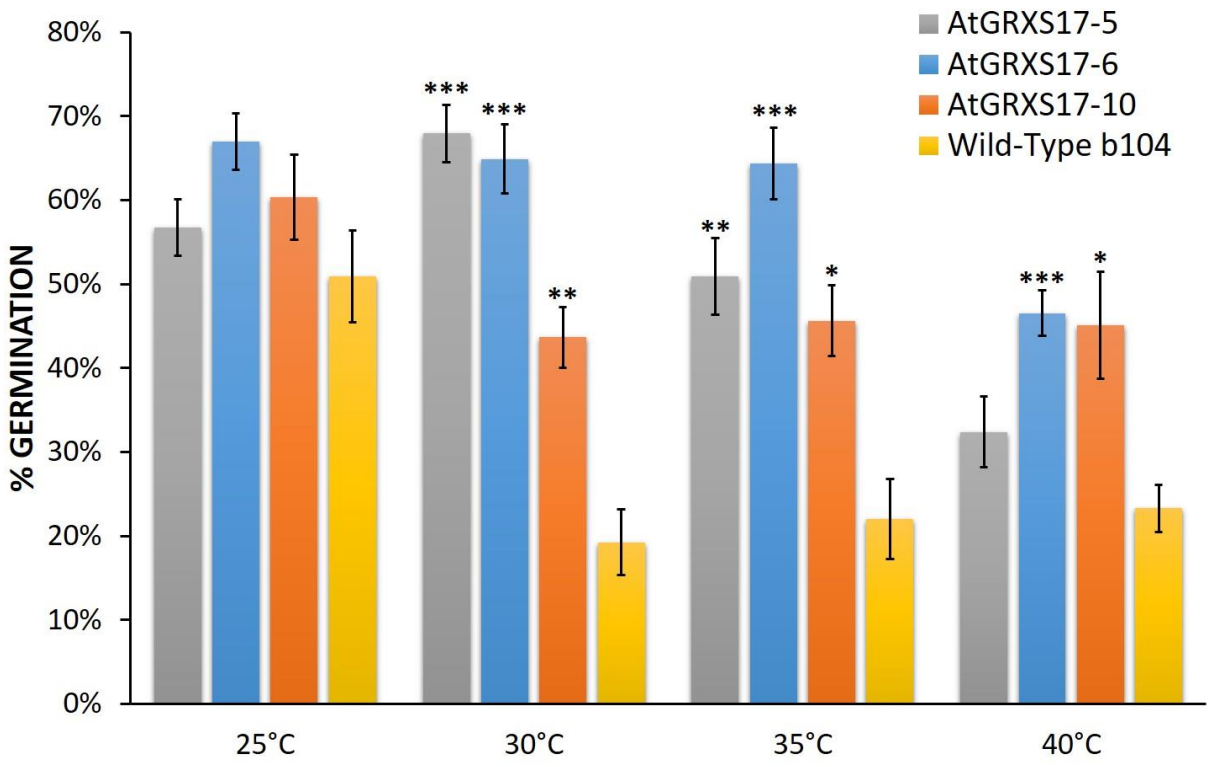

Figure 1. 8 Germination of pollen at different temperatures collected from plants stressed for two days at 37°C

(a) Representative image of pollen grains and germination tubes morphology of different genotypes. Red arrows indicate a pollen germination tube and the corresponding pollen grain. (b) germination rates at different incubation temperatures of all genotypes. Pollen was collected from plants two days after heat treatment was initialized. Data are means ± se of at least 8 images per genotype per treatment (n=8) and were analyzed using two-way ANOVA and Student's t-test. Asterisks indicate level of significance (*p≤.05, **p≤.01, *p≤.001).

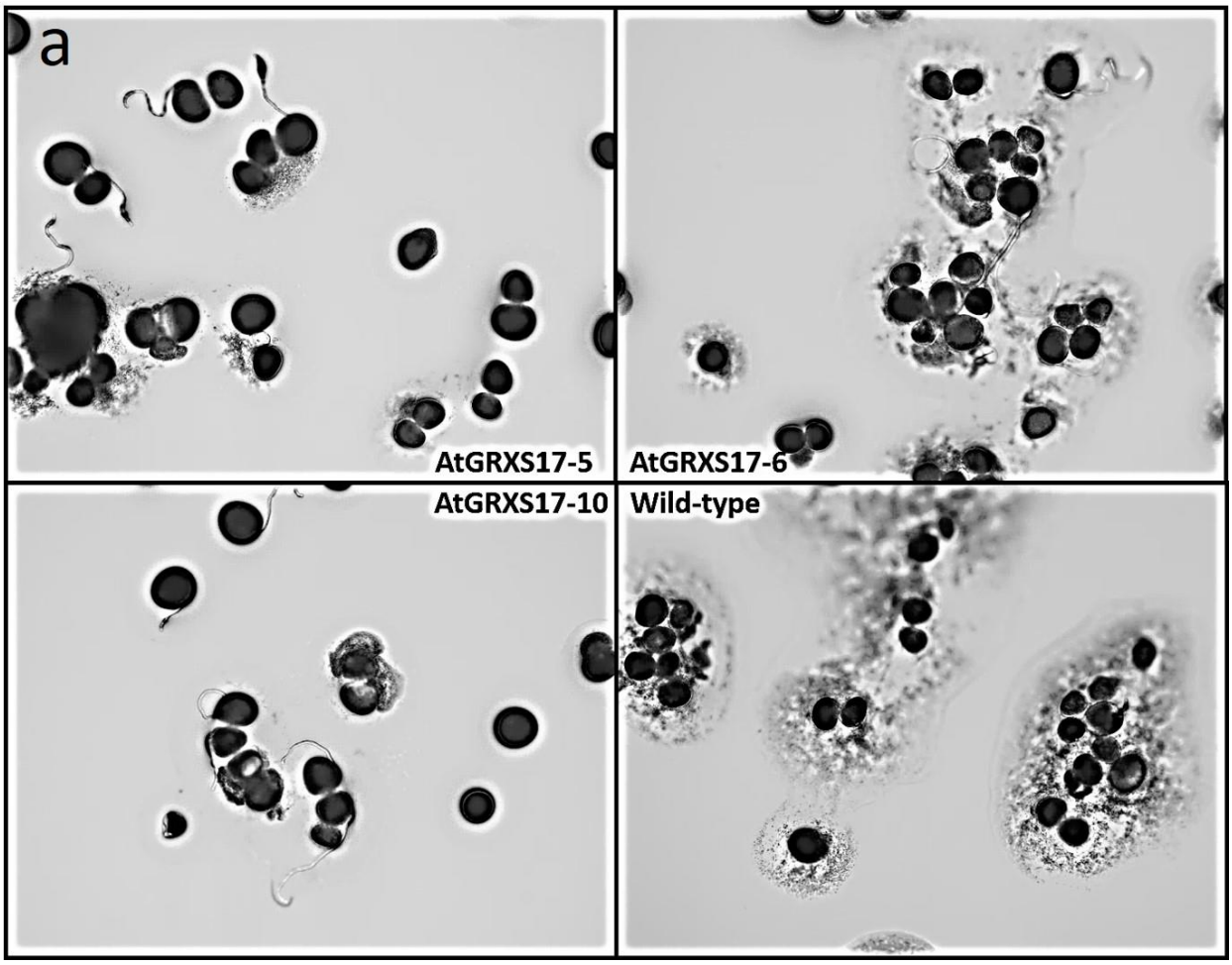
a
AtGRXS17-5
AtGRXS17-6
AtGRXS17-10
Wild-type

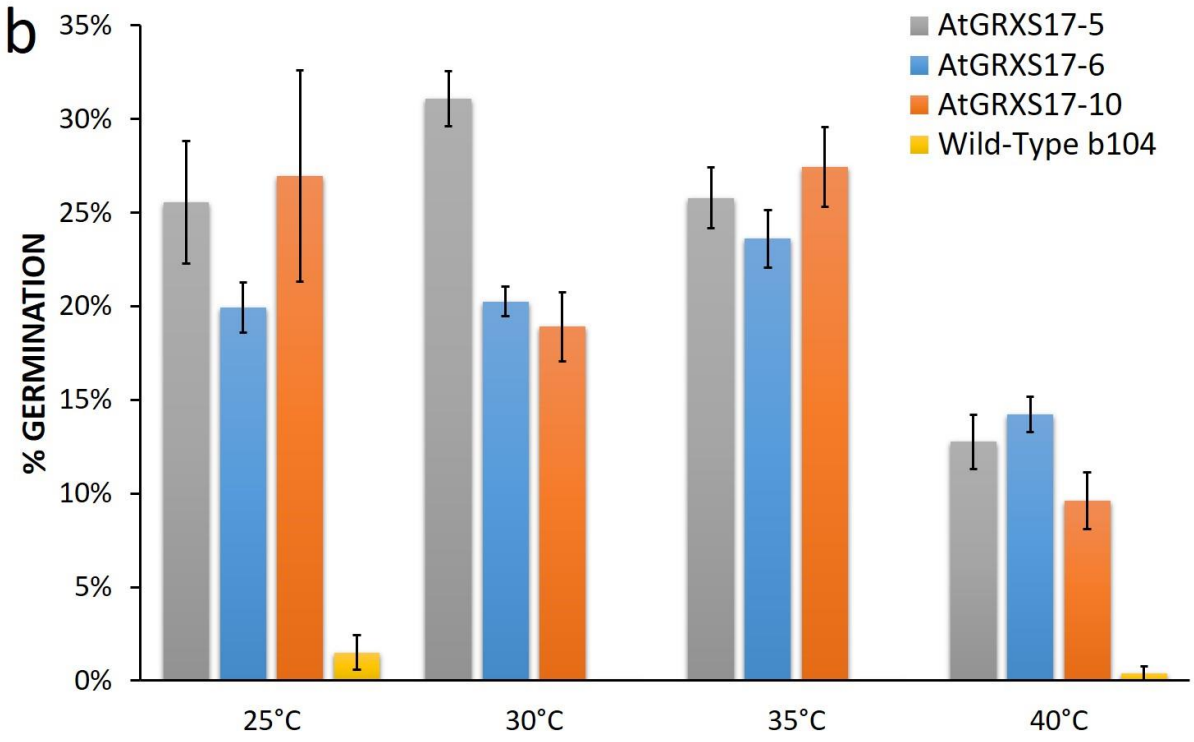

Figure 1. 9 Germination of pollen at different temperatures collected from plants stressed for three days at 37°C

(a) Representative image of pollen grains and germination tubes morphology of different genotypes. (b) Germination rates at different incubation temperatures of all genotypes. Pollen was collected from plants three days after heat treatment was initialized. Data are means ± SE of at least 8 images per genotype per treatment (n=8) and were analyzed using two-way ANOVA and Student's t-test. Asterisks indicate level of significance (*p≤.05, **p≤.01, *p≤.001).

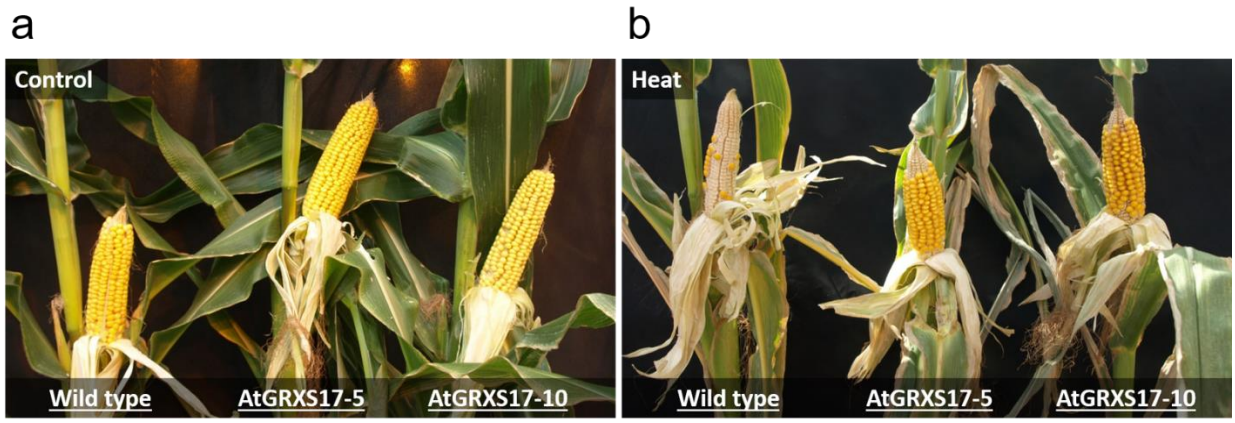
a
b
Control
Heat
Wild type
AtGRXS17-5
AtGRXS17-10
Wild type
AtGRXS17-5
AtGRXS17-10

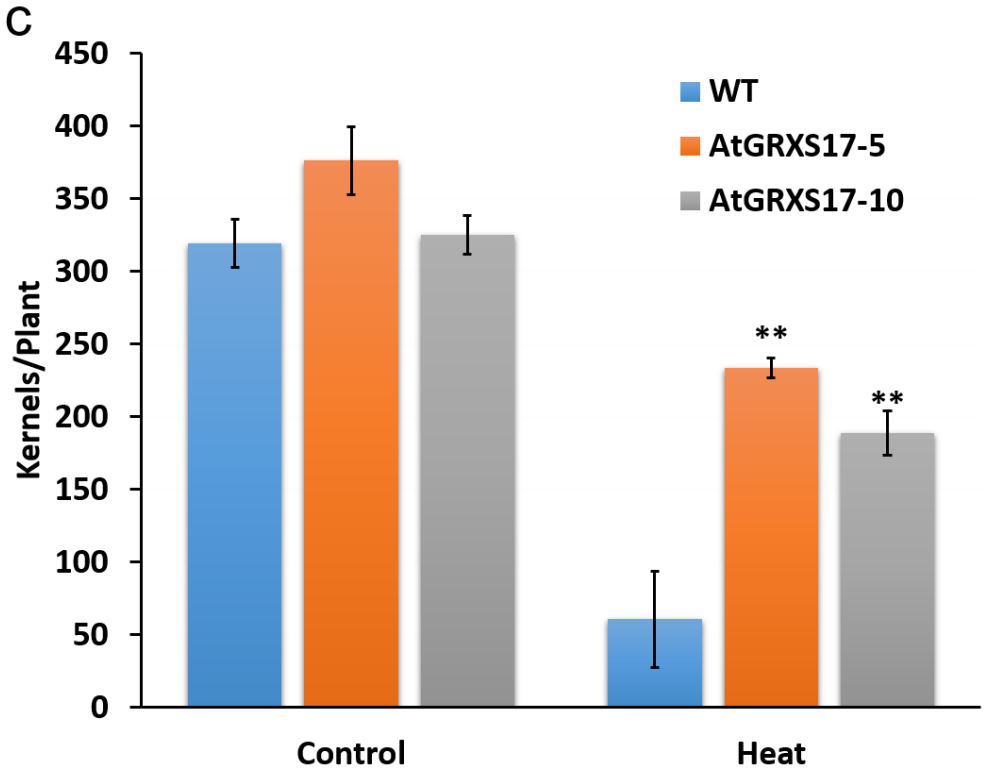
C
450
400
350
300
250
200
150
100
50
0
Kernels/Plant
WT
AtGRXS17-5
AtGRXS17-10
**
**
Control
Heat

Figure 1. 10 Kernel set response to high temperature treatment after pollination

(a) Representative plants with intact cobs grown in the greenhouse under optimal conditions. (b) Representative plants with intact cobs exposed to a 37°C temperature treatment 24 hours after pollination and continued through physiological maturity. (c) Kernel set of *AtGRXS17*-expressing and wild type plants are compared. Data are means ± SE of six per genotype (n=6) and were analyzed using two-way ANOVA. Student's t-test and asterisks indicate level of significance (*p≤.05, **p≤.01, *p≤.001).

Table 1. 1 Nutrient composition of maize kernels from 2017 field trial

Mineral	Genotype	Stress	Interaction
N	**0.001**	**0.029**	**0.024**
C	**0.032**	**0.000**	**0.013**
P	**0.201**	**0.006**	**0.357**
K	**0.344**	**0.079**	**0.911**
Ca	**0.038**	**0.523**	**0.303**
Mg	**0.028**	**0.006**	**0.200**
S	**0.164**	**0.702**	**0.939**
Cu	**0.372**	**0.045**	**0.318**
Fe	**0.457**	**0.847**	**0.362**
Mn	**0.197**	**0.408**	**0.645**
Zn	**0.034**	**0.000**	**0.407**

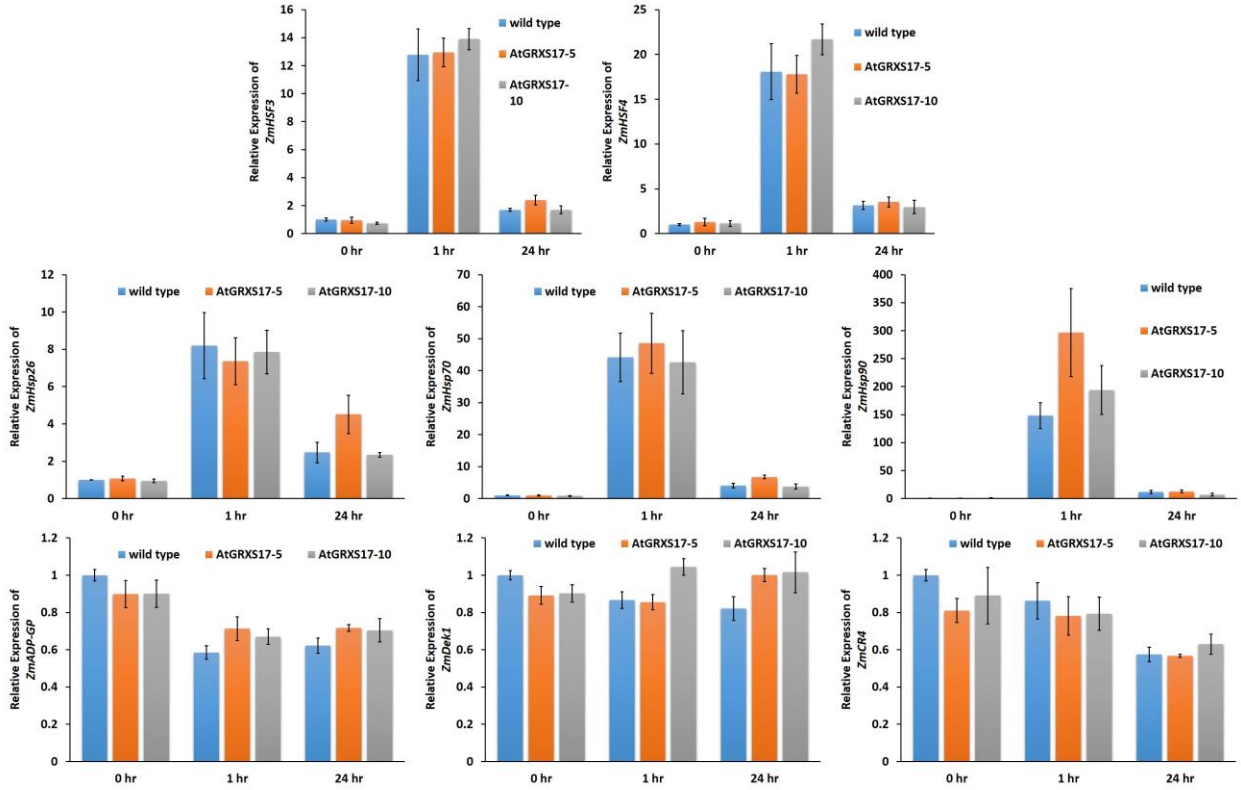

Figure 1. 11 Effects of *AtGRXS17* expression on expression patterns of stress responsive genes during heat stress.

Relative expression of heat shock factors (a) *ZmHSF3*, (b) *ZmHSF4*, heat shock proteins (c) *ZmHSP26*, (d) *ZmHSP70*, (e) *ZmHSP90*, starch synthesis (f) *ZmAGPase*, and membrane receptor signaling proteins (g) *ZmDEK1* and (h) *ZmCR4*. Data represent means ± SE; n=9 and were analyzed using two-way ANOVA and Student's t-test.

SUPPORTING INFORMATION

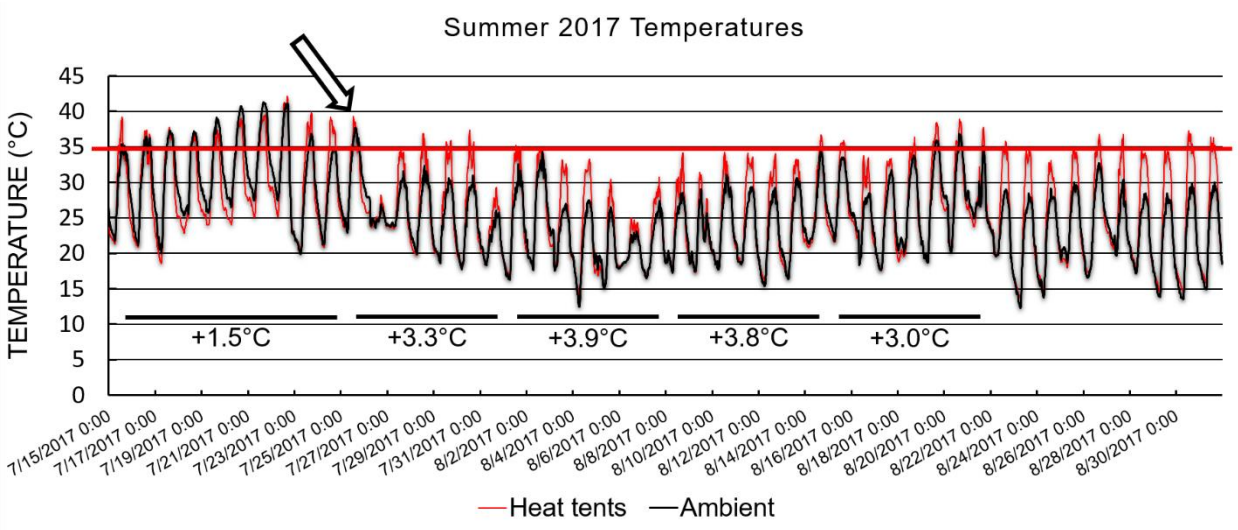

Figure 12 Temperatures measured in 2017 field trial.

Red line indicates temperatures measured within heat tents and the black line indicates ambient temperatures. Maximum daily temperatures within heat tents were slightly higher (1.5°C on average) in the ten-day period leading up to silking, indicated by arrow. Maximum daily temperatures within heat tents were 3.3°C, 3.9°C, 3.8°C, and 3.0°C higher, on average, than ambient in the first, second, third, and fourth week post silking, respectively. Temperatures often exceeded 35°C, indicated by the red bar.

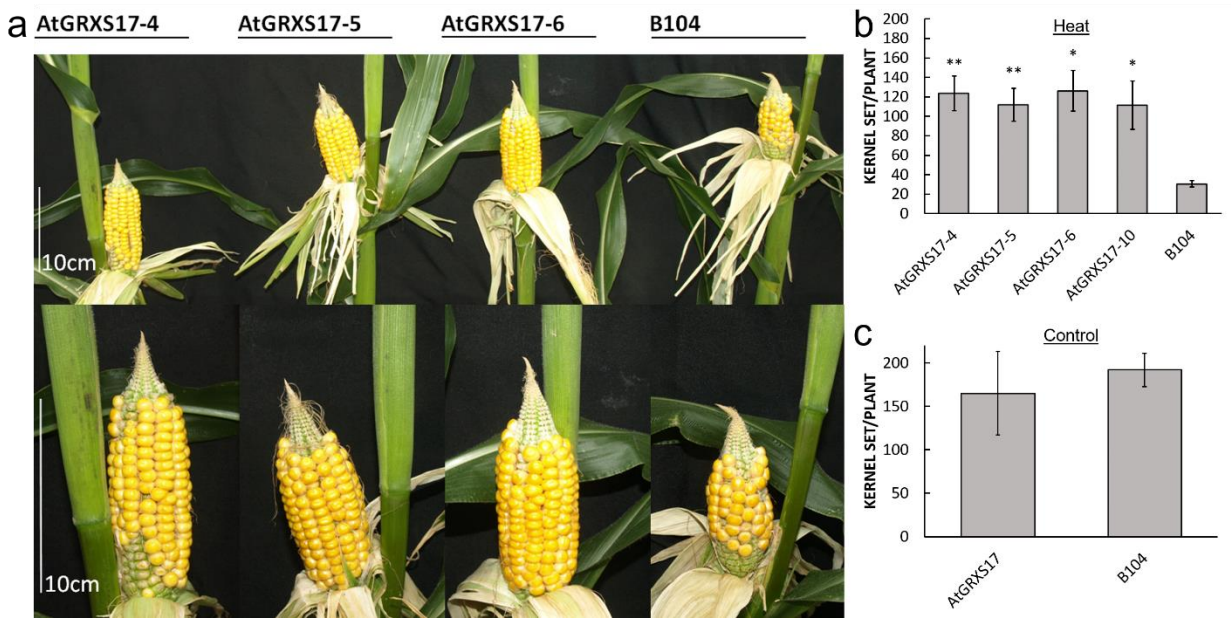

Figure 13 *AtGRXS17* expressing maize is more heat tolerant than wild type

(a) Representative cobs from greenhouse grown plants exposed to heat stress. (b) *AtGRXS17*-expressing lines have higher kernel set when exposed to heat stress during pollination and early kernel developmental stages. (c) *AtGRXS17*-expressing plants kernel set does not differ from wild type when grown at control temperatures. Data are means ± SE of four plants per genotype (n=4) and were analyzed with Student's t-test. Asterisks indicate level of significance (*p≤.05, **p≤.01, *p≤.001).

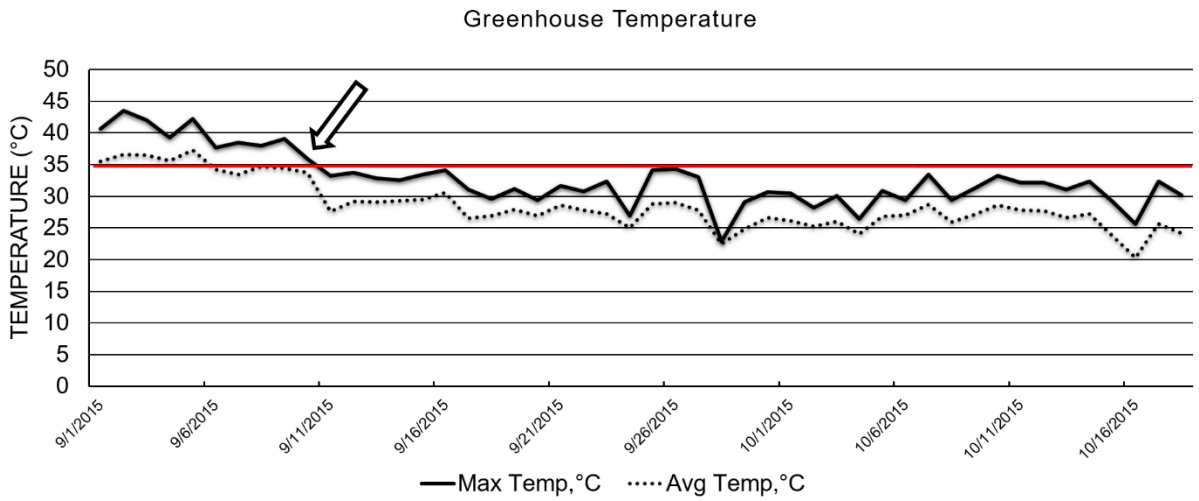

Figure 14 Average and maximum daily temperatures within heat treated greenhouses. During the heat stress period, temperatures often exceeded 35°C, indicated by the red bar, and maximum daily temperatures neared 40°C at midday, while average daily temperatures stayed near the climate control target of 37°C. Arrow indicates conclusion of the heat stress period. When reverted back to optimal conditions, greenhouse temperatures never exceed 35°C, and average daily temperatures hover near the target of 28°C.

Chapter 2 - Metabolic Profiling Reveals Altered Sulfur and Carbohydrate Pathways in Response to Drought Stress Between Differentially Expressed *GRXS17* in Rice Increases Drought Tolerance.

ABSTRACT

Plant water status is a tightly controlled process and is critical for optimal growth, development, and yield. Metabolite profiles change substantially under water deficit. Osmolytes, including amino acids and sugars, antioxidants, and phytohormones are vital for reducing the loss of water and controlling oxidation under stress conditions. Previously, our work has identified the *Arabidopsis* monothiol glutaredoxin, AtGRXS17, and the rice homolog OsGRXS17, as a key regulators for water status in tomato and rice, respectively. Ectopic expression of *AtGRXS17* in rice plants resulted in higher chlorophyll content, water content, and an increase in survival rate. *AtGRXS17*-overexpressing rice plants have altered sulfur assimilation pathways, less glutathione degradation, and increased sucrose synthase cleavage activity, impacting sugar signaling pathways. While *OsGRXS17*-silenced rice plants accumulate less aspartate, less free amino acids, and higher fumarate and pyruvate content, contributing to the previously reported drought tolerant phenotype. Both plants with ectopic expression or silenced GRXs accumulate less metabolites that are correlated with oxidative stress. To date, no metabolomics profiling experiment has been devised to elucidate the effect of differential glutaredoxin expression on the metabolic profile of rice plants grown under non-stressed, mild water deficit stress, and severe water deficit stress conditions. Our results provide insight into how glutaredoxin expression affects the rice metabolome and, thus, further our understanding and ability to engineer drought resistant plants.

INTRODUCTION

Water limitations represent the largest challenge to global food production in the foreseeable future (Arnauld et al., 2016). Global climate change predictions indicate an increase in the unpredictability of rainfall and temperature events (Passioura, 2007). Coupled with this unpredictability, increases to both world population and average global surface temperatures put further strain on the fresh groundwater supplies utilized for irrigated crops. It is estimated that by the year 2050 the demand for food will double (FAO). Certain portions of fresh water stores, such as the High Plains Aquifer, are predicted to be depleted to as low as 18% of initial levels by 2060 (Steward et al., 2013). This necessitates the need for drought tolerant rice due to its role as a staple food in South Asia, which is already one of the most undernourished regions in the world (Bishwajit et al., 2013). This provides a tremendous opportunity and responsibility for plant scientists to increase the drought resistance of rice through tolerance and avoidance mechanisms to help alleviate this strain.

Drought stress elicits several distinct responses from plants that are together referred to as drought tolerance mechanisms (Valliyodan et al., 2006). Drought tolerance is the acclimation of plants to water limited conditions and is distinct from drought escape, drought avoidance, and drought resistance. Together with drought avoidance, drought tolerance contributes to drought resistance (Yue et al., 2006). Plant responses categorized as drought tolerance include Abscisic acid (ABA) production, translocation, and response, osmotic adjustment (OA) through compatible osmolytes, and increased enzymatic and non-enzymatic antioxidant capacity resulting in lower reactive oxygen species (ROS) accumulation thus higher protein and membrane stability (Zhang et al., 2006; Reddy et al., 2004; Gill and Tuteja, 2010). Metabolomics experiments have defined metabolite groups with altered accumulation profiles in response to

drought stress including soluble sugars, amino acids, organic acids, nucleotide related metabolites, and metabolites directly involved in photosynthesis and respiration (Ramanjulu and Sudhakar, 1997; Shu et al., 2011). OA is frequently positively correlated with plant production, and soluble sugars and amino acid accumulation is often higher in the more tolerant genotypes (Blum, 2017). Despite this, individual metabolites may have accumulation profiles negatively correlated with drought tolerance (Degenkolbe, 2013). Amino acids, osmolytes and nitrogen stores consistently accumulate across many species in response to osmotic stress and, in some cases, have been shown to be an effective indicator of leaf relative water content (RWC) (Rampino et al., 2006; Di Martino et al., 2003; Charlton et al., 2008;). In maize, some amino acids increase while others decrease due to drought stress, however, the only drought susceptible genotype tested did not increase amino acid content (Witt et al., 2012).

ROS are highly oxidized oxygen containing molecules such as singlet oxygen ($^{-}O_2$), superoxide radical (O_2^{-}), hydrogen peroxide (H_2O_2), and hydroxyl radical (OH^{-}). These molecules are produced through aerobic respiration processes within the chloroplasts, mitochondria, and peroxisomes (Allen, 1995). Under optimal environmental conditions, plants are able to quickly detoxify these potentially damaging ROS molecules through enzymatic and non-enzymatic antioxidants (Gill, 2010). In addition to ROS being byproducts of natural plant processes, they also serve as important signaling molecules and are critical for drought stress response (Carvalho, 2008). However, during prolonged periods of stress, ROS accumulation can reach severely elevated concentrations, which, in turn, overwhelms the antioxidant capacity of the cell. These toxic byproducts oxidize many biological macromolecules they come into contact with including carbohydrates, nucleic acids, proteins, and lipids. This compromises basic cellular functions as well as the entire cell through damage to the phospholipid bilayer (Van Breusegem

and Dat, 2006). Glutaredoxins are small ubiquitous proteins that are able to control redox status of cells by reducing proteins through their thiol-disulfide transfer (Wu, et al., 2017). Reduced glutathione (GSH) is critical for reduction of glutaredoxin's oxidized thiol groups. Through the use of a loss of function *Arabidopsis* mutant, *atgrxs17*, glutaredoxins have been experimentally shown to be critical for abiotic stress tolerance, iron homeostasis, and floral development and signaling (Cheng et al., 2011; Yu et al., 2017). AtGRXS17 is an *Arabidopsis* class II CGFS type monothiol glutaredoxin and has been experimentally shown to increase abiotic stress tolerance when ectopically overexpressed in crops (Wu et al., 2012; Hu et al., 2015; Wu et al., 2017). Paradoxically, reduction in the expression of the rice homolog, *OsGRXS17*, results in increased drought tolerance through more efficient ABA-dependent stomatal closure signaling (Hu et al., 2017). Many reports implicate glutaredoxins importance in stress tolerance and ROS detoxification, but there is evidence for an additional role as interacting partner with CCAAT-box binding factor (CBF) regulatory proteins such as nuclear factor Nuclear Factor Y Subunit C11/Negative Cofactor 2α (NF-YC11/NC2α) (Knuesting et al., 2015). Ectopic overexpression of the maize *NF-YB2* resulted in increased drought tolerance and yield in maize grown under water limited conditions (Nelson et al., 2007). Interestingly, it conferred drought stress tolerance through ABA-independent and CBF-independent pathways as marker genes for both of these pathways were not upregulated. Taken together, this suggests that the role of AtGRXS17 in abiotic stress tolerance is through both the direct reduction in ROS species accumulation and altered redox status as well as interactions with regulatory proteins.

In this study we investigated the effect of ectopic overexpression of *AtGRXS17*(OE) and *OsGRXS17*-silencing in rice (*Oryzae sativa* L. cv. Nipponbare) on the metabolome during water limited conditions. We present data using a unique set of material to gain insight into the effect

of *GRXS17* expression on drought stress response in rice. We previously reported that *OsGRXS17* silenced plants (RNAi) display increased drought tolerance through modulation of stomatal closure resulting in increased relative water content (RWC) (Hu et al., 2017). Perplexingly, we found that OE lines also displayed increased drought tolerance and RWC. Survival rates and visual phenotype was measured and was consistently higher than wild type (WT) plants across multiple experiments. All three genotypes (WT, OE, and RNAi) metabolomes were analyzed for comparison.

MATERIALS AND METHODS

Plant Material and Treatments

Wild-type and *AtGRXS17*-expressing Nipponbare rice plants for all experiments were grown in climate controlled growth chambers with a 16h light (28°C)/8h dark (22°C) photoperiod at 300 μmols/m^2/s light intensity. Until drought initiation, plants were grown in pots sitting in trays with excess water for constant sub irrigation. Drought was initiated by removing pots from sub irrigated trays. For the first phenotype assay, 5-leaf stage plants were first stressed for 11 days and survival rates were scored. The second drought stress assay was initiated at tillering and water was withheld for 8 days. The third experiment was initiated when plants displayed two tillers and water was withheld for 8 days. For metabolic profiling, four week old plants were used and treatments were randomly assigned to uniform experimental units. After 0 days water stress (0DWS), 5 days (5DWS), or 8 days (8DWS) of not receiving water, the youngest fully expanded leaves were collected, immediately frozen in liquid nitrogen, lyophilized and sent to Metabolon, Inc. for metabolite analysis.

Statistical Analysis

Data were normalized by processing a constant weight of sample per volume of solvent. Statistical analysis was preformed using natural log-transformed scaled imputed data. Data were scaled to the mean and imputed based on the minimum detected value for the compound. Statistics were run as pair wise ANOVA contrasts between different genotypes within the same time point (genotype effect) and between time points within a given genotype (stress effect).

Metabolite Extraction and Analysis

Sample Preparation: Samples were prepared using the automated MicroLab STAR® system from Hamilton Company. Several recovery standards were added prior to the first step in the extraction process for QC purposes. To remove protein, dissociate small molecules bound to protein or trapped in the precipitated protein matrix, and to recover chemically diverse metabolites, proteins were precipitated with methanol under vigorous shaking for 2 min (Glen Mills GenoGrinder 2000) followed by centrifugation. The resulting extract was divided into five fractions: two for analysis by two separate reverse phase (RP)/UPLC-MS/MS methods with positive ion mode electrospray ionization (ESI), one for analysis by RP/UPLC-MS/MS with negative ion mode ESI, one for analysis by HILIC/UPLC-MS/MS with negative ion mode ESI, and one sample was reserved for backup. Samples were placed briefly on a TurboVap® (Zymark) to remove the organic solvent. The sample extracts were stored overnight under nitrogen before preparation for analysis.

RESULTS

AtGRXS17-expressing Plants Have Improved Drought Tolerance

Three independent phenotyping experiments with T3 *AtGRXS17*-expressing (OE) and wild-type (WT) rice plants were conducted to evaluate drought tolerance. Three independent transgenic events were chosen because of their relatively high *AtGRXS17* expression (Figure 1A). These lines displayed normal growth and development and showed no obvious phenotypic variation from WT plants (Figure 1B, C). Yield parameters such as panicle number, grain number, and 100 grain weight showed no differences (Supplemental Figure 1). OE lines showed higher drought tolerance than WT plants. After an 8-day water withholding period, both OE and WT were severely wilted in appearance, although OE lines -3, -6, and -7 slightly less than WT plants. (Figure 2B). After a recovery period, most transgenic plants completely recovered and maintained high vigor, while most WT did not recover (Figure 2C, D). Additional experiments displayed similar results (Supplemental Figure 2, 3, 4). Because of the variability in transgene expression and drought tolerance, *AtGRXS17-7* was selected as a candidate for metabolite profiling. *AtGRXS17-7* maintained higher leaf relative water content than WT plants at nine days of drought stress, resulting in higher chlorophyll fluorescence and lower H_2O_2 accumulation (Supplemental Figure 5, 6).

Metabolic Profile of Drought Stressed AtGRXS17-expressing and Wild-type Rice Plants

In total, 357 metabolites were detected in leaf tissue. All detected metabolites were sorted into groups: amino acids (117), lipids (69), nucleotide (50), carbohydrate (42), cofactors, prosthetic groups, and electron carriers (28), peptides (25), secondary metabolites (23), xenobiotics (2), and hormones (1) (Figure 3A). Of the 357 detected metabolites, 273 were significantly affected by drought stress, 113 displayed significant differences between genotypes, and 34 displayed

interaction (Figure 3B). These differences occurred in in all biochemical groups with the largest proportion of affected metabolites to total metabolites as follows: hormones, peptides, secondary metabolites, nucleotide, amino acid, co factors, carbohydrates, lipids, and xenobiotics (Figure 3C). Over one third of the total metabolites that were affected by stress were involved in amino acid metabolism (34.1%). Lipid metabolism (15.4%), nucleotide metabolism (15%), carbohydrate metabolism (11.7%), cofactor, prosthetic group, and electron carrier metabolism (8.1%), peptide metabolism (8.1%), secondary metabolites (7%), hormones (.4%) and xenobiotics (.4%) were the remaining categories (Supplemental Figure 7A, B).

Amino acids

Amino acids were the largest group of metabolites impacted by drought stress, accounting for over one third of all metabolites affected (Supplemental Figure 7A). Most amino acid groups had a greater proportion of metabolites increasing than decreasing (Supplemental Figure 7B). Aromatic amino acids including tryptophan, phenylalanine, tyrosine, and histidine all increased due to drought stress and ranged from 1.62-fold increase for tyrosine to a 14.58-fold increase for tryptophan (Figure 4A; Table 1). RNAi accumulated less aromatic amino acids than WT at 8DWS. Branched chain amino acids followed a similar pattern with consistent increases between 4.24-fold (valine) to 5.61-fold (isoleucine) at 8DWS, but no genotypic differences were observed within this group (Figure 4B). Glutamate amino acids continued this trend as glutamine, proline, arginine, and glutamate all increased (Figure 4C). Proline was the largest increase within this group with an average 7.04-fold increase due to stress. However, proline and glutamine accumulated much less in both OE and RNAi than WT, while RNAi accumulated less arginine than both wild type and OE. Aspartate family amino acids alanine, lysine, asparagine, methionine, threonine, and aspartate were all significantly affected by drought stress and

generally increased by 8DWS (Figure 4D). Most of these amino acids followed a pattern of slight decrease or stay constant from 0DWS to 5DWS but then increase sharply by 8DWS. Lysine and aspartate were the exceptions. Lysine gradually increased, while aspartate gradually decreased as drought stress progressed. RNAi and OE both accumulated much less asparagine, methionine, and threonine than WT at 8DWS and aspartate accumulation was lower in RNAi than WT and OE plants at all timepoints.

Glutathione and Sulfur Metabolism

Several metabolites involved in GSH and oxidized glutathione disulfide (GSSG) synthesis and degradation pathways were impacted (Figure 5A, B). GSSG increased at 8DWS across all genotypes. The two first byproducts of glutathione degradation, oxidized cysteine-glycine dipeptide, and gamma-glutamyl-amino acid (GGAA) peptides were impacted due to drought stress (Figure 5A, B). OE had less accumulation of cys-gly dipeptide than WT at 5DWS. Of the total ten GGAA that were affected by drought stress, nine increased (Table 2). In three cases, GG-methionine, GG-glutamine, and GG-tryptophan, RNAi had less accumulation than WT at 8DWS. OE had less accumulation of GG-glutamine than WT at 8DWS (Figure 5B). 5-Oxoproline (5OP), the next product in the GSH/GSSG degradation pathway, was much lower in RNAi and OE than WT at 8DWS. Alpha-ketoglutarate, a carbon metabolism product and glutathione synthesis precursor decreased by 8DWS (Figure 5A). Sulfate assimilation metabolites were impacted by both stress and *GRXS17* expression. The amino acid serine, the carbon backbone for cysteine, increased due to drought stress but only in WT (Figure 6). In WT, serine slightly decreased at 5DWS and was sharply induced at 8DWS, following the pattern of several aspartate family amino acids. RNAi and OE did not follow the same pattern. RNAi started with higher serine content than WT at 0DWS and 5DWS and did not differ from WT at

8DWS. OE only differed at 8DWS with less accumulation than WT. Adenosine 3',5'-diphosphate (PAP) is a byproduct of sulfonyl-transferase reactions and was unaffected by drought stress but OE accumulated 4.26-, and 4.99-fold more than RNAi at 0DWS and 5DWS, respectively (Figure 6). PAP degradation leads to an increase in free phosphate which decreased under drought stress. Again, OE showed differences and accumulated more than either other genotype at all timepoints with the largest differences of 2.04-, 1.86, and 1.67-fold more than RNAi at 0DWS, 5DWS, and 8DWS, respectively (Figure 6).

Carbohydrate Metabolism

Metabolites comprising soluble sugars, energy metabolism, respiration and photosynthesis were all greatly affected by drought stress. The soluble sugar sucrose accounted for 30% of all carbohydrates detected, followed by the citric acid cycle intermediate malate representing 28% (Supplemental Table 1). In general, metabolites classified into sugar metabolism increased while metabolites classified as energy metabolism related decreased (Supplemental Figure 8). Soluble sugars, amino and nucleotide sugars, and raffinose family oligosaccharides (RFO) increased to multiple times their nonstressed values (Table 3A; Figure 7). The RFO precursor, galactinol, increased 18.3-fold by 8DWS (Figure 8). OE had less than half the galactinol content at 0DWS than both RNAi and WT but this difference disappeared by 8DWS (Table 3B, C). However, OE accumulated more of the galactinol upstream precursors, uridine diphosphate-glucose (UDP-glucose) and uridine diphosphate-galactose (UDP-galactose), than WT (2.8-fold; 8.9-fold) and RNAi (2.2-fold; 4.9-fold) at 5DWS (Figure 8). At 8DWS, OE maintained 4.3-fold and 5.7-fold higher UDP-galactose content than WT and RNAi, respectively, and had 3.4-fold more UDP-glucose accumulation than RNAi. Differences in RFO precursor accumulation did not affect the accumulation of raffinose. The soluble sugars sucrose, glucose, and fructose increased 1.34-fold,

2.50-fold, and 2.50 fold by 8DWS, respectively (Figure 7). OE accumulated less glucose (.71-fold) and fructose (.70-fold) than WT at 0DWS and by 8DWS these genotypes did not differ. In addition to the accumulation of the glycolysis input sucrose, the glycolysis intermediate phosphoenolpyruvate (PEP) drastically decreased in all genotypes and the final product of glycolysis, pyruvate, significantly increased in RNAi plants by 8DWS (Figure 9A, B). The citric acid cycle was similarly affected with a large reduction in most intermediates (Table 4). Isocitrate, an intermediate upstream of alpha-ketoglutarate, was the largest decrease among carbohydrate related metabolites with only .008-fold at 8DWS. Fumarate, a citric acid cycle intermediate unaffected by stress, displayed genotypic differences (Figure 9C). Photosynthesis also displayed clear reductions, as the first stable intermediate of carbon fixation, 3-phosphoglycerate (3PGA), was decreased to .49 at 8DWS (Figure 9D).

DISCUSSION

GRXS17 is involved in drought stress tolerance as well as multiple additional roles in abiotic stress tolerance and auxin perception and signaling (Hu et al., 2017; Wu et al., 2017; Cheng et al., 2011). Despite this, how the increase or decrease of expression of *GRXS17* impacts metabolic pathways in response to drought stress remains unclear. Paradoxically, both overexpression of *AtGRXS17* in rice and silencing of *OsGRXS17* in rice increased drought tolerance. The result was hypothesized to likely occur through mutually exclusive pathways. Here, we report that *AtGRXS17-expressing* plants consistently showed higher survival rates and better recovery after 8-day drought treatments than their wild type counterparts (Figure 2; Supplemental Figure 2, 3, 4, 5, 6) and, utilizing a nontargeted metabolomics approach, detected differences that occurred in several biochemical groups including amino acids, carbohydrates, lipids, enzyme cofactors, nucleotides, peptides, hormones and secondary metabolites (Figure 3A). Differences in metabolomics profiles between genotypes within amino acids, glutathione metabolism and sulfate assimilation, and carbohydrate metabolism provided insight into the mechanistic action of GRXS17 in response to drought.

Amino acids and their metabolic profiles in plants have been well studied in response to osmotic stress, including drought and salt stress, and tend to increase greatly during stress (Shu et al., 2011; Sanchez et al., 2012). Amino acids have diverse roles as osmolytes, membrane stabilizers, and modulators of enzyme activity (Rai et al., 2002). In response to drought, tolerant genotypes of rice, such as N22, have higher free amino acid accumulation in shoot tissue than susceptible genotypes (Casartelli et al., 2018). At 8DWS, 18 amino acids were detected to increase by drought stress with average values ranging from 1.09 to 14.58-fold increases, while only one amino acid, aspartate, was detected to decrease (Table 1, Figure 4). Amino acids

positively correlated with abiotic stress may be more critical in rice than other species because rice is not able to accumulate glycinebetaine, one of the most important osmolytes, because it lacks a functional copy of choline monooxygenase, the first step in conversion of choline to glycinebetaine (Shirasawa, et al., 2006). Proline, arginine, and glutamate are all important as osmotic adjustors, nitrogen storage compounds, membrane and protein stabilizers. However, proline may play a larger role as an indicator of drought stress than remedy. Exogenous application of ABA induces proline accumulation in Arabidopsis, but only in plants with low water potential (Verslues, 2006). Water potential dependent proline accumulation suggests, in the presence of ABA, proline accumulation is primarily controlled by an alternate mechanism sensing plant water status. Our results indicated that proline followed the trend of previously discussed amino acids and is consistent with our previous work that demonstrated, while proline levels were elevated in all genotypes due to abiotic stress, OE and RNAi plants accumulate much less proline than WT plants despite their increased abiotic stress tolerance (Figure 4C, Hu et al., 2015). Proline is strongly controlled by water status and ROS accumulation tends to be positively correlated with proline accumulation (Liang et al., 2013). OE display significantly less DAB staining than WT, indicating less H2O2 accumulation (Supplemental Figure 6). Amino acids that differed between RNAi and OE were limited to serine, aspartate, and arginine. RNAi accumulated less arginine at 8DWS, more serine at 5DWS, and less aspartate at all timepoints compared to WT (Figure 4C, D, Figure 6). OE had less serine accumulation than wild type at 8DWS and less than RNAi at 5DWS. (Figure 6).

Amino acid accumulation does not always positively correlate with tolerance. As drought stress progresses, protein synthesis decreases resulting in an increased abundance of free amino acids that are negatively correlated to drought stress tolerance. Asparagine, glutamine, serine,

and threonine accumulation are negatively correlated with physiological data including water use efficiency, fresh and dry weights, and yield, in rice (Degenkolbe et al., 2013). Negative correlation of amino acid accumulation and desired traits is witnessed in other plant species as well, as phenylalanine, tyrosine, and glutamine are negatively correlated with biomass accumulation in *Arabidopsis* (Meyer et al., 2007). Given these discrepancies, it is important to distinguish amino acids positively correlated with drought tolerance and those negatively correlated. Interestingly, both OE and RNAi displayed significantly less accumulation of amino acids that are negatively correlated with drought tolerance including asparagine, glutamine, and threonine, than WT at 8DWS. Asparagine displayed the largest differences with RNAi accumulating 18% that of WT and OE accumulating 37% that of WT. Differences in amino acid accumulation patterns may explain the increased relative water content that both transgenic lines consistently displayed (Supplemental Figure 5, Hu et al., 2017).

RNAi lines accumulated an average of .47-fold and .46-fold less aspartate than WT and OE, respectively across timepoints (Figure 4D). Aspartate accumulation has been linked to stomatal opening and the irreversible breakdown of aspartate by aspartate oxidase (AO) was demonstrated to be critical for stomatal closure through the perception of ROS induced by NADPH oxidase RBOHD (Macho et al., 2012). Hu et al. demonstrated RNAi lines accumulate more H_2O_2 within the guard cells, leading to smaller stomatal aperture and lower stomatal conductance, which may provide evidence for lower AO-mediated aspartate content in RNAi. An aspartyl-tRNA ligase-like protein, aspartyl-tRNA synthetase (AspRS), was identified as a potential interacting partner with AtGRXS17 (Knuesting et al., 2015). AspRS catalyzes the synthesis of aspartyl-tRNA from aspartate and tRNA and is active under normal conditions (Luna et al., 2014). When primed by stress, β-aminobutyric acid (BABA) inhibits AspRS, and

aspartate and uncharged tRNA accumulate. BABA is an endogenous stress inducible molecule in plants and BABA-mediated stress tolerance is ABA-dependent (Thevenet et al., 2017; Jakab et al., 2005). RNAi plants accumulate less aspartate across all timepoints, promoting ROS-mediated stomatal signaling and closure.

Serine is a precursor to cysteine and GSH biosynthesis and functions in the primary sulfur assimilation pathway in plants (Chan et al., 2013). In addition to differences in serine content, the secondary sulfur metabolite, adenosine 3'-5'-diphosphate (PAP), content is greatly affected by *GRXS17*-expression but not stress (Figure 6). OE lines accumulate 4.26-fold and 4.99-fold more PAP than RNAi at 0DWS and 5DWS, respectively. PAP is a byproduct of sulfotransferase reactions where 3'-phosphate 5'-phosphosulfate (PAPS) is the sulfuryl group donor and a hydroxyl group is the acceptor in the secondary sulfate assimilation pathway (Klein and Papenbrock, 2004; Hirschmann et al., 2014). This metabolite responded in step with *GRXS17*-expression. That is, OE displayed the highest content and RNAi had the lowest. In *E. coli*, PAPS conversion to PAP by PAPS reductase can be carried out with glutathione-coupled glutaredoxin as a cofactor (Tsang, 1981). An adenosine bisphosphate phosphatase (SAL1), the enzyme that dephosphorylates PAP, loss of function mutant (*alx8*) accumulated more PAP and resulted in increased drought tolerance through the inhibition of nuclear 5' to 3' exoribonucleases (XRNs), thus reducing the post transcriptional deactivation of drought responsive genes (Estavillo et al., 2011). *alx8* plants had lower H_2O_2 accumulation and higher expression of an ascorbate peroxidase gene, *APX2*. *alx8* and *XRN* mutants expressed multiple genes in a similar fashion including genes involved in auxin response, cytokinin response, and sugar and starch metabolism, suggesting PAP is an upstream regulator of XRNs. PAP accumulation was not affected by stress in our study, despite Estavillo et al.'s evidence of a

drought induced PAP increase in wild-type plants. The dephosphorylation of PAP results in adenosine monophosphate (AMP) and an inorganic phosphate group (Pi), which explains the higher phosphate accumulation pattern OE displayed compared to WT and RNAi (Figure 6). High accumulation of Pi in OE lines suggest that increased PAP accumulation in OE was due to increased biosynthesis and not an inhibition of a PAP dephosphorylation enzyme. This data proposes a role for AtGRXS17 in sulfur metabolism and activation of PAP biosynthesis and suggests that the increased drought tolerance of OE plants is due to the effect of PAP accumulation.

GRXs affect cellular redox status utilizing the electrons from GSH by reducing target proteins and ROS accumulation (Wu et al., 2017). Less H_2O_2 accumulation in plant cells results in less oxidative damage to proteins and less protein catabolism (Davies, 2016). GSH synthesis and degradation is dependent upon amino acid biosynthesis and sulfur assimilation, and the cytosol has been implicated as the most important compartment of GSH localization for plant growth and development (Pasternak et al., 2008). Gamma-glutamyl-amino acid dipeptides (GGAA) are the first byproduct of GSH/GSSG degradation and recycling, and generally increase due to strain on the GSH/GSSG system. Our results indicated GSSG accumulated in response to drought in all genotypes, indicating a significant strain on the GSH/GSSG system, and an increase in nine of eleven GGAAs detected (Figure 5, Table 2). Compared to WT, RNAi accumulated less GG-methionine and GG-glutamine at 8DWS, less GG-tryptophan at 5DWS, and more GG-alanine, only at 0DWS and 5DWS. Like RNAi, OE accumulated less GG-methionine and GG-glutamine than wild type at 8DWS (Figure 5). Despite only four statistically significant GGAA genotype effects, in all but one (GG-leucine) of the nine GGAAs that increased, both RNAi and OE had a lower mean value at 8DWS. Overall, RNAi and OE have

less total accumulation of GGAAs, indicating less GSH degradation. Consistently, an oxidized cysteine-glycine dipeptide (cys-gly) was demonstrated as an indicator of gamma-glutammyl transferase (GGT)-mediated GSH degradation (Ferretti et al., 2009). Our results indicated that OE has less cys-gly accumulation than WT at 5DWS suggesting less degradation of GSH (Figure 5). Two pathways for GSH recycling are known, operating in the apoplast and the cytosol, with the latter accounting for most GSSH turnover (Masi et al., 2015; Ohkama-Ohtsu et al., 2008). In the cytosolic pathway, GSSH degradation must produce 5OP and cys-gly. 5OP content is lower in OE and RNAi than WT at 8DWS and cys-gly is lower in OE than WT at 5DWS, further suggesting less degradation and altered GSH pathways. It was hypothesized that glutaredoxins may be able to modulate a key enzyme in GSH synthesis, glutamate cysteine ligase, due to the similar redox potential similarities (Galant et al., 2011). However, no differences between genotypes were detected in cysteine or glutamine content and GG-cysteine was undetected in this study (Figure 5). Taken together, this data suggests that RNAi and OE lines modulate GSH recycling to effectively decrease ROS accumulation.

Soluble sugar accumulation and photosynthesis inhibition is a well-known effect of drought stress (Munns, 2002). Raffinose, fructose, glucose, and sucrose all increased dramatically by 8DWS and no differences between genotypes were detected at this time point (Figure 7). Raffinose, the first product of the RFO family, increased 3.3-fold followed by fructose, glucose, and sucrose increasing 2.5, 2.5, and 1.3-fold, respectively (Table 3A; Figure 7). Accumulation of these sugars reduces osmotic potential, helps stabilize macromolecules and organelles, and prevents oxidation of macromolecules through the reduction of hydroxyl radicals (Nishizawa-Yokoi et al., 2008). Galactinol accounted for the largest increase at 5DWS and 8DWS (Table 3A). RFOs have well-documented roles in abiotic stress tolerance. Overexpression

of an *Arabidopsis* galactinol synthase, *AtGolS2*, in *Arabidopsis* resulted in increased galactinol and raffinose content, and increased drought tolerance (Taji et al, 2002). In *Arabidopsis*, raffinose and galactinol drastically increased in response to overexpression of heat shock factors, methyl viologen treatments, and overexpression of a galactinol synthase, resulting in less lipid peroxidation and increased chlorophyll fluorescence (Nishizawa et al., 2008). Our results indicated galactinol increased 18.32 fold by 8DWS and no genotypic differences existed at 8DWS (Table 3B, C; Figure 8). OE differed from WT and RNAi at 0DWS displaying less than half the galactinol accumulation. OE also had less fructose and glucose than WT at 0DWS and had more accumulation of galactinol upstream precursors UDP-galactose and UDP-glucose at 5DWS and 8DWS (Table 3B, C; Figure 7; Figure 8).

The disaccharide sucrose can be degraded through two separate pathways. Invertase (Inv) degradation results in the hydrolyses of sucrose to yield glucose and fructose. Sucrose synthase (SUS) catalyzes the reversible synthesis of sucrose and activity in the cleavage direction yields a UDP-glucose molecule and a fructose molecule from sucrose. Sucrose degradation through Inv or SUS has been demonstrated to have signaling implications for plant growth and development (Ruan, 2012). Our results indicated sucrose degradation preferentially went through the Inv pathway as drought stress progressed, evident by the decrease in UDP-glucose as it was metabolized to RFO, as well as the simultaneous increase of glucose and fructose (Table 3A; Figure 7; Figure 8). As drought stressed progressed it was clear that OE lines maintained more UDP-glucose and UDP-galactose than both other genotypes at 5DWS, and maintained over 3-fold higher levels than RNAi at 8DWS (Table 3B, C; Figure 8). Together, this suggests that expression levels of *GRXS17* impact sucrose degradation pathways. This agrees with a previous report indicating that AtGRXS17 may be an interacting partner with an *Arabidopsis* sucrose

synthase (Knuesting et al., 2015). The link between redox status, thiol groups, and sugar signaling has been well studied. Thiol groups capable of thiol-disulfide exchange reduce, and activate or inactivate, proteins involved in carbohydrate metabolism. These proteins sense the redox status of the cell because they are highly reduced in a highly reduced environment, and vice versa, and are able to react accordingly (Griffiths et al., 2016). It is plausible that AtGRXS17 interacts with and reduces SUS through monothiol mechanisms. Indeed, it was previously reported that wheat SUS could interact with GSH/GSSG and a thioredoxin (TRX) through thiol-disulfide exchange. SUS cleavage to synthesis ratios increase when incubated with GSH, resulting in breakdown of sucrose to UDP-glucose and fructose, while SUS incubated with oxidized TRX or GSSG results in decreased cleavage to synthesis ratios (Pontis et al., 1981). Therefore, SUS reduced through thio-disulfide exchange has higher cleavage ratios and higher UDP-glucose production. Our results suggest AtGRXS17 was able to reduce SUS and maintain higher levels of UDP-glucose as drought stress progressed. This potential interaction provides additional evidence for the less oxidized status of OE plants. Altered sucrose degradation activity in other species has been shown to impact floral development, leaf development, pollen viability, and seed development, all topics in which GRXs are implicated (Ruan, 2012). For example, sugar metabolism mediated by SUS1 and SUS4 is necessary for photoperiod responsive flowering (Seo et al., 2011). It is also well documented that sugar signaling impacts auxin biosynthesis, transport, and signaling as well as cell cycle control (Mishra et al., 2009; LeClere et al., 2010; Slewinski, 2011). *Arabidopsis* loss of function *atgrxs17* mutants lack the ability to respond to heat stress through reduced auxin perception, transport, and signaling, and mutant lines displayed altered cell cycle control and abnormal flowering patterns in response to temperature and photoperiod (Cheng et al., 2011; Knuesting et al., 2015). UDP-glucose is a

signaling molecule in plants involved in programmed cell death and ROS signaling (Janse van Rensburg and Van den Ende, 2017). It is conceivable that the *atgrxs17* mutant line's phenotype is at least partially attributable to reduced regulation of SUS and subsequent UDP-glucose sugar signaling pathways. Our results indicated overexpression of *AtGRXS17* results in increased UDP-glucose content, possibly through modulation of SUS activity, resulting in altered signaling pathways.

Soluble sugar and sugar alcohol accumulation further reduce photosynthetic activity as negative regulators of photosynthesis (Xiao et al., 2000). Our results indicated that several key metabolites within glycolysis and the citric acid cycle pathways declined significantly while many soluble sugars increased. Of the 7 citric acid cycle metabolites that changed, 6 decreased, and a Calvin cycle metabolite decreased (Table 4; Figure 9). The glycolysis metabolite pyruvate was one of the few metabolites that increased by 8DWS and RNAi experienced the largest increase at 1.95-fold. Pyruvate, and the translocation into the mitochondrion via a mitochondrial pyruvate shuttle, has been implicated as a negative regulator of stomatal closure (Wang, et al., 2014). That is, if pyruvate is shuttled into the mitochondrion and broken down, stomatal closure is inhibited. Conversely, if pyruvate is not shuttled into the mitochondrion and accumulates in the cytosol, ABA signaling is amplified and stomatal closure is enhanced (Li et al., 2014). Pyruvate dehydrogenase activity affects pyruvate accumulation and pyruvate dehydrogenase kinase activity is regulated through both thiol-disulfide interactions and phosphorylation (Pettit, et al., 1982). The dramatic increase in pyruvate RNAi lines displayed, may provide a further link between GRXS17-mediated metabolic pathways and the documented increased ABA sensitivity and stomatal closure (Hu et al., 2017). Citric acid cycle intermediates significantly decrease due to stress and may be partially explained by the increase of amino acids derived from alpha-

ketoglutarate. Citrate and isocitrate, two upstream precursors to alpha-ketoglutarate derived amino acid biosynthesis, decreased to .39-fold and .01-fold respectively, coinciding with the increase in glutamate, glutamine, and proline. The only difference between genotypes detected for citric acid cycle intermediates was fumarate. The greatest difference between means was between OE and RNAi, with RNAi accumulating 1.7-fold more. Fumarate accumulation may be related to the decrease in aspartate that RNAi experienced. Fumarate is an upstream precursor in oxaloacetate dependent aspartate synthesis in the citric acid cycle, a bottleneck at this stage, in RNAi, could provide an alternative hypothesis for the reduced accumulation of aspartate. Additionally, pyruvate can be carboxylated to oxaloacetate, but, as discussed above, RNAi accumulated pyruvate under drought stress suggesting a bottleneck. This data suggests that GRXS17 mediated redox status is a regulator of citric acid cycle steps.

REFERENCES

Allen, R.D. (1995) Dissection of oxidative Stress Tolerance Using Transgenic Plants. *Plant Physiology* 107: 1049-1054.

Bishwajit, G., Sarker, S., Kpoghomou, M.A., Gao, H., Jun, L., Yin, D., Ghosh, S. (2013) Self-sufficiency in rice and food security: a South Asian perspective. *Agriculture & Food Security* (2013) 2: 10.

Blum, A. (2017) Osmotic adjustment is a prime drought stress adaptive engine in support of plant production. *Plant, Cell & Environment* 40: 4–10.

Bruinsma, J., Alexandratos, N. (2012) *World Agriculture: Towards 2030/2050*. (Global Perspective Studies Unit, Food and Agriculture Organization of the United Nations, Rome).

Casartelli, A., Riewe, D., Hubberten, H.M., Altmann, T., Hoefgen, R., Heuer, S. (2018) Exploring traditional aus-type rice for metabolites conferring drought tolerance. *Rice* 11:9.

Chan, K.X., Wirtz, M., Phua, S.Y., Estavillo, G.M., Pogson, B.J. (2013) Balancing metabolites in drought: the sulfur assimilation conundrum. *Trends in Plant Science* 18: 18-29.

Charlton, A.J., Donarski, J.A., Harrison, M., Jones, S.A., Godward, J., Oehlschlager, S., Arques, J.L., Ambrose, M., Chinoy, C., Mullineaux, P.M., Domoney, C. (2008) Responses of the pea (*Pisum sativum* L.) leaf metabolome to drought stress assessed by nuclear magnetic resonance spectroscopy. *Metabolomics* 4: 312.

Cheng, N.H.,1, Liu, J.Z., Liu, X., Wu, Q., Thompson, S.M., Lin, J., Chang, J., Whitham, S.A., Park, S.H., Cohen, J.D., Hirschi, K.D. (2011) Arabidopsis Monothiol Glutaredoxin, AtGRXS17,

Is Critical for Temperature-dependent Postembryonic Growth and Development via Modulating Auxin Response. *The Journal of Biological Chemistry* 286: 20398-20406.

Davies, M.J. (2016) Protein oxidation and peroxidation. *Biochemical Journal*. 473(7):805-825.

Degenkolbe, T., Do, P.T., Kopka, J., Zuther, E., Hincha D.K., Köhl, K.I. (2013) Identification of Drought Tolerance Markers in a Diverse Population of Rice Cultivars by Expression and Metabolite Profiling. *PLOS ONE* 8(5): e63637.

Di Martino, C., Delfine, S., Pizzuto, R., Loreto, F., Fuggi, A. (2003) Free amino acids and glycine betaine in leaf osmoregulation of spinach responding to increasing salt stress. *New Phytologist* 158: 455-463.

Estavillo, G.M., Crisp, P.A., Pornsiriwong, W., Wirtz, M., Collinge, D., Carrie, C., Giraud, E., Whelan, J., David, P., Javot, H., Brearley, C., Hell, R., Marin, E., Pogson, B.J.. (2011) Evidence for a SAL1-PAP Chloroplast Retrograde Pathway That Functions in Drought and High Light Signaling in Arabidopsis. The Plant Cell 23(11):3992-4012.

Ferretti, M., Destro, T., Tosatto, S. C., La Rocca, N., Rascio, N. Masi, A. (2009) Gamma-glutamyl transferase in the cell wall participates in extracellular glutathione salvage from the root apoplast. *New Phytologist* 181: 115-126.

Galant, A., Preuss, M.L., Cameron, J.C., Jez, J.M. (2011) Plant Glutathione Biosynthesis: Diversity in Biochemical Regulation and Reaction Products. *Frontiers in Plant Science* 2:45.

Gill, S.S., Tuteja, N. (2010) Reactive oxygen species and antioxidant machinery in abiotic stress tolerance in crop plants. *Plant Physiology and Biochemistry* 48:909-930.

Griffiths, C.A., Paul, M.J., Foyer, C.H. (2016) Metabolite transport and associated sugar signaling systems underpinning source/sink interactions. *Biochimica et Biophysica Acta* 1857(10):1715-1725.

Yu, H., Yang, J., Shi, Y., Donelson, J., Thompson, S.M., Sprague, S., Roshan, T., Wang, D.-L., Liu, J., Park, S., Nakata, P.A., Connolly, E.L., Hirschi, K.D., Grusak, M.A., Cheng, N. (2017) Arabidopsis Glutaredoxin S17 Contributes to Vegetative Growth, Mineral Accumulation, and Redox Balance during Iron Deficiency. *Frontiers in Plant Science*. 8:1045.

Hu, Y., Wu, Q., Peng, Z., Sprague, S.A., Wang, W., Park, J., Akhunov, E., Jagadish, K.S.V., Nakata, P.A., Cheng, N.H., Hirschi, K.D., White, F.F., Park, S.H. (2017) Silencing of OsGRXS17 in rice improves drought stress tolerance by modulating ROS accumulation and stomatal closure. *Scientific Reports* 7: 15950.

Hu, Y., Wu, Q., Sprague, S.A., Park, J., Oh, M., Rajashekar, C.B., Koiwa, H., Nakata, P.A., Cheng, N.H., Hirschi, K.D., White, F.F., Park, S.H. (2015) Tomato expressing Arabidopsis glutaredoxin gene AtGRXS17 confers tolerance to chilling stress via modulating cold responsive components. *Horticulture Research* 2: 15051.

Hirschmann, F., Krause, F., Papenbrock, J. (2014) The multi-protein family of sulfotransferases in plants: composition, occurrence, substrate specificity, and functions. *Frontiers in Plant Science* 5:556.

Irino, Y., Toh, R., Nagao, M., Mori, T., Honjo, T., Shinohara, M., Tsudu, S., Nakajima, H., Satomi-Kobayashi, S., Shinke, T., Tanaka, H., Ishida, T., Miyata, O., Hirata, K.(2016) 2-Aminobutyric acid modulates glutathione homeostasis in the myocardium. *Scientific Reports*. 6:36749.

Jakab, G., Ton, J., Flors, V., Zimmerli, L., Métraux, J.P., Mauch-Mani, B. (2005) Enhancing Arabidopsis Salt and Drought Stress Tolerance by Chemical Priming for Its Abscisic Acid Responses. *Plant Physiology* 139(1): 267-274.

Janse van Rensburg, H.C., Van den Ende, W. (2017) UDP-Glucose: A Potential Signaling Molecule in Plants?. *Frontiers in Plant Science* 8: 2230.

Klein, M., Papenbrock, J. (2004) The multi-protein family of Arabidopsis sulphotransferases and their relatives in other plant species. *Journal of Experimental Botany* 55:1809–1820.

Knuesting, J., Riondet, C., Maria, C., Kruse, I., Becuwe, N., Konig, N., Berndt, C., Tourrette, S., Guilleminot-Montoya, J., Herrero, E., Gaymard, F., Balk, J., Belli, G., Scheibe, R., Reichheld, J.P., Rouhier, N., Rey, P. (2015) Arabidopsis Glutaredoxin S17 and its partner the nuclear factor Y subunit C11/Negative Cofactor 2 alpha, contribute to maintenance of the shoot apical meristem under long-day photoperiod. *Plant Physiology*. 167: 1643-U1822.

LeClere, S., Schmelz, E.A., Chourey, P.S. (2010) Sugar Levels Regulate Tryptophan-Dependent Auxin Biosynthesis in Developing Maize Kernels. *Plant Physiology* 153(1): 306-318.

Li, C.L., Wang, M., Ma, X.Y., Zhang, W. (2014) NRGA1, a Putative Mitochondrial Pyruvate Carrier, Mediates ABA Regulation of Guard Cell Ion Channels and Drought Stress Responses in Arabidopsis. *Molecular Plant* 7: 1508-1521.

Liang, X., Zhang, L., Natarajan, S. K., & Becker, D. F. (2013). Proline Mechanisms of Stress Survival. *Antioxidants & Redox Signaling* 19(9): 998–1011.

Luna, E., van Hulten, M., Zhang, Y., Berkowitz, O., López, A., Pétriacq, P., et al. (2014) Plant perception of β-aminobutyric acid is mediated by an aspartyl-tRNA synthetase. *Nature Chemical Biology* 10: 450-456.

Macho, A.P., Boutrot, F., Rathjen, J. P., Zipfel, C. (2012). ASPARTATE OXIDASE Plays an Important Role in Arabidopsis Stomatal Immunity. *Plant Physiology* 159(4): 1845–1856.

Masi, A., Trentin, A.R., Agrawal, G.K., Rakwal, R. (2015) Gamma-glutamyl cycle in plants: a bridge connecting the environment to the plant cell? *Frontiers in Plant Science* 6:252.

Meyer, R.C., Steinfath, M., Lisec, J., Becher, M., Witucka-Wall, H., Törjék, O., Fiehn, O., Eckardt, Ä., Willmitzer, L., Selbig, J., Altmann, T. (2007) The metabolic signature related to high plant growth rate in Arabidopsis thaliana. *Proceedings of the National Academy of Sciences* 104 (11): 4759-4764.

Mishra, B.S., Singh, M., Aggrawal, P., Laxmi, A. (2009) Glucose and Auxin Signaling Interaction in Controlling Arabidopsis thaliana Seedlings Root Growth and Development. *PLOS ONE* 4(2): e4502.

Munns, R. (2002) Comparative physiology of salt and water stress. *Plant, Cell & Environment* 25: 239-250.

Nelson, D.E., Repetti, P.P., Adams, T.R., Creelman, R.A., Wu, J., Warner, D.C., Anstrom, D.C., et al. (2007) Plant nuclear factor Y (NF-Y) B subunits confer drought tolerance and lead to improved corn yields on water-limited acres. *Proceedings of the National Academy of Sciences* 104: 16450-16455.

Nishizawa-Yokoi, A., Yabuta, Y., Shigeoka, S. (2008) The contribution of carbohydrates including raffinose family oligosaccharides and sugar alcohols to protection of plant cells from oxidative damage. *Plant Signaling & Behavior* 3(11):1016-1018.

Nishizawa, A., Yabuta, Y., Shigeoka, S. (2008) Galactinol and Raffinose Constitute a Novel Function to Protect Plants from Oxidative Damage. *Plant Physiology* 147(3):1251-1263.

Naoko, O.O., Oikawa, A., Zhao, P., Xiang, C., Saito, K., Oliver, D.J. (2008) A γ-Glutamyl Transpeptidase-Independent Pathway of Glutathione Catabolism to Glutamate via 5-Oxoproline in Arabidopsis. *Plant Physiology* 148(3):1603-1613.

Passioura John. (2007) The drought environment: physical, biological and agricultural perspectives. Journal of Experimental Botany 58: 113–117.

Pasternak, M., Lim, B., Wirtz, M., Hell, R., Cobbett, C.S., Meyer, A.J. (2008) Restricting glutathione biosynthesis to the cytosol is sufficient for normal plant development. *The Plant Journal* 53: 999-1012.

Pettit, F.H., Humphreys, J., Reed, L.J. (1982) Regulation of pyruvate dehydrogenase kinase activity by protein thiol-disulfide exchange. *Proceedings of the National Academy of Sciences* 79(13): 3945-3948.

Pontis, H.G., Babio, J.R., Salerno, G. (1981) Reversible unidirectional inhibition of sucrose synthase activity by disulfides. *Proceedings of the National Academy of Sciences* 78(11): 6667-6669.

Rai, V. (2002) Role of Amino Acids in Plant Responses to Stresses. *Biologia Plantarum* 45: 481.

Ramanjulu, S., Sudhakar, C. (1997) Drought tolerance is partly related to amino acid accumulation and ammonia assimilation: A comparative study in two mulberry genotypes differing in drought sensitivity. *Journal of Plant Physiology* 150: 345-350.

Rampino, P., Pataleo, S, Gerardi, C., Mita, G., Perrotta, C. (2006) Drought stress response in wheat: physiological and molecular analysis of resistant and sensitive genotypes. *Plant, Cell & Environment* 29: 2143-2152.

Reddy, A.R., Chaitanya, K.V., Vivekanandan, M. (2004) Drought-induced responses of photosynthesis and antioxidant metabolism in higher plants. *Journal of Plant Physiology* 161: 1189-1202.

Ruan, Y.L. (2012) Signaling Role of Sucrose Metabolism in Development. *Molecular Plant* 5: 763-765.

Sanchez, D.H., Schwabe, F., Erban, A., Udvardi, M.K., Kopka, J. (2012) Comparative metabolomics of drought acclimation in model and forage legumes. *Plant, Cell & Environment* 35: 136-149.

Seo, P.J., Ryu, J., Kang, S.K., Park, C. (2011) Modulation of sugar metabolism by an INDETERMINATE DOMAIN transcription factor contributes to photoperiodic flowering in Arabidopsis. *The Plant Journal* 65: 418-429.

Shirawawa, K., Takabe, T., Kishitani, S. (2006) Accumulation of Glycinebetaine in Rice Plants that Overexpress Choline Monooxygenase from Spinach and Evaluation of their Tolerance to Abiotic Stress. *Annals of Botany* 98(3):565-571.

Shu, L., Lou, Q., Ma, C., Ding, W., Zhou, J., Wu, J., Feng, F., Lu, X., Luo, L., Xu, G., Mei, H. (2011) Genetic, proteomic and metabolic analysis of the regulation of energy storage in rice seedlings in response to drought. *Proteomics* 11: 4122-4138.

Slewinski, T.L. (2011) Diverse Functional Roles of Monosaccharide Transporters and their Homologs in Vascular Plants: A Physiological Perspective. *Molecular Plant* 4:641-662.

Steward, D.R., Bruss, P.J., Yang, X., Staggenborg, S.A., Welch, S.M., Apley, M.D. (2013) Tapping groundwater stores for agriculture. *Proceedings of the National Academy of Sciences* 110: E3477-E3486.

Taji, T., Ohsumi, C., Iuchi, S., Seki, M., Kasuga, M., Kobayashi, M., Yamaguchi-Shinozaki, K., Shinozaki, K. (2002) Important roles of drought- and cold-inducible genes for galactinol synthase in stress tolerance in Arabidopsis thaliana. *The Plant Journal* 29: 417-426.

Thevenet, D., Pastor, V., Baccelli, I., Balmer, A., Vallat, A., Neier, R., Glauser, G., Mauch-Mani, B. (2017) The priming molecule β-aminobutyric acid is naturally present in plants and is induced by stress. *New Phytologist* 213: 552-559.

Thiry, A.A., Chavez Dulanto, P.N., Reynolds, M.P., Davies, W.J. (2016) How can we improve crop genotypes to increase stress resilience and productivity in a future climate? A new crop screening method based on productivity and resistance to abiotic stress. *Journal of Experimental Botany* 67: 5593–5603.

Tsang, M.L. (1981) Assimilatory sulfate reduction in Escherichia coli: identification of the alternate cofactor for adenosine 3'-phosphate 5'-phosphosulfate reductase as glutaredoxin. *Journal of Bacteriology*. 146:3 1059-1066.

Valliyodan, B., Nguyen, H.T. (2006) Understanding regulatory networks and engineering for enhanced drought tolerance in plants. *Current Opinion in Plant Biology* 9:189-195.

Van Breusegem, F., Dat, J.F. (2006) Reactive Oxygen Species in Plant Cell Death. *Plant Physiology* 141: 384-390.

Verslues, P.E., Bray, E.A. (2006) Role of abscisic acid (ABA) and Arabidopsis thaliana ABA-insensitive loci in low water potential-induced ABA and proline accumulation. *Journal of Experimental Botany* 57: 201–212.

Wang, M., Ma, X., Shen, J., Li, C., Zhang, W. (2014) The ongoing story: the mitochondria pyruvate carrier 1 in plant stress response in Arabidopsis. *Plant Signaling & Behavior* 9:10.

Witt, S., Galicia, L., Lisec, J., Cairns, J., Tiessen, A., Araus, J.L., Palacios-Rojas, N., Fernie, A.R. (2012) Metabolic and Phenotypic Responses of Greenhouse-Grown Maize Hybrids to Experimentally Controlled Drought Stress. *Molecular Plant* 5:401 – 417.

Wu, Q., Yang, J., Cheng, N.H., Hirschi, K.D., White, F.F., Park, S.H. (2017) Glutaredoxins in plant development, abiotic stress response, and iron homeostasis: From model organisms to crops. *Environmental and Experimental Botany* 139: 91-98.

Wu, Q., Lin, J., Liu, J., Wang, X., Lim, W., Oh, M., Park, J., Rajashekar, C.B., Whitham, S. A., Cheng, N., Hirschi, K.D., Park, S. (2012) Ectopic expression of Arabidopsis glutaredoxin AtGRXS17 enhances thermotolerance in tomato. *Plant Biotechnology Journal* 10: 945-955.

Wu, Q., Hu, Y., Sprague, S.A., Kakeshpour, T., Park, J., Nakata, P.A., Cheng, N.H., Hirschi, K.D., White, F.F., Park, S.H. (2017) Expression of a monothiol glutaredoxin, AtGRXS17, in

tomato (Solanum lycopersicum) enhances drought tolerance. *Biochemical and Biophysical Research Communications* 491:1034-1039.

Xiao, W., Sheen, J. & Jang, JC. (2000) The role of hexokinase in plant sugar signal transduction and growth and development. *Plant Molecular Biology* 44: 451.

Yue, B., Xue, W., Xiong, L., Yu, X., Luo, L., Cui, K., Jin, D., Xing, Y., Zhang, Q. (2006) Genetic Basis of Drought Resistance at Reproductive Stage in Rice: Separation of Drought Tolerance From Drought Avoidance. *Genetics* 172: 1213-1228.

Zhang, J., Jia, W., Yang, J., Ismail, A.M. (2006) Role of ABA in integrating plant responses to drought and salt stresses. *Field Crops Research* 97: 111-119.

FIGURES

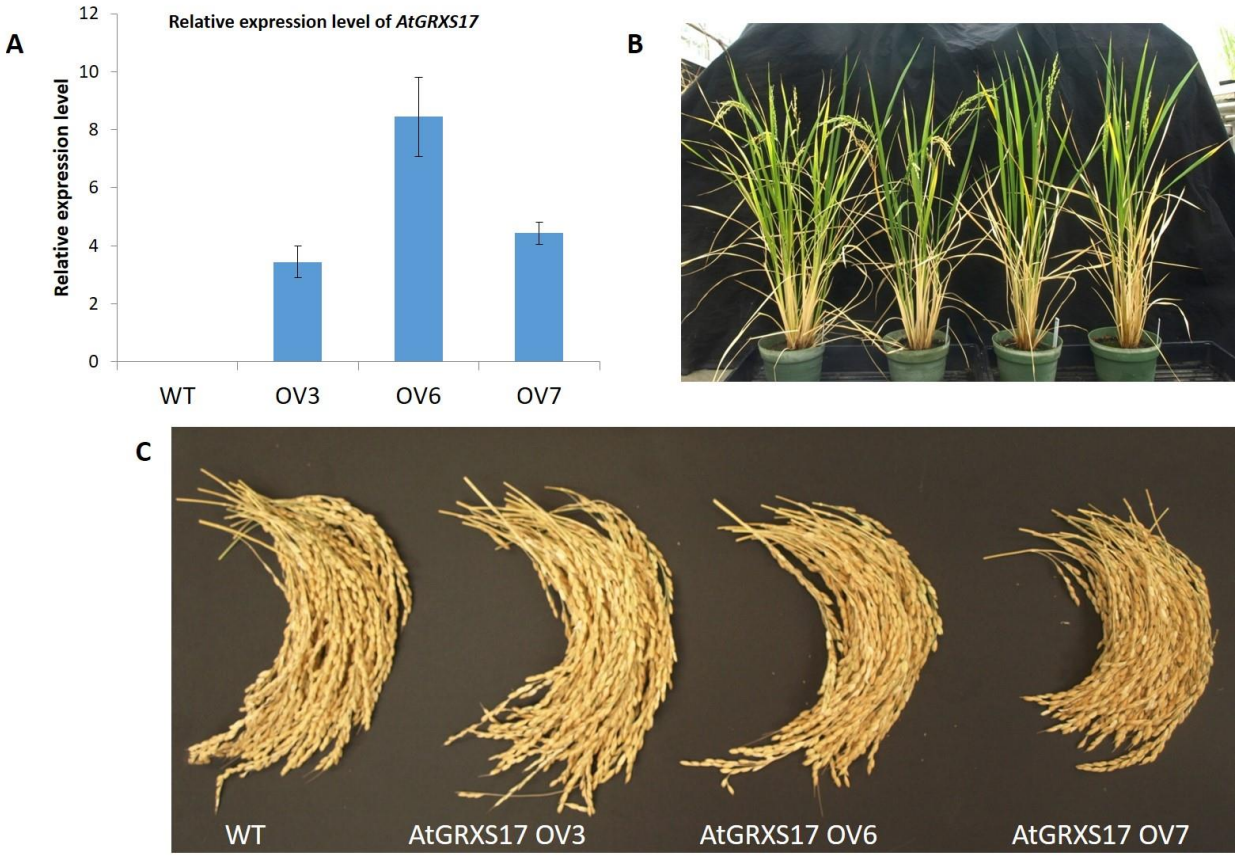

Figure 2. 15 *AtGRXS17*-expressing rice plants are phenotypically indistinguishable from wild-type plants.

(A) Relative expression levels of *AtGRXS17* in lines -3, -6, and -7 and (B) growth and general morphology (C) and grain yield was analyzed. Error bars indicate mean ± SD (n=3).

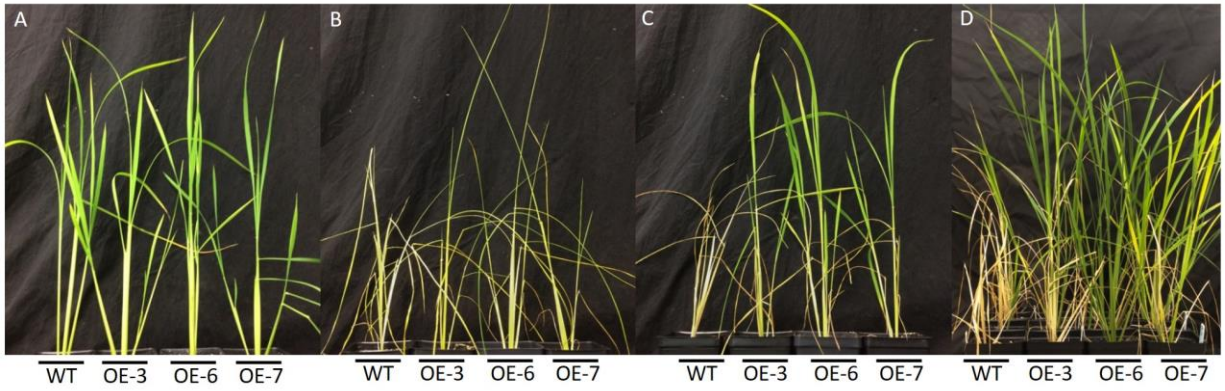

Figure 16 *AtGRXS17*-expressing plants are more drought tolerant than wild-type plants. Uniform rice plants at the two tiller stage are assessed for drought tolerance. (A) Two-tiller stage rice plants are indistinguishable from one another before drought treatment. (B) Rice plants 8 days after withholding water. (C) OE rice plants recover after one week and (D) some WT plants re-grow from new tillers several weeks later.

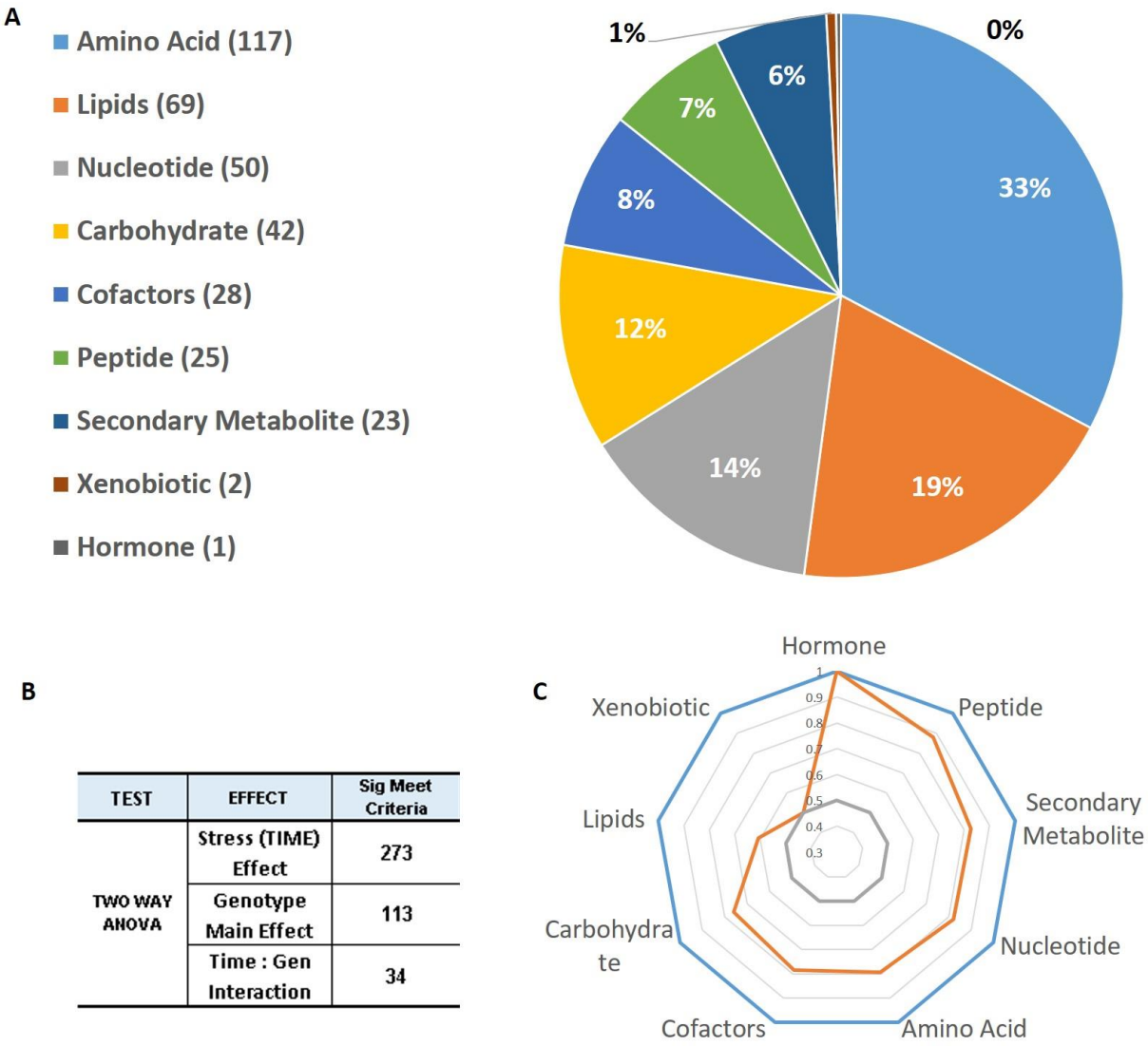

TEST	EFFECT	Sig Meet Criteria
TWO WAY ANOVA	Stress (TIME) Effect	273
	Genotype Main Effect	113
	Time : Gen Interaction	34

Figure 17 The rice metabolome is significantly impacted by drought stress and GRXS17 expression.

(A) 357 metabolites were detected and categorized into groups. (B) 273 metabolites were affected by stress and 113 were affected by *GRXS17*-expression. (C) Proportion of metabolites affected by stress to total metabolites within each categorized group. Most metabolite groups had a large proportion affected by stress.

Amino acid	Stress p val	8DWS
tryptophan	3.00E-15	14.58
histidine	1.21E-11	7.34
proline	1.56E-13	7.04
isoleucine	7.49E-12	5.61
leucine	2.23E-11	4.80
valine	8.17E-13	4.24
glycine	3.51E-13	2.36
phenylalanine	1.18E-06	2.25
lysine	5.08E-07	1.83
glutamine	2.93E-06	1.77
arginine	0.0002	1.70
tyrosine	6.16E-05	1.62
methionine	7.22E-05	1.38
alanine	5.48E-05	1.25
threonine	1.32E-05	1.23
glutamate	0.0211	1.20
serine	0.0014	1.19
asparagine	1.28E-07	1.09
aspartate	0.0003	0.75

Table 2. 1 Amino acid profiles at 8 days of water stress.

Fold increase at 8DWS of all amino acids detected to change in response to drought stress. P-values for stress effect from two-way ANOVA are reported.

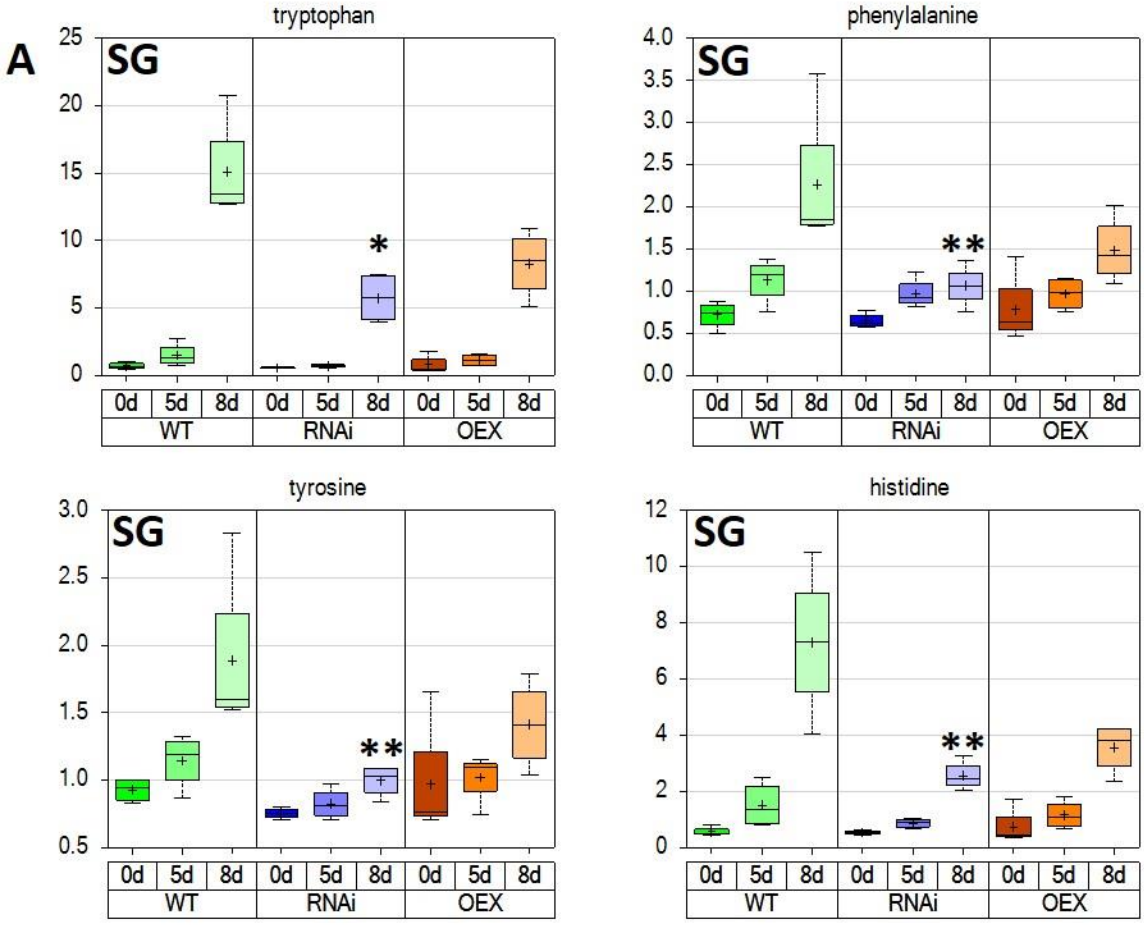
A
tryptophan
SG
25
20
15
10
5
0
*
0d 5d 8d 0d 5d 8d 0d 5d 8d
WT RNAi OEX
phenylalanine
SG
4.0
3.5
3.0
2.5
2.0
1.5
1.0
0.5
0.0
**
0d 5d 8d 0d 5d 8d 0d 5d 8d
WT RNAi OEX
tyrosine
SG
3.0
2.5
2.0
1.5
1.0
0.5
**
0d 5d 8d 0d 5d 8d 0d 5d 8d
WT RNAi OEX
histidine
SG
12
10
8
6
4
2
0
**
0d 5d 8d 0d 5d 8d 0d 5d 8d
WT RNAi OEX

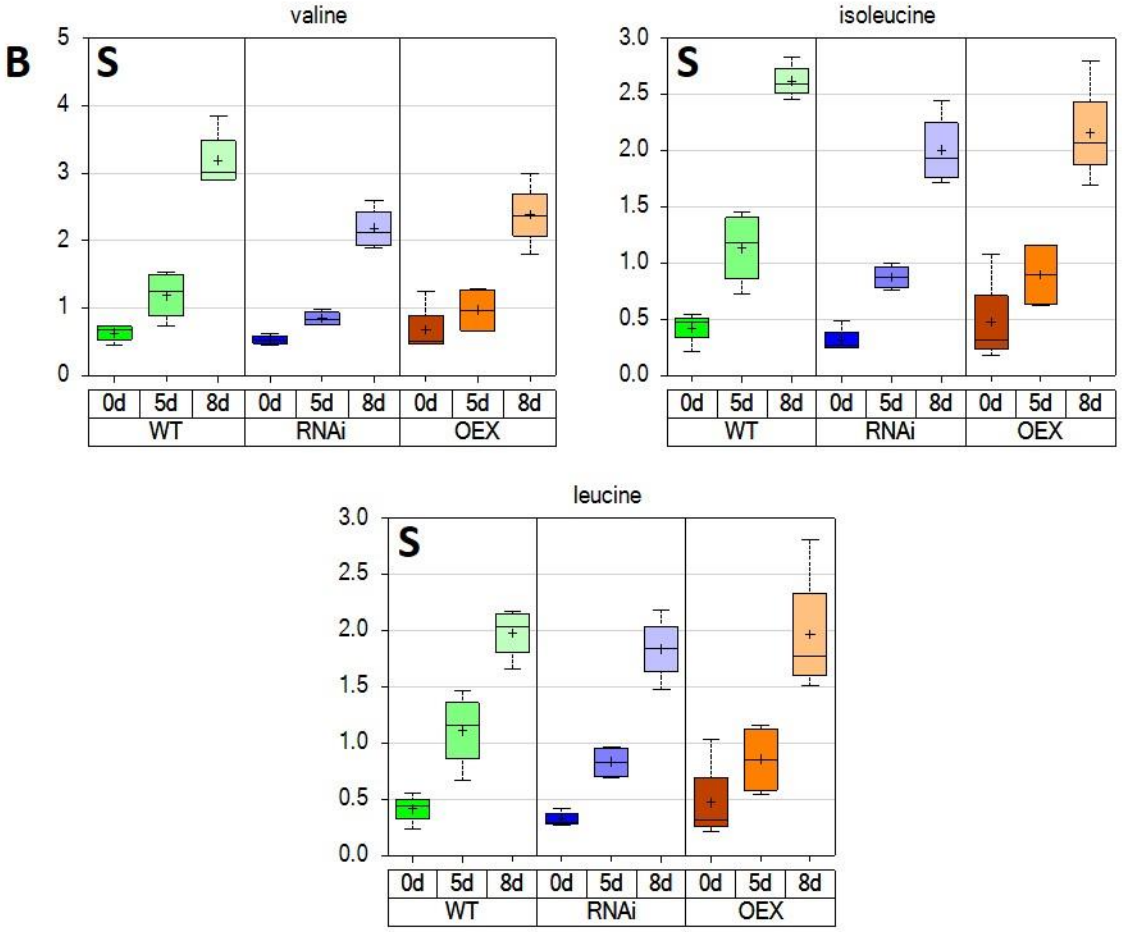
B
valine
S
5
4
3
2
1
0
0d 5d 8d 0d 5d 8d 0d 5d 8d
WT RNAi OEX
isoleucine
S
3.0
2.5
2.0
1.5
1.0
0.5
0.0
0d 5d 8d 0d 5d 8d 0d 5d 8d
WT RNAi OEX
leucine
S
3.0
2.5
2.0
1.5
1.0
0.5
0.0
0d 5d 8d 0d 5d 8d 0d 5d 8d
WT RNAi OEX

C

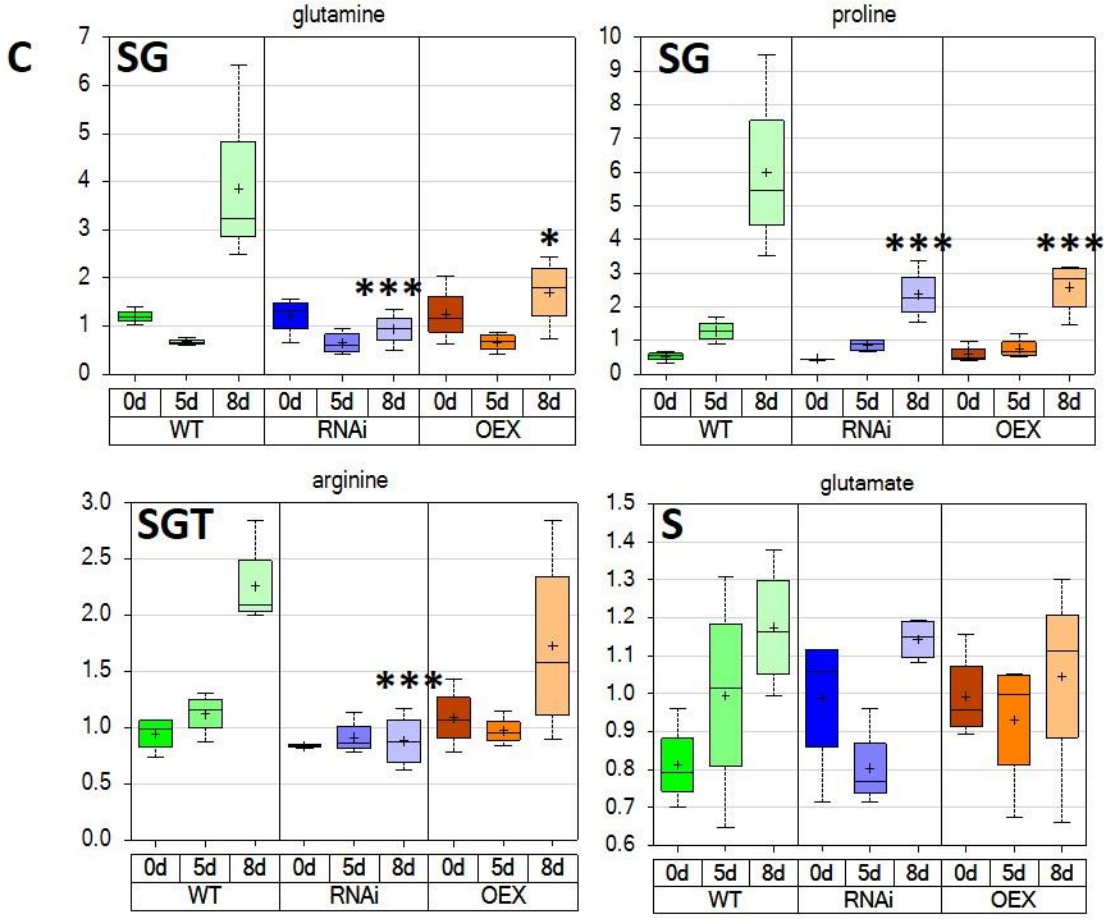
glutamine
SG
***
*
proline
SG
***
***
arginine
SGT
***
glutamate
S
0d
5d
8d
WT
RNAi
OEX

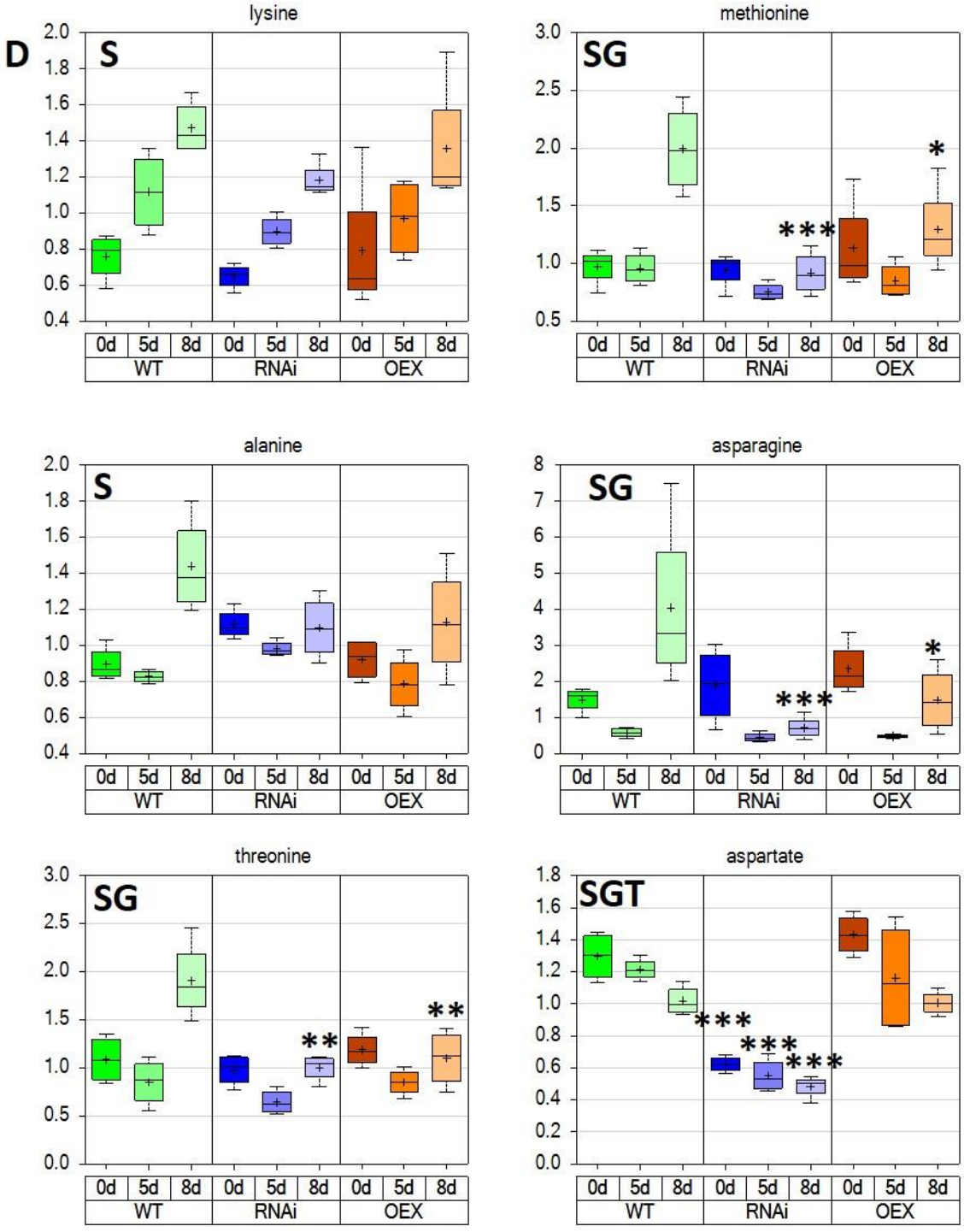
D
lysine
S
methionine
SG
alanine
S
asparagine
SG
threonine
SG
aspartate
SGT
0d
5d
8d
WT
RNAi
OEX

Figure 18 Amino acids profiles in response to drought stress and GRXS17 expression. (A) Aromatic, (B) branched chain, (C) glutamate family and (D) aspartate family amino acids are significantly affected by drought stress. Data were analyzed using two-way ANOVA and Student's t-test. S denotes a significant change due to stress ($p \leq .05$); G denotes a significant effect of *GRXS17* expression ($p \leq .05$); T denotes significant differences between OE and RNAi within the same time point ($p \leq .05$). Asterisks denote difference between WT within the same time point (*P<0.05, **P<0.01, ***P<.001).

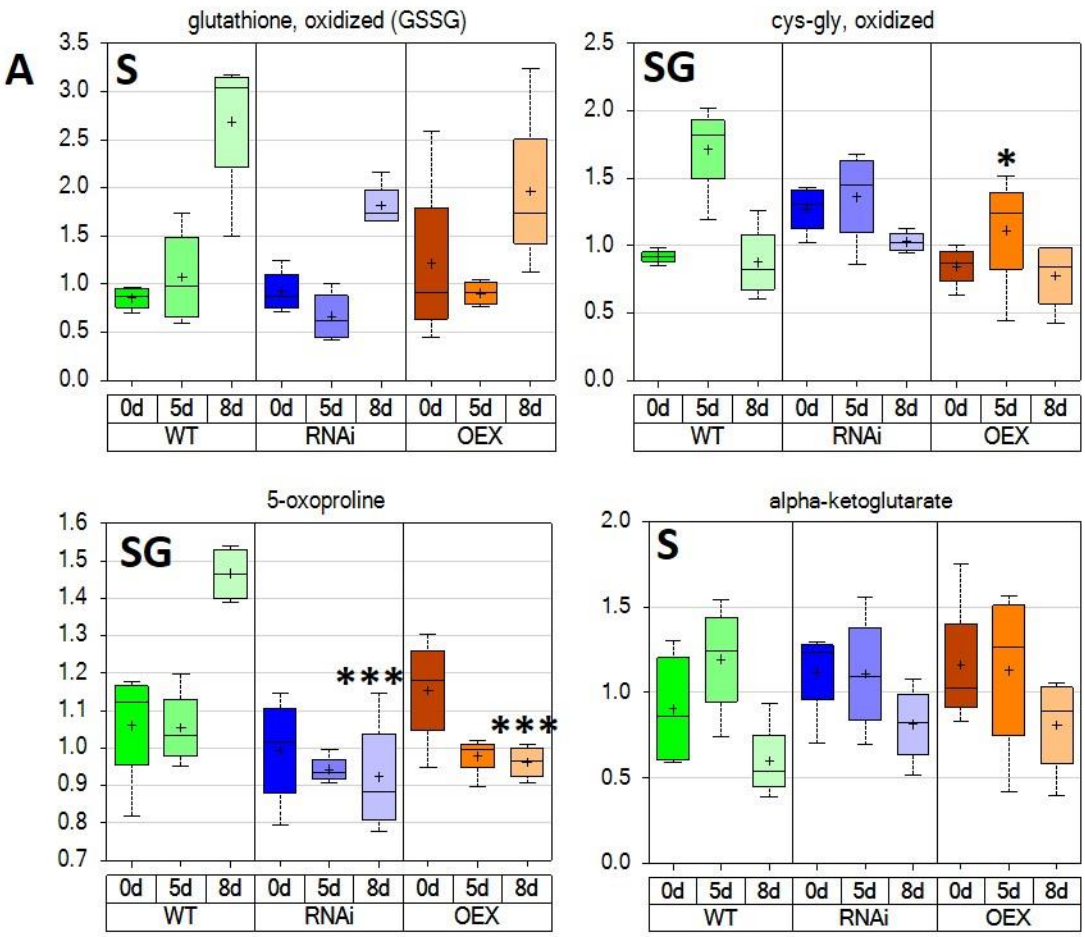
A
glutathione, oxidized (GSSG)
S
cys-gly, oxidized
SG
5-oxoproline
SG
alpha-ketoglutarate
S
0d
5d
8d
WT
RNAi
OEX
*
***
***

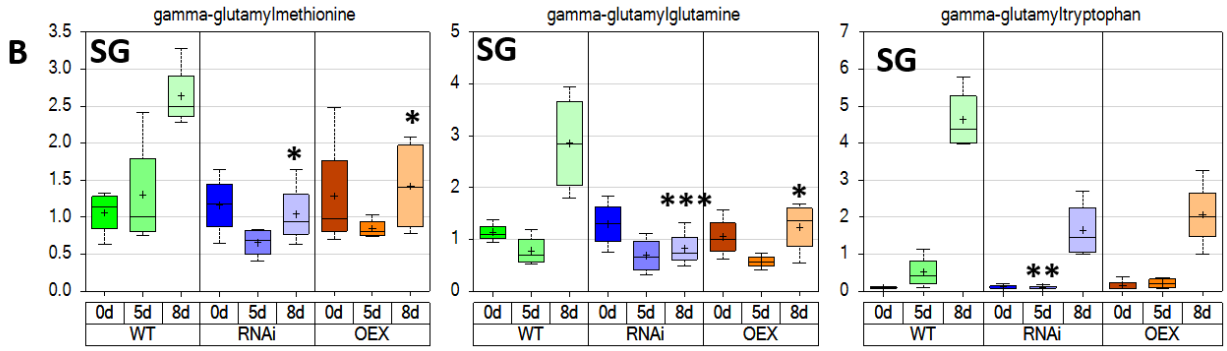

Figure 19 Glutathione metabolite profiles in response to drought stress and GRXS17 expression.

(A) Oxidized glutathione and related degradation metabolites 5-OP and cys-gly, (B) gamma-glutamyl-amino acids presented. Data were analyzed using two-way ANOVA and Student's t-test. S denotes a significant change due to stress ($p \leq .05$);

G denotes a significant effect of GRXS17 expression ($p \leq .05$); T denotes significant differences between OE and RNAi within the same time point ($p \leq .05$). Asterisks denote difference between WT within the same time point (*P<0.05, **P<0.01, ***P<.001).

Biochemical	P Value		Fold Change	
	Stress	Genotype	5DWS	8DWS
gamma-glutamyltryptophan	1.25E-12	0.016	2.27139	23.131
gamma-glutamylhistidine	9.08E-12	0.0548	2.30834	8.68055
gamma-glutamylisoleucine*	1.50E-11	0.506	3.21327	7.37194
gamma-glutamylleucine	3.49E-07	0.6804	1.79739	3.03149
gamma-glutamyl-epsilon-lysine	2.63E-07	0.1462	1.61044	2.96876
gamma-glutamylphenylalanine	8.32E-05	0.1335	1.85596	2.57758
gamma-glutamylvaline	9.82E-07	0.5891	1.63231	2.5661
gamma-glutamylmethionine	0.0059	0.0137	0.79814	1.45174
gamma-glutamylglutamine	0.0002	0.0138	0.58408	1.41302
gamma-glutamylalanine	0.1418	0.0008	0.93563	0.7949
gamma-glutamylglutamate	0.0124	0.7803	0.84022	0.78995

Table 2. 2 Gamma-glutamyl amino acids increase as drought stress progresses.

All gamma-glutamyl amino acids detected in this experiment were sorted according to fold change at 8DWS. P value from two-way ANOVA for stress and genotype effect is reported.

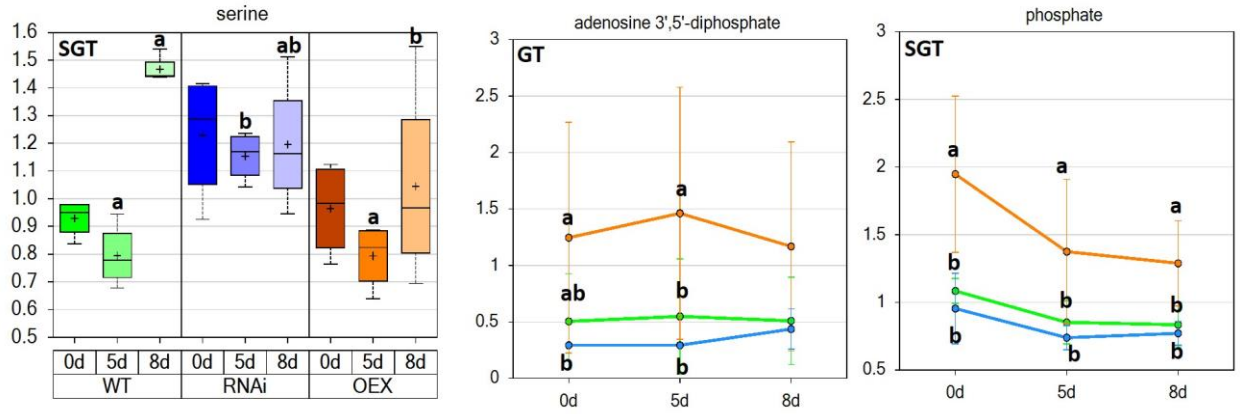

Figure 20 Sulfate assimilation amino acids and metabolites are affected by *AtGRXS17* expression.

Serine, adenosine 3',5'-diphosphate (PAP), and phosphate accumulation differ between genotypes. Green indicates WT, blue indicates RNAi and orange indicates OE. Data were analyzed using two-way ANOVA and Student's t-test. S denotes a significant change due to stress ($p \leq .05$); G denotes a significant effect of GRXS17 expression ($p \leq .05$); T denotes significant differences between OE and RNAi within the same time point ($p \leq .05$). Different letters indicate differences between genotypes within the same time point ($p \leq .05$).

A

Biochemical	P Value		Fold Change	
	Stress	Genotype	5DWS	8DWS
galactinol	0.000	0.002	2.821	18.317
raffinose	0.000	ns	1.277	3.326
ribitol	0.000	0.000	1.454	3.017
fructose	0.000	0.006	1.127	2.502
ribonate	0.000	ns	1.357	1.921
xylose	0.013	ns	1.116	1.628
N-acetylglucosaminylaspar	0.000	ns	1.151	1.424
arabitol/xylitol	0.001	ns	0.924	1.424
mannitol/sorbitol	0.000	ns	1.052	1.395
sucrose	0.000	ns	1.143	1.374
erythronate*	0.001	0.000	1.143	1.334
arabonate/xylonate	0.036	0.034	1.110	1.314
myo-inositol	0.008	ns	1.188	1.185
erythritol	0.013	ns	0.675	1.041
ribose	0.033	0.005	0.849	0.874
UDP-glucose	0.000	0.002	0.611	0.324
UDP-galactose	0.000	0.001	0.366	0.198

B

	OE vs RNAi					
	0DWS		5DWS		8DWS	
	P Value	Fold Change	P Value	Fold Change	P Value	Fold Change
glycerate	0.021	0.860	0.008	0.840	0.000	0.760
ribitol	0.000	0.530	0.001	0.590	0.012	0.650
erythronate*	ns	ns	0.000	1.590	0.008	1.370
UDP-galactose	ns	ns	0.008	4.850	0.017	5.690
UDP-glucose	ns	ns	0.029	2.210	0.009	3.420
galactinol	0.004	0.430	ns	ns	ns	ns
ribose	0.001	0.690	0.043	0.810	ns	ns
2-phosphoglycerate	0.002	88.260	ns	ns	ns	ns
arabonate/xylonate	0.042	0.710	ns	ns	ns	ns

Table 2. 3 Carbohydrate patterns in response to drought stress and comparison between OE and RNAi.

Carbohydrates are sorted by fold change at 8DWS and include p value from two-way ANOVA for stress and genotype effect (A) and carbohydrate related metabolites that differ between OE and RNAi (B). Fold change was calculated as OE value divided by RNAi value and statistical analysis was carried out with Student's t test.

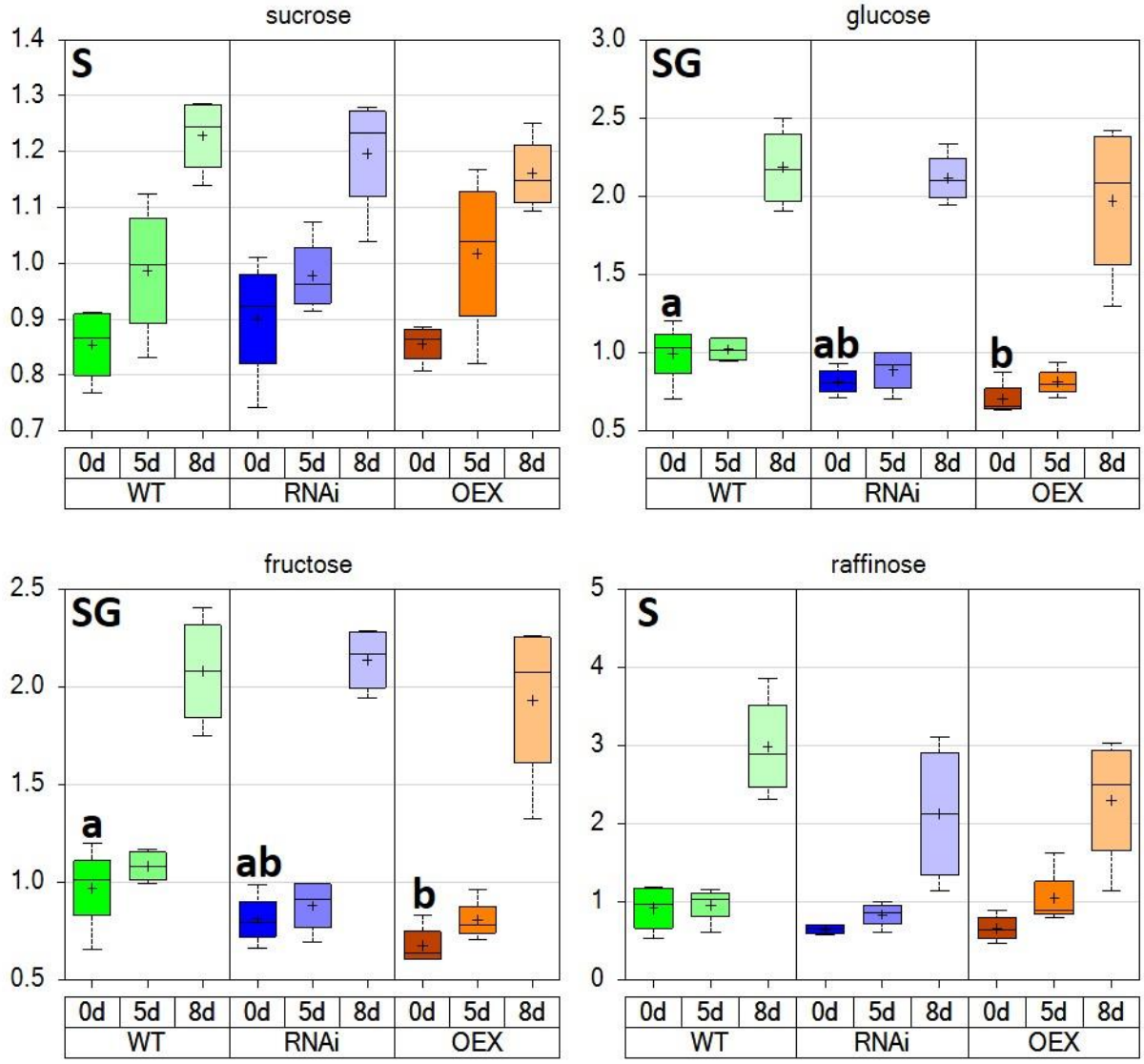

Figure 21 Soluble simple sugars and raffinose accumulation in response to drought stress and *GRXS17* expression.

Sucrose, glucose, fructose and raffinose accumulation was affected by stress while fructose and glucose also differed between genotypes. Data were analyzed using two-way ANOVA and Student's t-test. S denotes a significant change due to stress ($p \leq .05$); G denotes a significant effect of GRXS17 expression ($p \leq .05$); T denotes significant differences between OE and RNAi within the same time point ($p \leq .05$). Different letters indicate differences between genotypes within the same time point ($p \leq .05$).

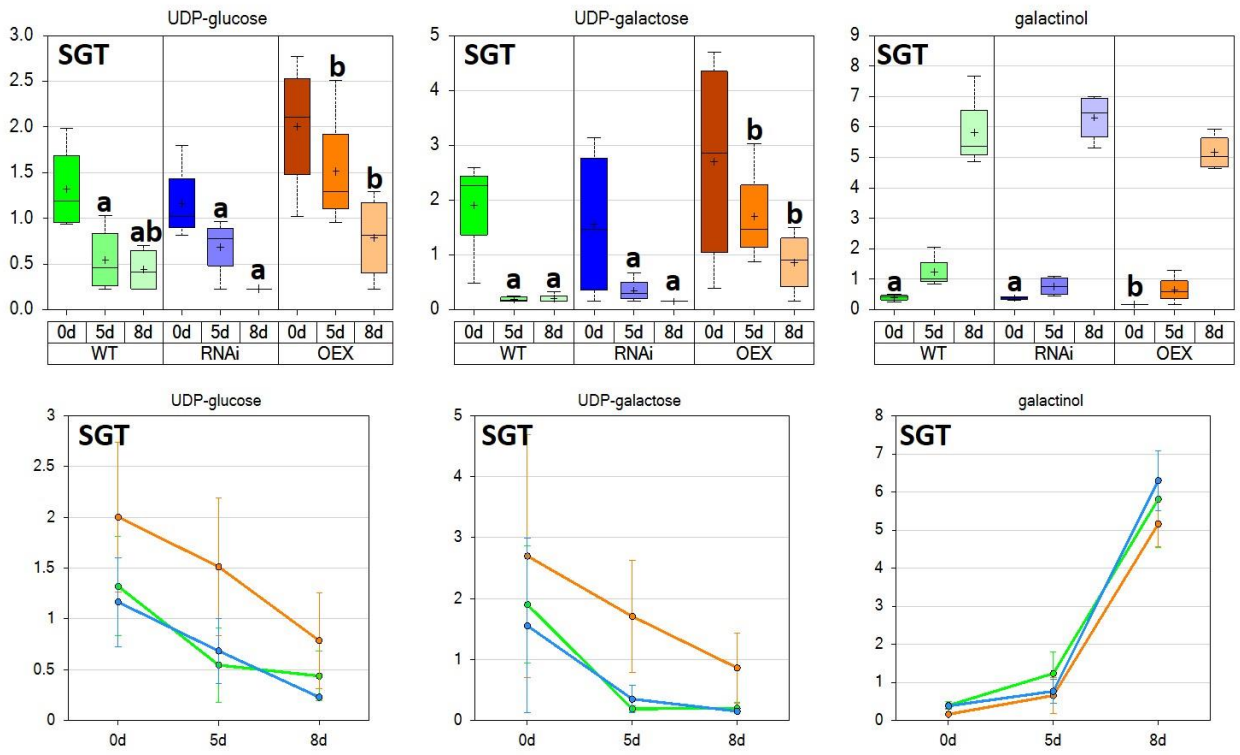

Figure 22 Raffinose family oligosaccharide precursors are affected by stress and GRXS17 expression.

UDP-glucose, UDP-galactose, and galactinol accumulation differ between genotypes. Green indicates WT, blue is RNAi and orange is OE. Letters indicate differences between genotypes within timepoints. Data were analyzed using two-way ANOVA and Student's t-test. S denotes a significant change due to stress ($p \leq .05$); G denotes a significant effect of GRXS17 expression ($p \leq .05$); T denotes significant differences between OE and RNAi within the same time point ($p \leq .05$). Different letters indicate differences between genotypes within the same time point ($p \leq .05$).

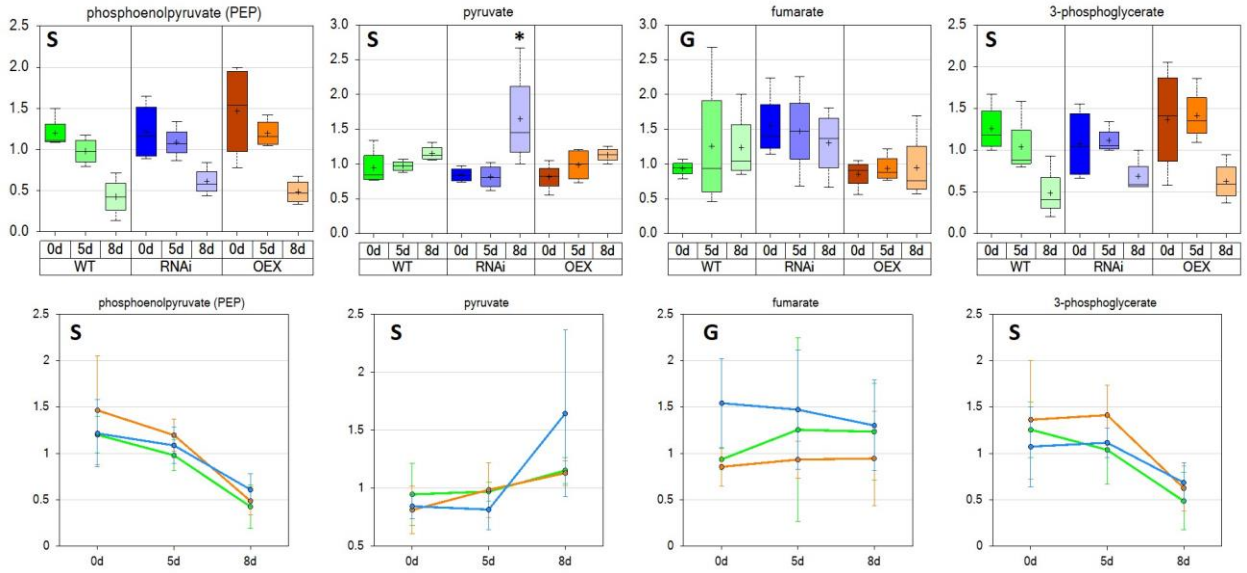

Figure 23 The effect of stress and GRXS17 expression on glycolysis, the citric acid cycle, and the Calvin cycle.

Phosphoenolpyruvate (PEP) and pyruvate are both glycolysis related metabolites affected by stress. The citric acid cycle intermediate fumarate accumulation differs between genotypes. Calvin cycle intermediate 3-phosphoglycerate is affected by stress. Green indicates WT, blue is RNAi and orange is OE. Data were analyzed using two-way ANOVA and Student's t-test. S denotes a significant change due to stress ($p \leq .05$); G denotes a significant effect of GRXS17 expression ($p \leq .05$); T denotes significant differences between OE and RNAi within the same time point ($p \leq .05$). Different letters indicate differences between genotypes within the same time point ($p \leq .05$). Asterisks denote difference between time point indicated and 0DWS (*P<0.05, **P<0.01, ***P<.001).

Biochemical	P Value		Fold Change	
	Stress	Genotype	5DWS	8DWS
isocitrate	0.000	ns	1.260	0.008
aconitate [cis or trans]	0.000	ns	1.162	0.084
2-methylcitrate	0.006	ns	0.842	0.274
citrate	0.000	ns	0.953	0.387
alpha-ketoglutarate	0.024	ns	1.079	0.699
succinate	0.025	ns	0.902	0.777
maleate	0.003	ns	1.136	1.634

Table 2. 4 Citric acid cycle intermediates response to drought stress and *GRXS17* expression.

All citric acid cycle intermediates detected to change due to drought stress were sorted by fold change. P value from two-way ANOVA for stress and genotype effect is reported.

SUPPORTING INFORMATION

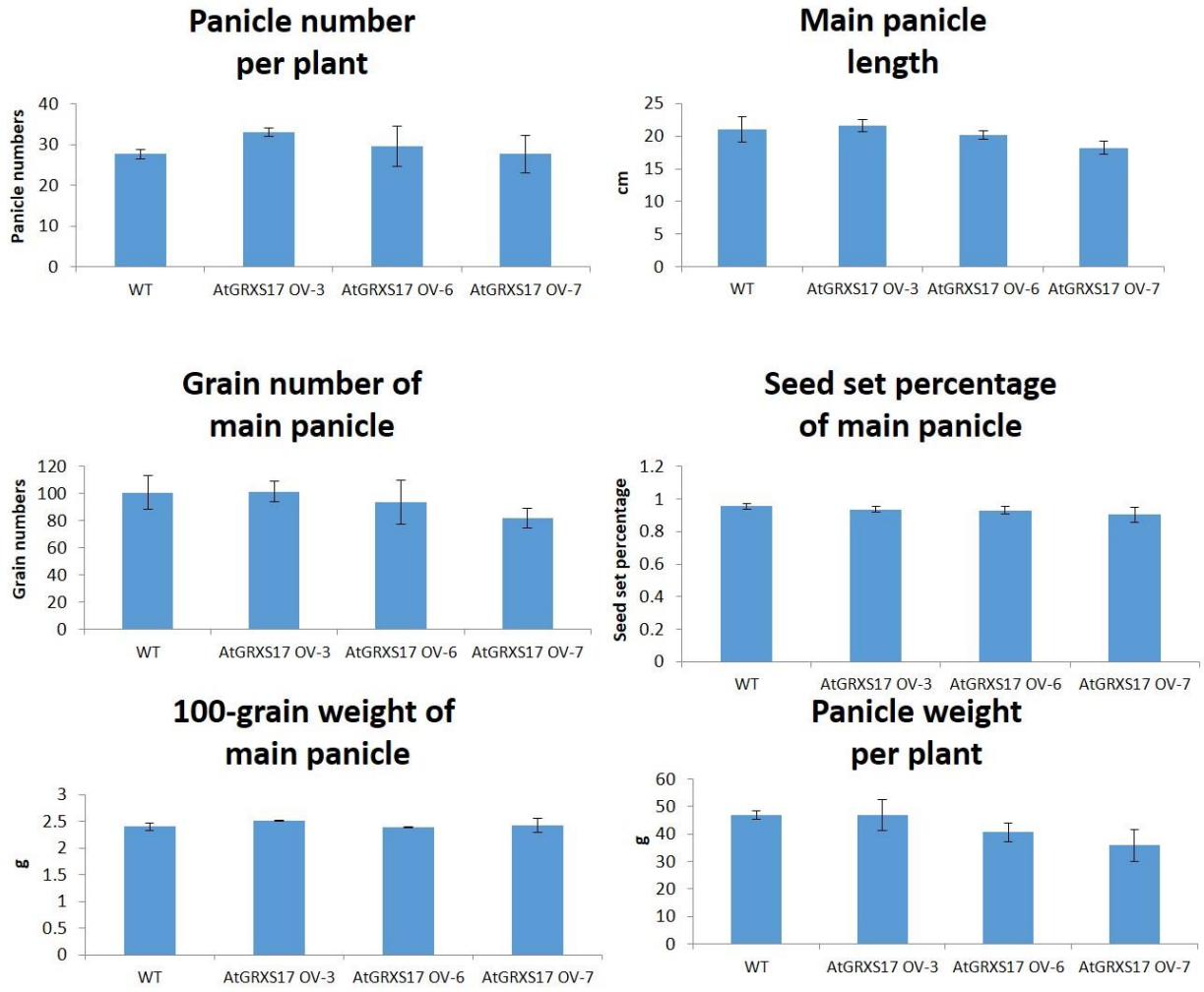

Figure 24 Yield parameters of wild-type and *AtGRXS17*-expressing rice plants.

Panicle number, panicle length, grain number per panicle, seed set percentage, average grain weight, and total grain weight per panicle were measured. Error bars indicate ± SD.

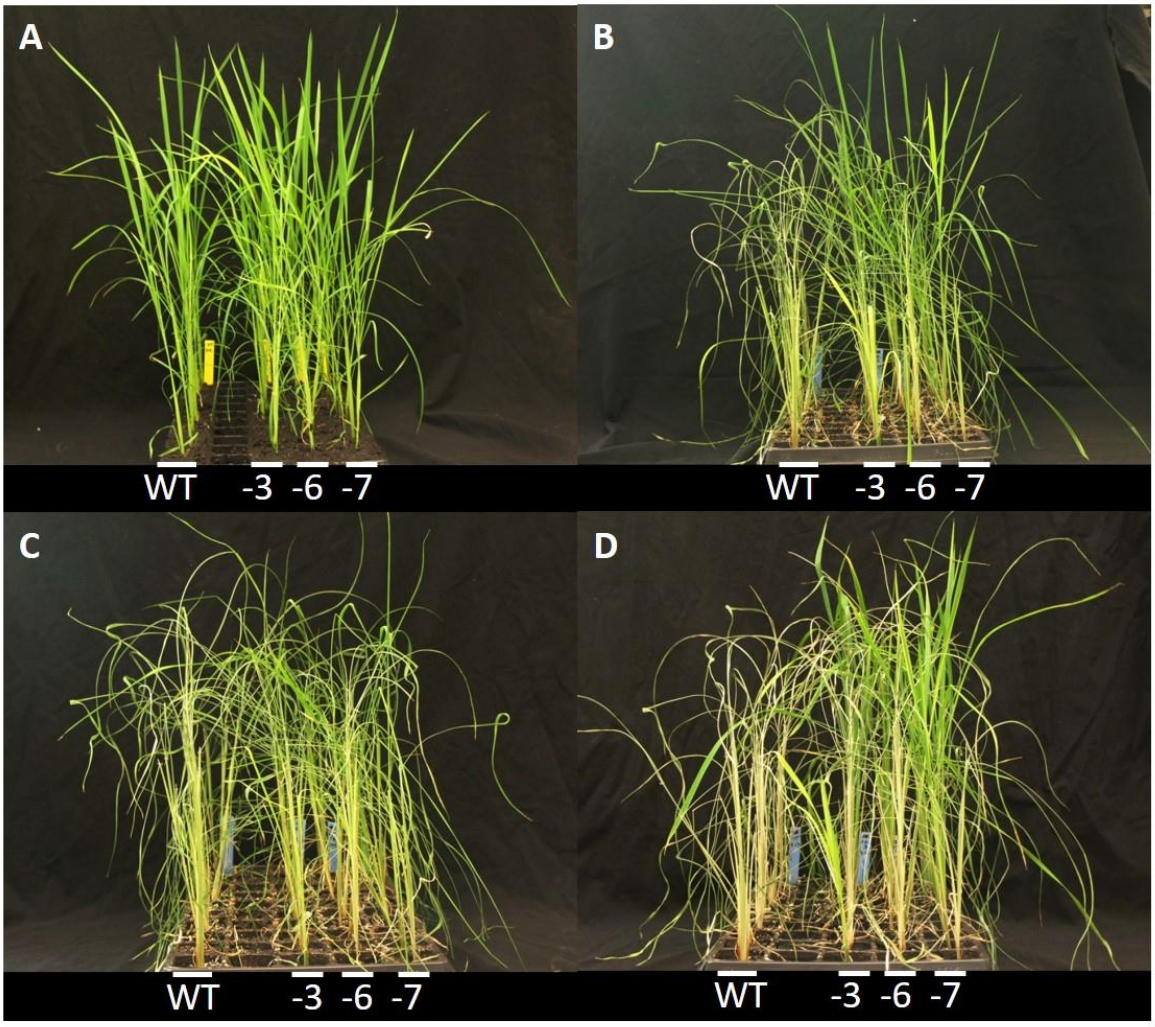

Figure 25 *AtGRXS17*-expressing plants are more drought tolerant than wild-type plants. (A) Wild type and *AtGRXS17*-3, -6, -7 rice plants are indistinguishable from one another before drought treatment. (B) Rice plants 6 days after withholding water. (C) Rice plants 8 days after withholding water. (D) OE lines, but not WT, recover after two weeks.

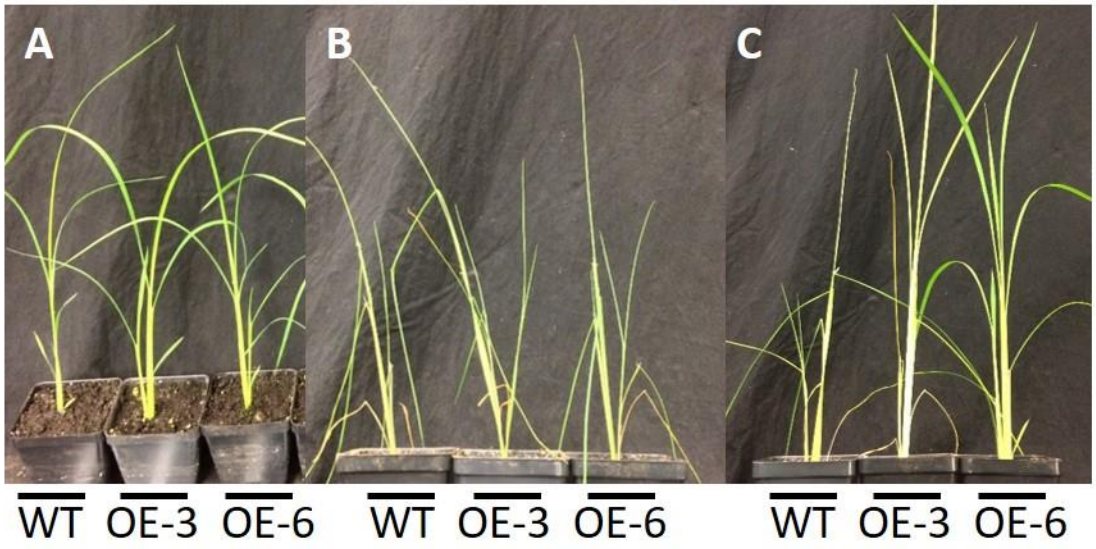

Figure 26 *AtGRXS17*-expressing plants are more drought tolerant than wild-type plants. (A) Wild type and *AtGRXS17*-3, -6 rice plants are indistinguishable from one another before drought treatment. (B) Rice plants 8 days after withholding water. (C) Rice plants 8 days after withholding water.

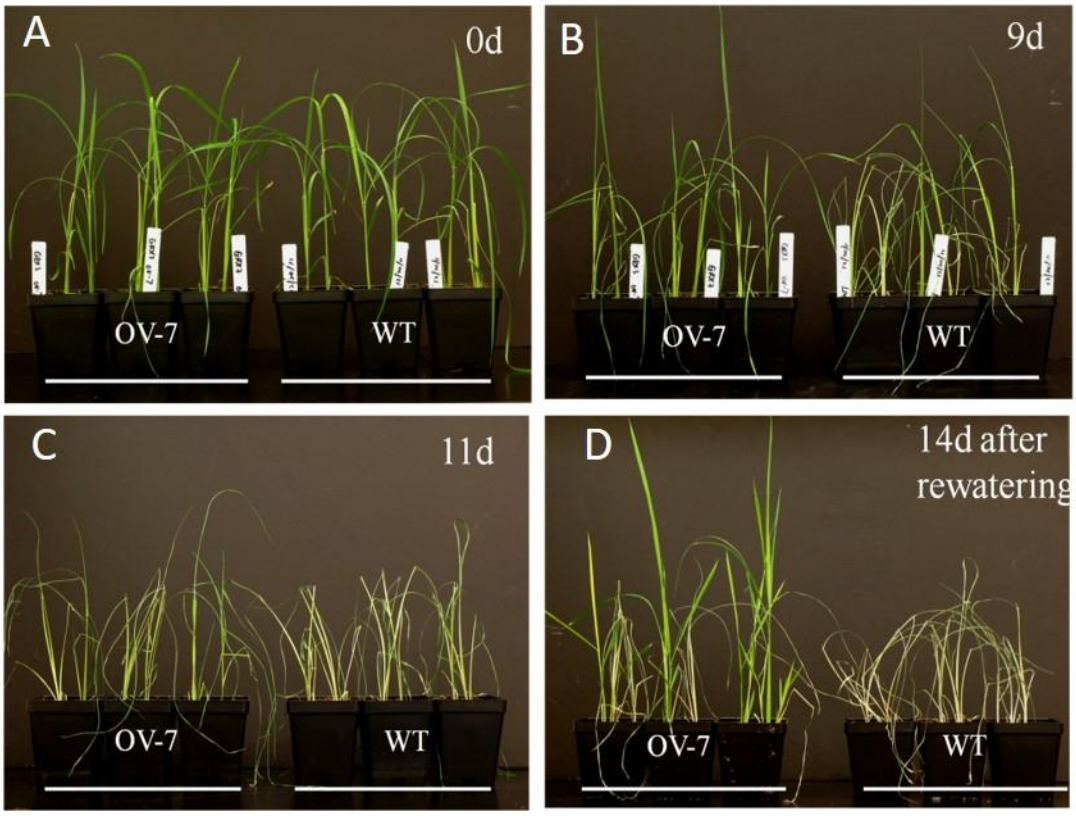

Figure 27 Drought test of WT and *AtGRXS17*-7 (OE) rice.

(A) Wild type and *AtGRXS17*-7(OE) rice plants before treatment on the initial day of withholding water. (B) Rice plants 9d and (C) 11d after withholding water. (D) OE plants recover after rewatering.

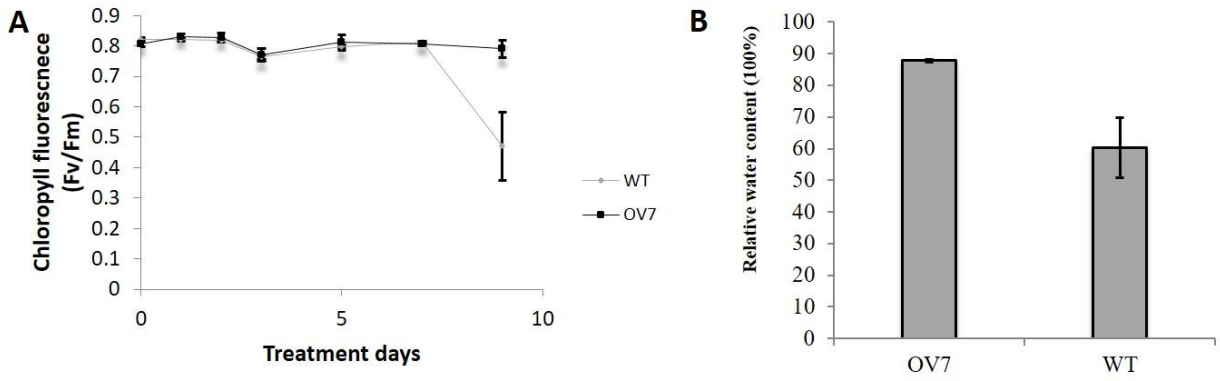

Figure 28 Chlorophyll fluorescence and relative water content of WT and OE.

(A) Drought tolerance was analyzed after nine days through chlorophyll fluorescence and (B) relative water content. Error bars indicate mean ± SD (n=3).

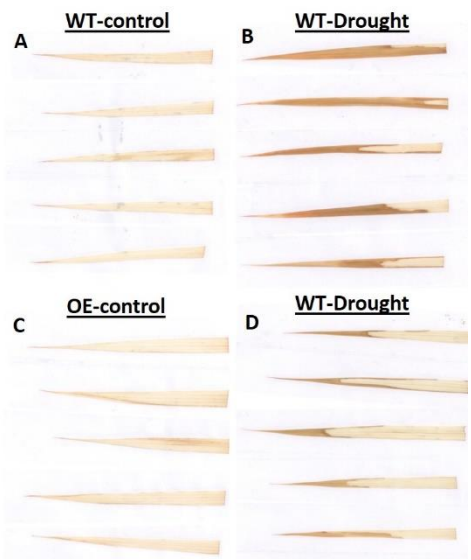

Figure 29 H_20_2 accumulation in response to drought stress in WT and OE leaves.

(A) Little DAB staining occurred in non-stressed WT or (C) OE rice plants. (B) WT and (D) OE rice plants H_2O_2 accumulation in response to drought stress.

A

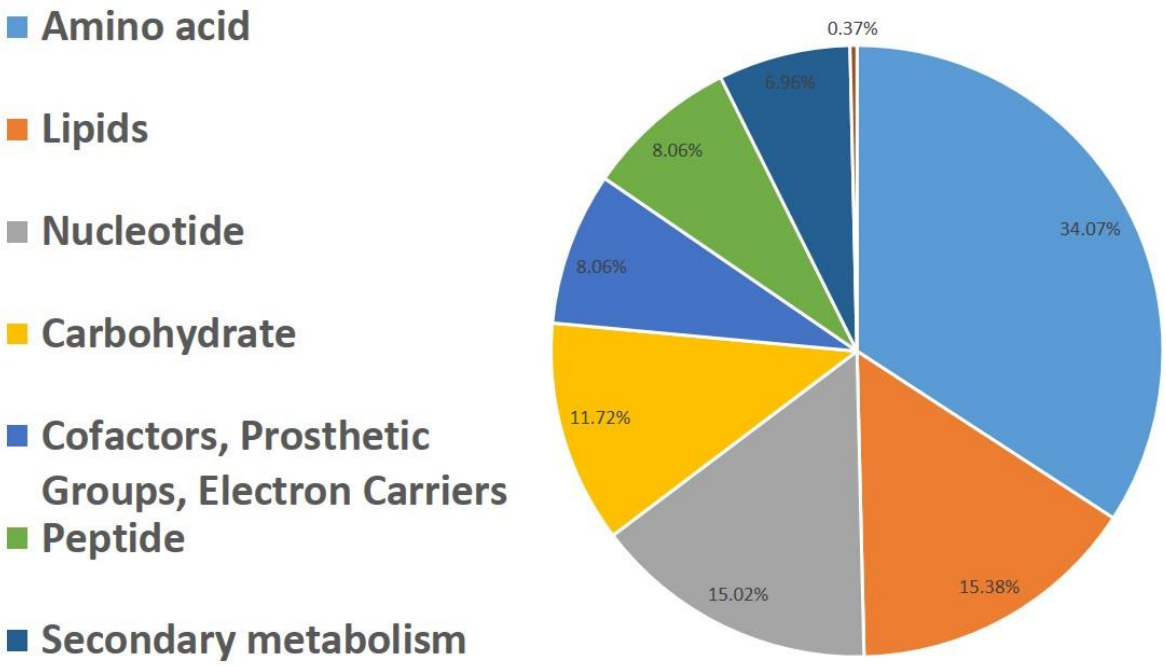
Amino acid
Lipids
Nucleotide
Carbohydrate
Cofactors, Prosthetic Groups, Electron Carriers
Peptide
Secondary metabolism
0.37%
6.96%
8.06%
34.07%
8.06%
11.72%
15.02%
15.38%

B

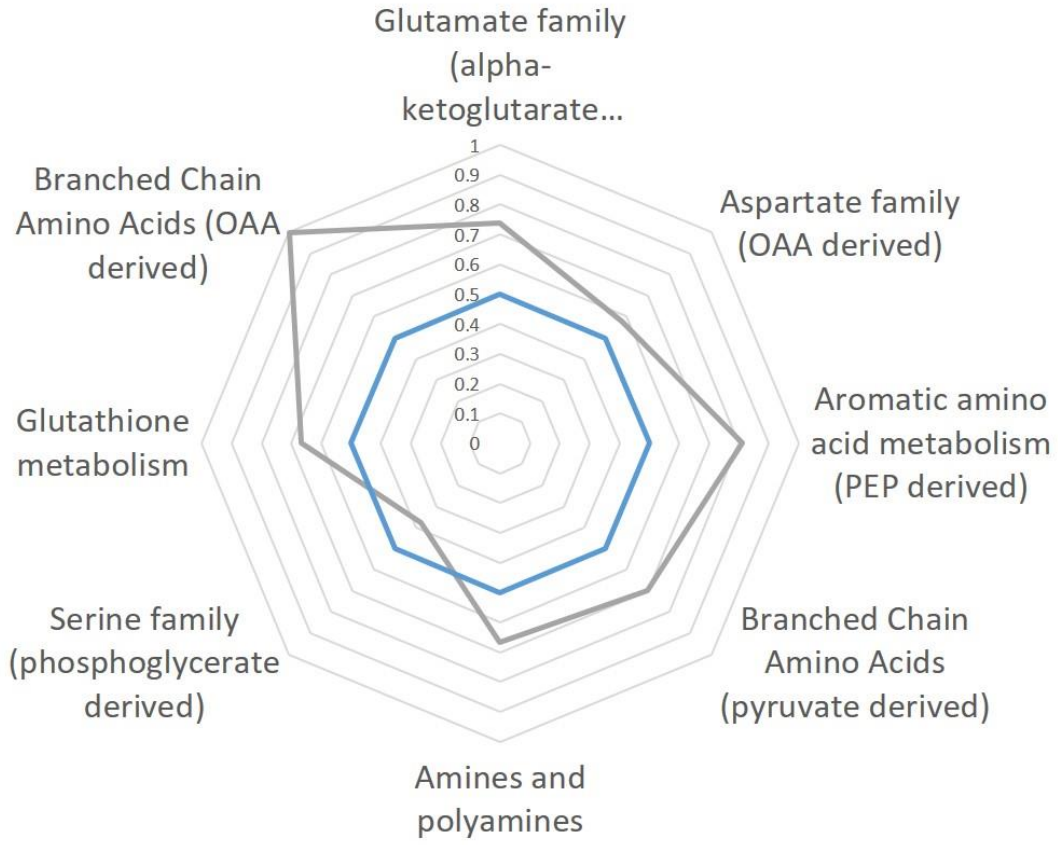
Glutamate family (alpha-ketoglutarate...
Aspartate family (OAA derived)
Aromatic amino acid metabolism (PEP derived)
Branched Chain Amino Acids (pyruvate derived)
Amines and polyamines
Serine family (phosphoglycerate derived)
Glutathione metabolism
Branched Chain Amino Acids (OAA derived)
1
0.9
0.8
0.7
0.6
0.5
0.4
0.3
0.2
0.1
0

Figure 30 Amino acids are the largest group of metabolites affected by stress and mostly increase.

(A) Amino acid metabolism (34.1%). Lipid metabolism (15.4%), nucleotide metabolism (15%), carbohydrate metabolism (11.7%), cofactor, prosthetic group, and electron carrier metabolism (8.1%), peptide metabolism (8.1%), secondary metabolites (7%), hormones (.4%) and xenobiotics (.4%) were all affected by stress. (B) Most subgroups of amino acid metabolites increase (>50%) while serine related metabolites decrease.

Biochemical	Percentage of Total Carbohydrate
sucrose	30%
malate	28%
arabonate/xylonate	10%
oxalate (ethanedioate)	8%
glycerate	5%
glucose	4%
citrate	4%
fructose	3%
erythronate	2%

Table 2. S. 1 Composition of carbohydrates detected across all genotypes.

Composition of different carbohydrate related metabolites as a percentage of total carbohydrate related metabolites.

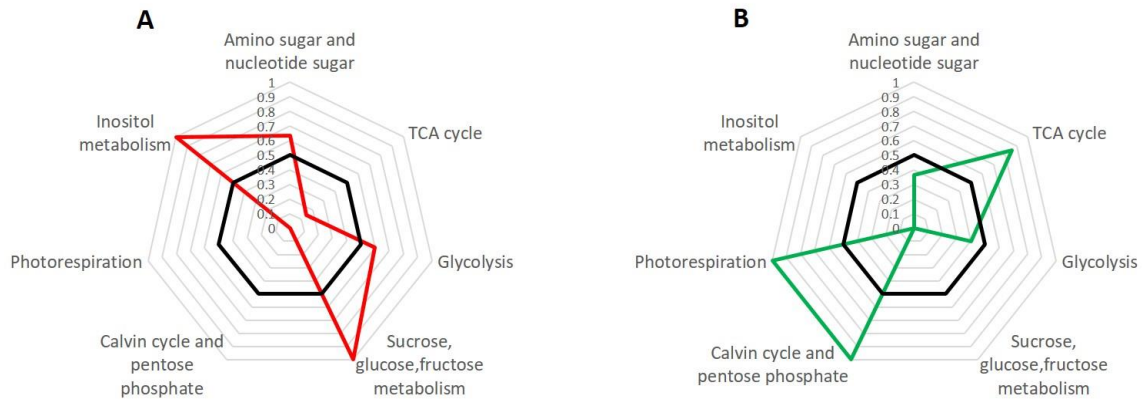

Figure 31 Radar plots of stress affected carbohydrate related metabolites indicate proportion that increase or decrease.

(A) Inositol metabolism, amino and nucleotide sugars, soluble sugars all mostly increased while

(B) photorespiration, Calvin cycle, and citric acid cycle related metabolites mostly decreased.